Doctoral Dissertation

Activation and characterization of cryptic phthoxazolin A biosynthetic gene cluster in *Streptomyces avermitilis*

(*Streptomyces avermitilis* におけるフトキサゾリ A 休眠生合成遺伝群の活性化および機能解析)

DIAN ANGGRAINI SUROTO

April 2018

Division of Advanced Science and Biotechnology
Graduate School of Engineering
Osaka University

Table of Contents

List of Figures

List of Tables

Abbreviations

A	adenylation
ACP	acyl carrier protein
antiSMASH	antibiotics and secondary metabolite analysis shell
APM	avermectin production medium
ARE	autoregulatory element
AT	acetyl transferase
ATP	adenosine triphosphate
BLAST	basic local alignment search tool
C	condensation
CDCl3	deuterated chloroform
CFU	colony forming unit
CoA	coenzyme-A
COSY	correlation spectroscopy
Cyp	cytochrome p450
DAD	diode array detector
DDBJ	DNA Data Bank of Japan
DH	dehydratase
DNA	deoxyribose nucleic acid
ER	enoyl reductase
F	formylation
FAD	flavin adenine dinucleotide
HMBC	heteronuclear multiple bond connectivity
HPLC	high performance liquid chromatography
HRCIMS	high resolution chemical ionization mass spectrometry
HTH	helix-turn-helix
IR	infra red
ISP4	International Streptomyces Project medium No.4
KR	ketoreductase
KS	ketosynthase
LAL	large ATP-binding regulator of the LuxR family
LB	Luria-Bertani medium
MeOH	methanol
MIC	minimum inhibitory concentration
MMF	methylenomycin furan

m/z	mass/charge ratio
MT	methyl transeferase
NADP-(H)	nicotinamide adenine dinucleotide (phosphate)
NCBI	National Center for Biotechnology Information, USA
NMR	nuclear magnetic resonance
NOESY	nuclear overhauser effect spectroscopy
NRPS	non-ribosomal peptide synthetase
OSMAC	one strain, many compounds
PCP	peptidyl carrier protein
PCR	polymerase chain reaction
PI	pimaricin inducer
PKS	polyketide synthase
RNA	ribonucleic acid
RT-PCR	reverse transcriptase-polymerase chain reaction
SALD	*Streptomyces avermitilis* large deletion
SAP	*Streptomyces avermitilis* plasmid
SARP	*Streptomyces* antibiotic regulatory protein
SCB	*Streptomyces coelicolor* butanolide
SRB	*Streptomyces rochei* butenolide
SUKA	Special Use of Kitasato Actinobacteria.
TE	thioesterase
TFA	trifluoroacetic acid
UV	ultra violet
VB	*virginiae* butanolide
YEME	yeast extract malt extract medium
YMD	yeast extract malt extract dextrin medium
YMS-MC	yeast extract malt extract soluble starch supplemented with magnesium chloride and calcium chloride
YPD	yeast extract peptone dextrose medium
YT	yeast extract tryptone medium

Chapter I

General Introduction

1.1. The habitat and life cycle of *Streptomyces*

The Streptomyces bacteria are Gram-positive belonging to the taxonomic order of Actinomycetales, with remarkably high-content of guanine and cytosine in their DNA (average 74 mol %) (1). They are the dominant, the most morphologically diverse genus in the family Streptomycetaceae, and the well-studied among actinomycetes (2). Generally, Streptomyces species grow by utilizing carbon from the remains of plants and animals in the soil (3) and give the typical earthy odor due to the production of geosmin (4,5). Nevertheless, Streptomyces also effectively live in the sea and freshwater ecosystems (5,6), live in symbiosis with plants (5-7), fungi, insects, and invertebrates (5,6) and in rare cases, they are causing human infections (8-10). Streptomyces have earned status as indispensable sources of therapeutic molecules because of the supreme wealth and diversity of the secondary metabolisms (11,12).

Most of the Streptomyces have intricate morphological development and reproduce by sporulation. The spores germinate and produce germ tubes to form vegetative mycelium that extent by apical growth at the hyphal tip (2, 13). The combination of tip growth and branching produces extensive and elaborate vegetative mycelium which actively explores the surroundings (13,14) and hydrolyzes natural polymers to supply nutrients (3). Due to nutritional scarcity and other physiological stresses, vegetative mycelium initiates the reproductive growth by forming vertical “aerial hyphae”. The aerial hyphae spread by apical growth escape the surface tension of the aqueous phase of

medium and expand into the air (13-15). Nutrients for the aerial hyphae are supplied from the degraded-substrate mycelium (13,14,16).

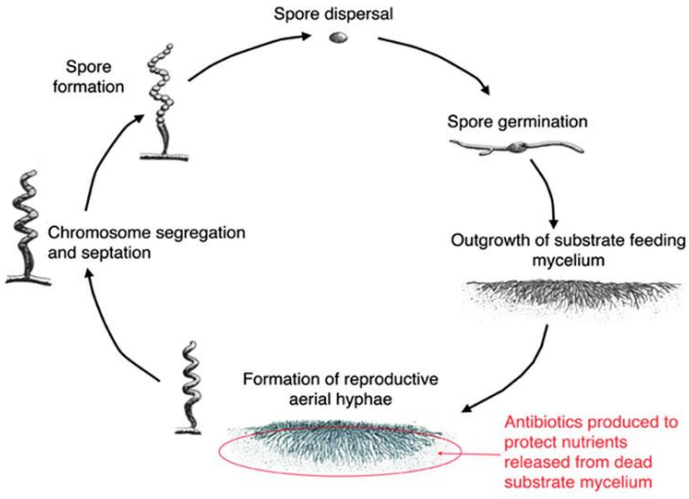

Figure 1.1. The life cycle of *Streptomyces* (5)

The sporulation is initiated by the development of the aerial hyphae into long chains of pre-spore compartments, subsequently, segregation and distribution of the copies of linear chromosomes occur so that a compartment contains a copy of the chromosome (2,13). Thick spore walls resistant to lysozyme are made, followed by production of a grey spore pigment (2,13,14). These spores are meant for distribution and survival of Streptomyces in a dormant state, thus they are able to endure extreme low moisture condition and other physicochemical threats (2,13,14).

In addition to the classical life cycle, the unique developmental competence of Streptomyces named as “exploratory growth” was recently discovered. The exploratory growth is driven by sugar limitation due to contact of Streptomyces with fungi (17). Many Streptomyces species have the ability to undertake exploratory growth mode which enables them to expand new territory using the rapid growth of vegetative hyphae sans sporulation process (17).

1.2. Secondary metabolites production in *Streptomyces*

The shift between vegetative growth and reproductive growth in *Streptomyces* have been linked with the production of secondary metabolites (18,19). The secondary metabolites have numerous bioactivities such as antibiotics, antitumor, insecticide, antiviral, herbicide, and antifungal etc (11) (Figure 1.2). These secondary metabolites are not necessary for the growth of *Streptomyces* under laboratory cultivation but may bestow advantageous defense to *Streptomyces* in natural habitat (3,20). The bioactive metabolites from actinomycetes have comprised more than 30% of the known microbial metabolites, with the *Streptomyces* genus produce for approximately 70-80% of those biologically active secondary metabolites (11).

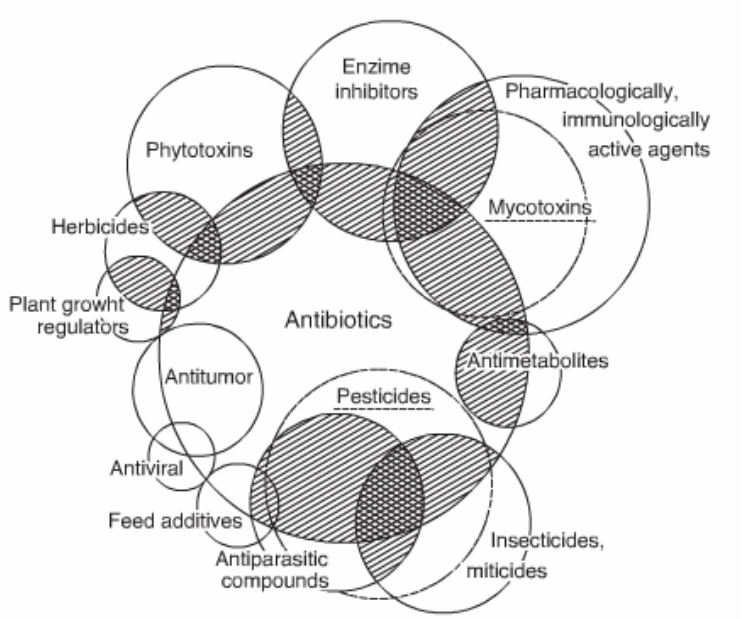

Figure 1.2. The bioactivities of secondary metabolites (11)

The typical lifestyle and habitat of *Streptomyces* as non-motile microorganism in soil with numerous environmental stresses are reflected in their capability to produce series of secondary metabolites (20). Their secondary metabolites were previously

considered as antibiotics to win the competition with others microorganisms for the food supplies (3,20.) In fact, these metabolites also act as signaling molecules for communication with various microorganisms in the natural habitat (3,21).

The secondary metabolites from *Streptomyces* have been industrially and scientifically exploited since in the 1940s, which were initiated by the discovery of streptomycin at Rutgers University by Selman Waksman and his student. With culmination at The Golden Age in which thousands of secondary metabolites were identified, including hundreds that were authorized for prescription drugs, for example, antibacterial drugs tetracycline, chloramphenicol, streptomycin, vancomycin, and chemotherapeutic drug doxorubicin (11,12). Examples of industrially exploited bioactive metabolites produced by *Streptomyces* are depicted in Figure 1.3.

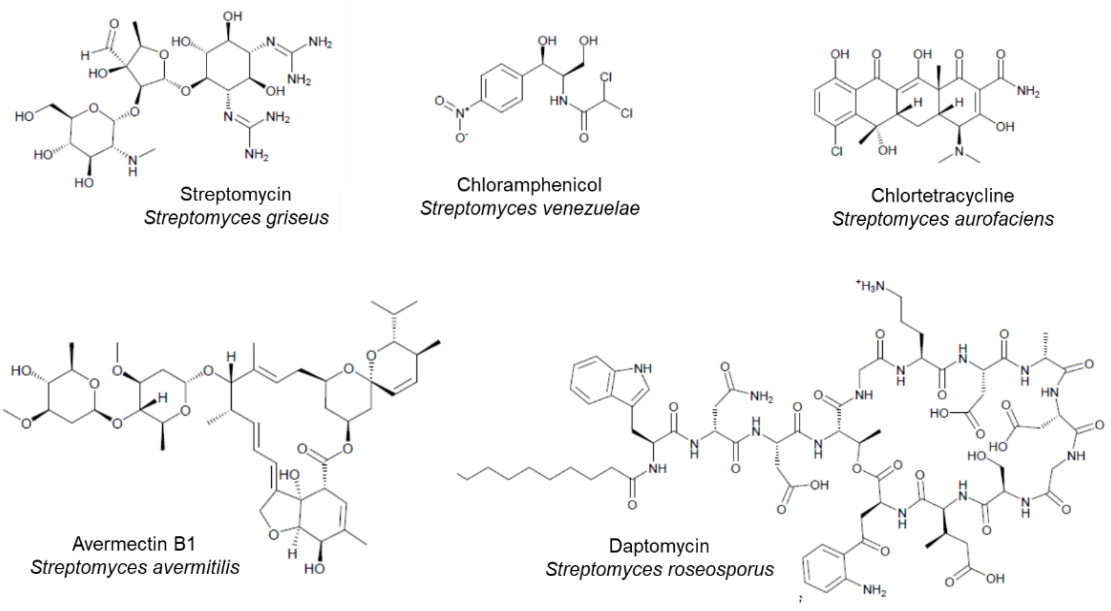

Figure 1.3. The metabolites of *Streptomyces* with industrial significance

Secondary metabolites have various and extraordinary intricate structures, with the different array of molecular weights and stereochemical properties which appealed the chemists for generating the synthetic derivatives, and biologists to understand the biosynthetic pathways. The structural features of secondary metabolites are the outcome of their biosynthesis in nature which required multiple enzymes to catalyze the process (22). Like other bacteria and fungi, the sequencing analysis of the *Streptomyces* genome shows that the biosynthetic genes and their regulators are usually grouped and polycistronically transcribed (23).

The microbial or *Streptomyces* secondary metabolites are classified into (i) polyketides synthesized by polyketide synthases; (ii) peptides synthesized by non-ribosomal peptide synthetases or by the conventional ribosomal pathway; (iii) terpenes which are developed from isoprene unit derived from mevalonate pathway; (iv) amino sugars and aminoglycosides in which have a modification of sugars structure with amine functional group; and (v) alkaloids, the nitrogenous small secondary metabolites derived from the complex biosynthetic pathway. Some secondary metabolites are sometimes produced in a combination of two pathways, termed as “hybrid”, such as hybrid polyketides synthase-non ribosomal peptide synthetase (24) and meroterpenoid which is produced by terpene and polyketide pathway (4).

1.2.1. The assembly line of polyketides

Polyketides represent one of the main family of secondary metabolites showing the high extent of structural diversity and numerous bioactivities for agricultural and medicinal applications, including commercially available drugs such as erythromycin, chloramphenicol, daunorubicin, avermectin, rifampicin, and tetracycline.

This group of secondary metabolites has a common mechanism of biosynthesis involving multifunctional enzymes polyketide synthases (PKSs). Basically, the polyketide carbon backbones are formed by repeated-decarboxylative condensations of an acyl starter unit with derivative of malonyl-CoA extender units which are very much alike to fatty acid biosynthesis (25).

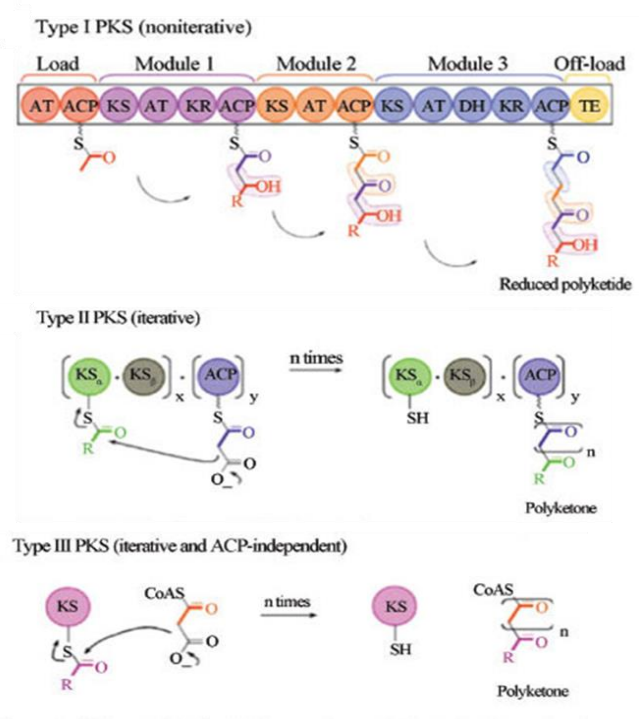

Figure 1.4. Graphic representation of polyketide synthases assembly lines (25)

A PKS module at least consists of an acyltransferase (AT), β-ketosynthase (KS) and acyl carrier protein (ACP) domain. A malonyl-CoA (other) extender unit is put into the ACP domain by AT domain and the KS domain catalyzes the C-C bond formation of the emerging polyketide with the extender unit. The polyketide chain may form saturated acyl structure due to the action of ketoreductase (KR), dehydratase (DH), and an enoyl reductase (ER) domains. Finally, the polyketide acyl chains are released from the ACP by thioesterase (TE) domains (22,25).

The PKSs are divided into three groups based on their structures and catalytic mechanisms (22,25,26) ; (i) the type I PKSs represent huge multidomain enzymes that are arranged into modules, in which each module is in charge for one set of C-C bond formation (elongation). These type I PKSs are classified into iterative and non-iterative (modular) based on how their ketosynthase domains act, whether or not each KS domain catalyzes repeatedly for elongation of polyketides; (ii) The type II PKSs represent small enzymes complexes that contain discrete functional domains for iterative elongation; (iii) Whereas the type III PKSs are homodimer enzymes that are repeatedly performing decarboxylation, condensation, cyclization, and aromatization. The type III PKS represents acting condensing enzymes of the chalcone synthase type.

Table 1.1. Type and distribution of PKSs (27)

PKS type	Mode of substrate activations, building blocks	Organisms
Type I PKS modular	ACP, various extender units	Bacteria (Protists)
Type I PKS iterative	ACP, only malonyl extenders	Fungi, some bacteria
Type II (iterative)	ACP, only malonyl extenders	Only bacteria
Type III (iterative)	Acyl-CoA, only malonyl extenders	Predominantly plants, some bacteria and fungi

Structural diversity in polyketides group of secondary metabolites was mainly due to the type and number of building blocks involved in the system (22,27). Non-acetate starter units were established for several polyketides such as propionate, malonamate, hydroxy-substituted and non-substituted cinnamoyl, benzoyl, as well as short linear or branched fatty acids (22,27). The diverse structures of polyketides may also come from the action of several modifying enzymes. These enzymes catalyze the complete change of the polyketide chains into their final product, which may include hydroxylation,

glycosylation, alkylation, oxidation, halogenation, epoxidation, and cyclization (22,27,28).

In contrast to standard modular type PKS (*cis*-AT PKS), there are PKS enzymes showing peculiar feature, in which the AT activity is provided by the discrete enzyme encoded by an individual gene (29). These type of PKSs termed as *trans*-AT PKS. They also show a high degree of variation on their modules including unique module organizations, non-elongating modules, modules which divided into two different polypeptides, thus the co-linearity rule to predict the structure of PKSs product based on the module organization is difficult to be applied in *trans*-AT PKSs (30). The *trans*-AT PKSs had been found in numerous therapeutic polyketides since the first discovery of *trans*-AT bacillaene biosynthesis from *Bacillus subtilis* in 1993 (30).

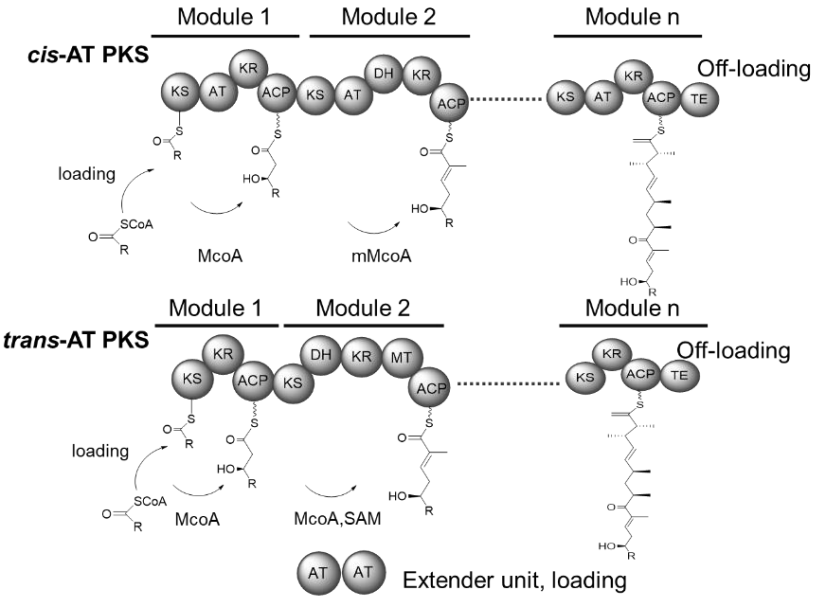

Figure 1.5. Graphic representation of a *cis*-AT PKS and a *trans*-AT PKS assembly lines (31)

1.2.2. The assembly line of nonribosomal peptides

The well-known nonribosomal peptides of natural products including penicillin, vancomycin, cephalosporin, cyclosporine, and anticancer bleomycin show a high degree of structural diversity. Nonribosomal peptide synthetases (NRPSs) have modular multienzyme assembly lines that are similar to those of PKSs, in which amino, hydroxy and carboxy acid monomers are incorporated into the system to produce peptide-containing compounds (32).

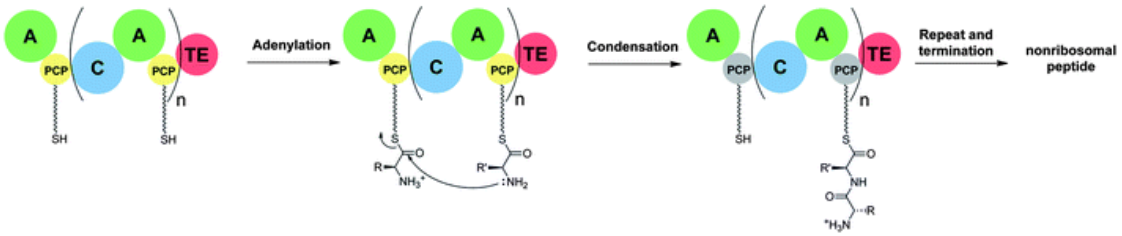

Figure 1.6. Graphic representation of non-ribosomal peptide synthetases (NRPS) assembly line (32)

In each NRPSs elongation module, an adenylation (A) domain activates its cognate amino acid and produces aminoacyl adenylate using ATP. The A domains dictate the amino acid substrates to be incorporated in the backbones. This capacity is reflected on the active site of any A-domain, called “specificity-conferring code” (33). Then, the aminoacyl activated by A-domain is loaded onto a peptidyl carrier protein (PCP).

Subsequently, a condensation (C) domain establishes an amide bond with the burgeoning peptidyl chain bound to the upstream PCP domain. The NRPSs machinery incorporates proteinogenic amino acids, D- and B-amino acids, methylated, glycosylated and phosphorylated residues, in total more than 500 substrates had been recognized (34). Like PKS machinery, NRPS also has modification enzymes such as oxidation, cyclization, glycosylation, hydroxylation (35).

1.3. Regulation of secondary metabolites production in *Streptomycetes*

The production of secondary metabolites in *Streptomyces* is reliant on the stage of growth, but it is also influenced by a diverse environmental and cellular signals, including nutrient limitation, the presence of different signaling molecules, and various physiological stresses (18,19). At the molecular level, the signals from these factors are transferred within the cell via a multilayered of regulators to the biosynthetic genes. The different intra- and extra-cellular factors interact at different levels with the cell regulatory networks or even with the secondary metabolite biosynthesis itself (36). This makes the entire regulatory network very complicated.

1.3.1. Nutrients availability

The presence of carbon source, nitrogen source, and phosphate influences the production of secondary metabolites and morphological development in *Streptomyces*. Simple and quickly utilized carbon sources such as glucose, galactose, glycerol, and mannose prevent the production of several secondary metabolites in *Streptomyces* (37). The *Streptomyces* prefer chitin as a nutrient source in nature (3), with majority obtained from fungi and the exoskeletons of insects and crustaceans. The hydrolyzed product of chitin, N-acetylglucosamine (GlcNAc) was reported to trigger the production of secondary metabolites of *Streptomyces* in minimal medium but showed opposite effect in rich medium (38).

The low amino acid condition in *Streptomyces* induces stringent response system in which production of the polyphosphorylated guanine nucleotide (ppGpp) is accelerated due to activation of the ribosome-associated protein RelA (19,36,39). The high level of ppGpp generally will trigger secondary metabolite production. In the same time, the

decrease of GTP level causes the initiation of morphological development (39).

The production of secondary metabolites also is considerably altered by the phosphate level in fermentation media. For decades, phosphate has a deleterious effect on the production of numerous secondary metabolites in *Streptomyces* (40). A high level of inorganic phosphate represses the transcription of secondary metabolite gene clusters and their regulatory genes, leads to inhibition of secondary metabolites production (19,36,40).

Complex interactions among carbon source, nitrogen source, and phosphate regulation were also reported. The PhoP-PhoR system regulates the transcription of nitrogen metabolism-related genes under phosphate scarcity, to reduce the consumption of excessive nitrogen sources (40). Additionally, the phosphofructokinase enzyme of the glycolytic pathway represents the interaction between carbon and phosphate regulation, deletion of phosphofructokinase gene caused the overproduction of secondary metabolite in *S. coelicolor* (41).

1.3.2. The hierarchical regulatory networks

To ensure secondary metabolites are produced in right time and appropriate amount, a streptomycete employs numerous regulatory proteins at the different hierarchical level, some of them respond to physiological and environmental cues. The high-level regulatory proteins or global regulators govern the expression of low-level pathway-specific regulatory genes (sometimes called "cluster-situated regulatory" genes) that directly dictate the expression of secondary metabolite biosynthetic gene clusters (18,19,36). The global regulators or pleiotropic regulators are usually encoded by genes outside of the physically clustered-biosynthetic genes. These regulators regulate at least one secondary metabolite production and/or morphological differentiation (19,36). The global regulators

mostly communicate to pathway-specific regulators in response to environmental or cellular signals through several series of signal transduction cascades to regulate the expression of pathway-specific regulatory genes (18,19,36). Particularly, the two-component system response regulatory systems are present in substantial number in *Streptomyces* genus than that in other genera (42). The two-component histidine-kinase response regulator AbsA in S*treptomyces coelicolor* is the well-characterized higher-level regulators, which controlled the production of several secondary metabolites: calcium-dependent antibiotic (CDA), actinorhodin, undecylprodigiosin, and methylenomycin (43). In addition, serine/threonine kinase signal transduction AfsK/AfsR system is also global regulator that regulates the production of undecylprodigiosin, actinorhodin, and calcium-dependent antibiotic in *Streptomyces coelicolor* A3(2) (44,45).

In contrast, pathway-specific (cluster-situated) regulators regulate the expression of genes from one specific biosynthetic pathway, the genes encoding these regulators are frequently situated in the biosynthetic gene clusters that they regulate (18,19). The transcriptional activators have dominated this type of regulator and they are unequivocally required for secondary metabolites biosynthesis. The pathway-specific regulators in *Streptomyces* are mostly the SARP family (*Streptomyces* antibiotic regulatory proteins) (19,46-48) followed by the LAL family (large ATP-binding LuxR regulators (19,47,48) The SARP family proteins are exclusively present in genus *Streptomyces* (19,46,47) and some of the other genera of actinomycetes (46), typically they have an N-terminal OmpR-type winged helix-turn-helix (HTH) DNA-binding domain (46). This domain binds to heptameric repeats located at -35 promoters region of target genes (46). The LAL family regulators have not been well studied regarding their overall role in regulating the onset of secondary metabolisms (19,47,48). Some regulators

of the LAL family were identified including PikD for pikromycin in *Streptomyces venezuelae* (49), AveR for avermectin in *Streptomyces avermitilis* (50), RapH for rapamycin in *Streptomyces hygroscopicus* (51) and MilR for milbemycin in *Streptomyces bingchenggensis* (52).

1.3.3. The autoregulator signaling molecules and the autoregulatory cascade

Small diffusible signaling molecules play important roles in triggering secondary metabolisms in *Streptomyces*. These signaling molecules (called as autoregulators) are present in minute quantities and usually active at nanomolar concentrations to induce secondary metabolisms and /or morphological development by controlling the DNA-binding activity of cytoplasmic cognate receptor proteins (as reviewed by 21,53,54). They deliver as quorum sensing to initiate secondary metabolites production, and have been regarded as "*Streptomyce*s hormones."

1.3.3.1. Structural classification of autoregulators

Until recently 29 autoregulators have been identified (21,55). Based on their chemical structures, the autoregulators are classified into five groups: three major well-studied group: the γ-butyrolactone types, the furan types, the butenolide types and two little-known group PI factor and N-methylphenylalanyl-dehydrobutyrine diketopiperazine. The γ-butyrolactone signaling molecules are the most widely distributed among streptomycetes. A recent study indicated that 64.1% of *Streptomyces* are predicted to produce γ-butyrolactones (56). At this time, the structure of nineteen γ-butyrolactones from seven *Streptomyces* species showing different features on fatty acid side-chain have been characterized (21,55). The γ-butyrolactones consist of the A-factor

from *S. griseus*; five congeners of virginiae butenolide (VBs A-E), possessing a 6-α-hydroxyl group from *S. virginiae*, Grafe's three factors; possessing a 6-α-hydroxyl group from *S. bikinensis* and *S. cyanofuscatus*; IM-2 possessing the 6-β-hydroxyl group, *S. coelicolor* butanolides (SCBs 1-8) from *S. coelicolor* A3(2); and Factor I from *S. viridochromogenes*.

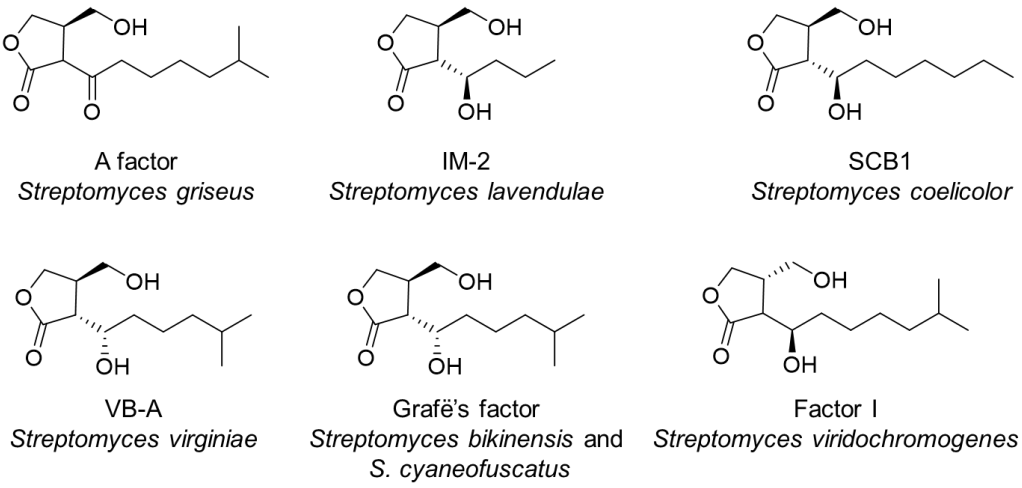

Figure 1.7. Representative of γ-butyrolactone-type autoregulators and their producers

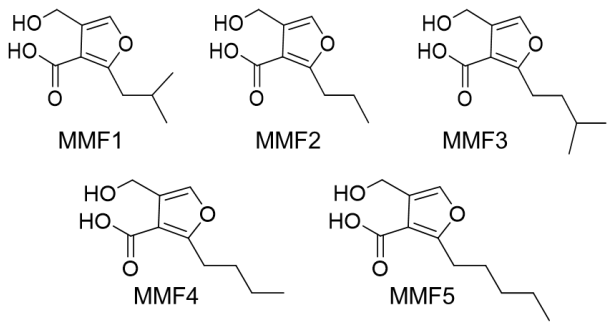

Figure 1.8. The methylenofuran signaling molecules

The methylenofuran (MMF) signaling molecules induce the production of methylenomycin in *Streptomyces coelicolor* A3(2), consist of five distinct methylenofurans, with different side chain lengths of the C2 alkyl group (57).

In comparison to the butyrolactone-type and methylenofuran-type autoregulators,

the butenolide-type autoregulators are relatively new autoregulator signaling molecules. The first butenolide type identified (in 2011) is the avenolide from *Streptomyces avermitilis*, which is essential for avermectin production (58). Two others butenolide, SRB1 and SRB2 are from *Streptomyces rochei*; they induce the production of lankacidin and lankamycin (59).

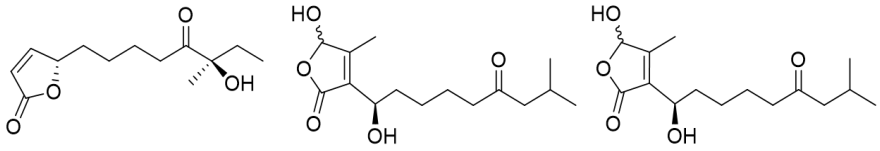

Figure 1.9. Structures of butenolide-type autoregulators and their producers

1.3.3.2. The receptor proteins in autoregulator signaling cascade

The autoregulators produced by *Streptomyces* recognize their specific receptors to initiate the organized-processes for secondary metabolism and/or morphological development (21,53,54). These receptors mostly are repressors belong to TetR transcriptional regulators, the binding of autoregulators to receptors induce the conformational changes and release the receptors from promoter regions (AREs, autoregulator response elements) allowing the expression of target genes (21,53). Which in turn, the regulatory and biosynthetic genes for secondary metabolisms and/or morphological development are coordinately expressed.

The autoregulator receptors and their homologues are widely distributed in genus *Streptomyces* (21, 53). The number may increase due to the increasing number of genome sequences. Many *Streptomyces* have more than one genes encoding autoregulator receptors/receptor homologues (53). Multiple autoregulator receptors establish regulatory cascade in which the main receptor controls other homologues preceding to the ultimate

pathway-specific regulators from SARP or LAL family (19,21,53). Interestingly, more than half of autoregulator receptors are found in the adjacent region of the secondary metabolite gene clusters, which indicates that the autoregulator receptors may possess pathway-specific function (19,53). Several homologues of the autoregulator receptors called "pseudo-autoregulator receptor regulators" are also involved in secondary metabolism, by binding and responding to secondary metabolite signals (60). In contrast to the A-factor type, it seems that most of *Streptomyces* autoregulators only regulate secondary metabolism (61).

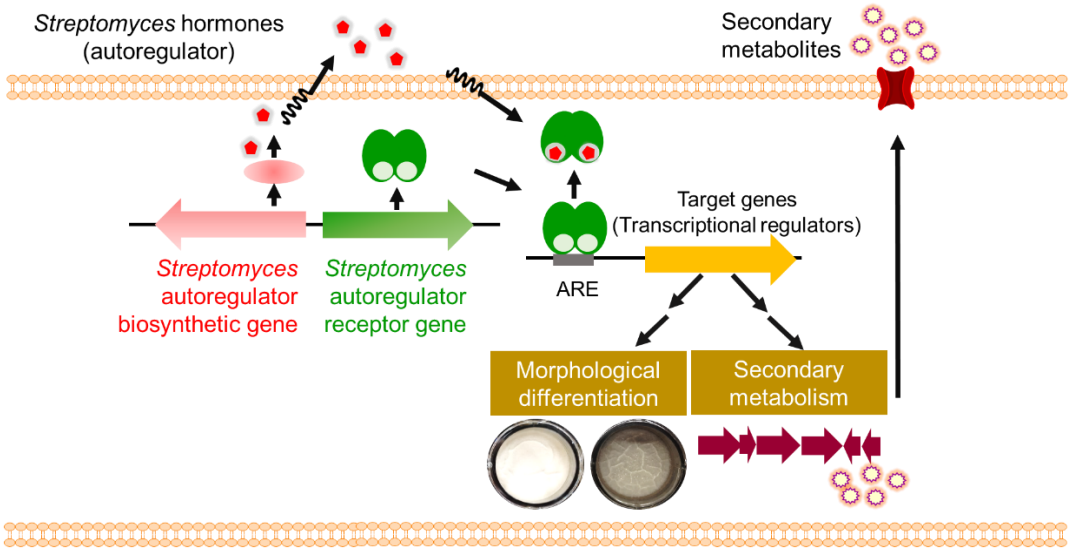

Figure 1.10. The molecular mechanism of autoregulatory signaling cascade

The genes for autoregulators biosynthesis and their receptors are close to each other (21,53). The detailed mechanism of autoregulator signaling cascade involving the autoregulator and its receptor is divergent among *Streptomycetes*. But two features are conserved; autoregulator synthase and receptor protein work as bistable switch in which autoregulator concentration positively correlates with expression of synthase, which in turn alleviates repression of autoregulator synthase gene by receptor protein; the

autoregulator signal detected by receptor proteins is transmitted to hierarchical regulatory cascade/network involving numerous transcriptional regulators (21). Simplification of the autoregulatory cascades is shown in Figure. 1.7. Deletion of autoregulator receptor genes mostly causes the higher production of secondary metabolite production (53), which made these receptors as an interesting target for strain improvement.

1.4. Cryptic secondary metabolisms in *Streptomyces*

The *Streptomyces* genome sequences showed that the gene clusters for production of secondary metabolites are noticeably beyond the number of their known products (23, 62-64). In average 30 distinct secondary metabolite gene clusters from different biosynthetic assembly lines are present in a streptomycete genome (23, 65, 66) (Table 1.2).

Table 1.2. Secondary metabolite biosynthetic gene clusters encoded in streptomycetes genomes (66)

Microorganism	Size (Mb)	NRPS/PKS clusters	Total clusters	% of genome
Streptomyces albus JA1074	6.84	11	24	14.9
Streptomyces toyocaensis A47934	7.34	8	27	10.1
Streptomyces venezuelae	8.23	9	31	12.2
Streptomyces collinus Tü 365	8.27	14	31	16.6
Streptomyces ambofaciens ATTC23877	8.39	10	27	13.2
Streptomyces griseus NBRC 13350	8.55	10	40	13.2
Streptomyces coelicolor A3(2)	8.67	11	27	10.7
Streptomyces hygroscopicus 5008	10.15	17	40	14.5
Streptomyces roseum DSM43201^T	10.34	15	26	11.4
Streptomyces violaceusniger Tu4113	10.66	22	43	21.9
Streptomyces bingchenggensis BCW-1	11.94	30	53	21.7
Streptomyces rapamycinus NRLL 5491	12.70	28	52	24.3

In fact, less 10% of the biosynthetic gene clusters produce adequate amounts of secondary metabolites to be observed by typical fermentation analyses, while most of them required manipulation of cultivation condition or genetic alterations to uncover their products (12, 66-68). Thus, those clusters are called as cryptic, or silent, or orphan pathways (65-68).

1.5 . Strategies for activation of cryptic secondary metabolisms

Since the great number of cryptic secondary metabolite gene clusters potentially produce secondary metabolites with new chemical entities or valuable bioactivities, these cryptic biosynthetic gene clusters need to be activated. For the last few years, several methods have been created to unlock the potential of these cryptic or silent biosynthetic gene clusters (65,67,68)) and also to improve the prediction of their structure based on bioinformatics analysis (69).

1.5.1 Alteration of cultivation conditions

Production of secondary metabolites is tightly correlated with nutritional supply and environmental condition. Exploration of fermentation media had been used as conventional methods to improve the yield of secondary metabolite production. The term "OSMAC (one strain many compounds)" strategy had been invented by Zeeck and co-workers, where the new secondary metabolite production can be triggered by altering cultivation condition (70). The other cultivation condition can be altered including media composition, temperature, salinity, aeration, the shape of the flasks (70).

The OSMAC application for discovery of new compound or new derivative of the

known compound had been fruitful. The cultivation of *Streptomyces* sp. Gö 40/10 using different culture vessels and aeration conditions resulted in the identification of 10 novel secondary metabolites out of 18 isolated metabolites, including butyrolactones, macrolides, cyneromycin, and ansamycins, which originated from different carbon skeletons (71). Similarly, by application of the OSMAC, three chaxalactins, the unusual class of 22-membered macrolactone polyketides were identified from *Streptomyces sp*. C34 (72). The manipulation composition of fermentation media to *S. albus* J1074 had successfully awakened the production of five paulomycin derivatives (73).

Stress responses to environmental factors often result in changes of secondary metabolisms. The addition of rare earth elements (scandium and/or lanthanum) in low concentration to *Streptomyces coelicolor* A3(2) culture improved the production of actinorhodin and induced the biosynthesis of unidentified metabolites (74). The supplementation of nickel ion to the culture medium led to the identification of a novel cyclizidine analogue from *Streptomyces* sp. WU20 by (75). Moreover, the addition of an antimicrobial compound that inhibits fatty acid biosynthesis such as triclosan, activated the production of actinorhodin in *S. coelicolor* (76).

In the natural habitat, *Streptomyces* have to compete against other microorganisms using their secondary metabolites (20), this knowledge preceded the co-cultivation strategy to activate cryptic secondary metabolite. Physical interaction or communication using a chemical signal between cells had been suggested as the key element to enhance the production of secondary metabolites (67,68). Co-cultivation of the mycolic acid producing bacterium *Tsukamurella pulmonis* with *Streptomyces endus* induced the production of the new antibiotic alchivemycin A, whereas co-cultivation of *T. pulmonis* with *S. lividans* activated the unidentified red pigment (77). In addition, *Streptomyces*

species had also been used to alter the metabolic profiles of fungi (67,68).

1.5.2. Ribosome engineering

Introduction of mutations in genes encoding RNA polymerase (RNAP) and ribosomal protein S12 — known as ribosome engineering — had been proven to increase the titer of several secondary metabolites (78-80). Selection of resistant mutant against antibiotics that target the ribosome (streptomycin, gentamycin) and target the RNA polymerase beta subunit (rifamycin) using plates containing antibiotics is easy and no information regarding genome sequence of target microorganism is needed (78). Using this strategy, the production of previously silent piperidamycin A, D, and F in *Streptomyces mauvecolor* had been established (80). Apparently, a mutation at Lys 88 to Glu or Arg in the ribosomal S12 is predicted to increase the protein synthesis in stationary phase (81,82). In turn, the primary metabolisms are altered causing a high production of secondary metabolites (81,82). Whereas a mutation at His437 to Asp or Leu, Tyr, Arg in RNA polymerase triggers secondary metabolite production by imitating the stringent response, which increases the ppGpp production (78,81,83).

Ribosome engineering strategy in combination with deletion of major secondary metabolite gene clusters in *S. coelicolor* A3(2) led to the activation silent cryptic polyketide cluster (*cpk)*, and identification of a novel polyketide alkaloid, coelimycin P1(84).

1.5.3. Alteration of the regulatory networks

The knowledge about the regulatory networks in *Streptomyces* can be applied to activate production of secondary metabolites. Deletion of transcriptional repressors or

overexpression of transcriptional activators are the basic concept for manipulation of regulators to activate secondary metabolite production, regardless they are global or pathway-specific regulators (25,65). Global regulators mostly have a prevalent effect on global transcription patterns (18,19,25), thus the activated-secondary metabolite is rather difficult to predict. But pathway-specific regulators are exclusively related to the cluster(s) where the genes encoding the regulators are located, hence the product may already be anticipated.

The overexpression of global regulators such as AbsA or BldA from *S. coelicolor* A3(2) altered the production of secondary metabolites in the *S. coelicolor* or others *Streptomyces* species. The heterologous expression of *absA* allele activated the cryptic production of pulvomycin in *Streptomyces flavopersicus* (85), whereas the introduction of *bldA* allele to *Streptomyces calvus* enabled the detection of annimycin (86). In A factor autoregulatory signaling cascade, AdpA is a global regulator and a target of autoregulator receptor protein ArpA, in which its expression is triggered by the presence of autoregulators (87). Recently, it was reported that deletion of AdpA in *S. ansochromogenes* activated the oviedomycin production, due to upregulation on the expression of the pathway-specific and biosynthetic gene cluster for oviedomycin (88).

The continuous expression of a pathway-specific transcriptional activator belonging to the Large ATP binding of the LuxR (LAL) family induced the expression of a giant PKS biosynthetic gene cluster, which enables for identification of stambomycins A-D, a unique 51-member glycosylated macrolides in *Streptomyces ambofaciens* (89). Similarly, the production of 6-epi-alteramides by *Streptomyces albus* J1074 was observed by overexpression of LuxR-family transcriptional activator (90). This strategy also worked well with a SARP family transcriptional activator as studied by

Du et al., led to the identification of ishigamide, a novel amide-containing polyene from *Streptomyces* sp. MSC090213JE08 (91). Furthermore, overexpression of LysR transcriptional regulator activated the production of four new glycosylated deferoxamine in marine-derived *Streptomyces albus* PVA94-07 (92).

The deletion of autoregulator receptor homologues, in particular, has been proven successful to activate the silent secondary metabolite gene clusters in the vicinity. For example, the deletion of *alpW* encoding a γ-butyrolactone receptor homologue in a cryptic angucyclin cluster led to the identification of kinamycins in *S. ambofaciens* (93). The deletion of *scbR2* (which encodes a γ-butyrolactone receptor homologue, a repressor in a *cpk* cluster of *S. coelicolor* A3(2) induced the production of yellow pigment and an unidentified new antibiotic (94), whereas in *S. rochei*, an azoxyalkene compound was accumulated by the deletion of the autoregulator receptor homologue *ssrB* and multiple genes for major secondary metabolites (95). The deletion of *jadR2* autoregulator receptor homolog in S. *venezuelae* activated the jadomycin production (60). Moreover, the deletion of *gbnR* encoding a methylenofuran receptor homologue induced the production of a novel family of microbial products (gaburedins) in *S. venezuelae* (96).

These strategies were also readily applied to non-*Streptomyces* actinomycetes *Kitasatospora setae*, the deletion of the *ksbC* gene (which encodes an autoregulator receptor homologue located far from secondary metabolite biosynthetic gene cluster) led to the identification of a new carboline alkaloid, kitasetaline (97,98).

1.5.4. Genome mining and heterologous expressions

Secondary metabolite gene clusters such as polyketide synthetase, non-ribosomal peptide synthetases, usually have conserved protein domain function. With the immense

number of available *Streptomyces* genomic sequences, computing algorithms, and databases for analysis and /or annotation of secondary metabolite gene clusters are unequivocally needed (69). A comprehensive bioinformatic software antiSMASH (antibiotics and Secondary Metabolite Analysis Shell) has been a robust tool for rapid identification of secondary metabolite biosynthetic gene base on genomic sequences assembly (99). Another web-based tool to identify secondary metabolites gene clusters is 2ndFind (http://biosyn.nih.go.jp/2ndfind/) developed by the Japanese scientist, furthermore database and computational tool for polyketide and nonribosomal peptide synthase domain prediction such as PKS/NRPS Analysis Website (http://nrps.igs.umaryland.edu/), NRPSPredictor (http://nrps.informatik.uni-tuebingen.de/), and MIBiG repository (http://mibig.secondarymetabolites.org/) are also useful for identification of the core structure of secondary metabolites.

Thus, genome mining strategies using bioinformatics analysis to isolate the product from a secondary metabolite gene cluster of a microorganism have been a powerful tool to facilitate the activation of cryptic secondary metabolites (100).

The genome mining is usually combined with expression of a gene cluster in a heterologous host for identifying and engineering the corresponding products (65-68). *Streptomyces avermitilis* and *S. coelicolor* were recently engineered to be reliable hosts for heterologous expression by the deletion of their own secondary metabolite biosynthetic gene clusters, which reduced the metabolic competition for the precursor by heterologous metabolites (101-102). Furthermore, transformation-associated recombination (TAR) system and BAC (bacterial artificial chromosome) had been developed to overcome the difficulty of handling large biosynthetic gene clusters (>50 kb) (103).

The heterologous expression has also been used to increase the titer of several known metabolites from different biosynthetic pathways, in which the production in their native hosts is extremely low (101,102,104-106). The heterologous expression strategy had facilitated the identification of the new ansamycin-like compounds chaxamycins A to D from *Streptomyces leeuwenhoekii* (107), several new terpenes from *Streptomyces* spp (108), novel derivatives of complestatin from *Streptomyces chartreusis* AN1542 (109), and novel PKS-NRPS hybrid product of macrolactam pactamides from marine-derived *Streptomyces pactum* SCSIO 02999 (110). With this strategy, a new diol-containing polyketide, lavendiol from *S. lavendulae* FR1-5 had been successfully activated and identified (111).

1.6. *Streptomyces avermitilis*

Streptomyces avermitilis was isolated in 1977 from a soil sample in Ito city, Shizuoka, Japan (112). S. *avermitilis* is the only producer of the polyketide macrolide avermectin (113) and a strong anthelmintic agent that is exceptionally effective against roundworms and arthropod parasites, with low toxicity in humans (114). Avermectins contain eight components (A1a, A1b, A2a, A2b, B1a, B1b, B2a, and B2b), the avermectin B1a component has the strongest anthelmintic activity (112) The ivermectin (22,23-dihydroavermectin B), semisynthetic derivative of avermectin, has been available since the 1980s for veterinary medicine (114) The avermectin under trademark name “Mectizan” also had been a great help to eradicate the lymphatic filariasis and onchocerciasis in developing countries (113,115). The annual sales of ivermectin have been over US$1 billion for the past 20 years (113,115). Furthermore, ivermectin also showed numerous bioactivity against the virus, parasitic insect, and Mycobacterium as reviewed elsewhere

(116).

Table 1.3. Secondary metabolite biosynthetic gene clusters in *S. avermitilis* (104)

No	Genes	Location (nt)	Actual or predicted product[a]
1	*sav76 (ams)*	86,073–87,080	**Avermitilol, avermitilone**
2	*sav100–101*	113,361–118,594	Polyketide
3	*sav257–259*	299,873–303,052	Microcin
4	*sav407–419 (pte)*	486,648–567,017	**Filipin**
5	*sav603–609*	754,376–763,277	Non-ribosomal peptide (siderophore)
6	*sav837–869*	991,134–1,042,269	Non-ribosomal peptide
7	*sav935–953 (ave)*	1,132,045–1,212,960	**Avermectin**
8	*sav1019–1025 (crt)*	1,285,187–1,293,904	**Isorenieratene**
9	*sav1136–1137 (melC)*	1,424,869–1,426,085	**Melanin**
10	*sav1249–1251*	1,549,424–1,554,224	Polyketide–non-ribosomal peptide hybrid
11	*sav1550–1552*	1,893,266–1,912,282	Polyketide
12	*sav1650–1654 (hop)*	2,020,191–2,026,846	**Squalene**
13	*sav2163 (geo)*	2,635,583–2,637,760	**Geosmin, germacradienol**
14	*sav2267–2269*	2,765,027–2,768,005	γ-Butyrolactone ?
15	*sav2277–2282*	2,775,228–2,784,841	Polyketide
16	*sav2367–2369*	2,878,682–2,894,413	Polyketide
17	*sav2372–2388*	2,896,543–2,914,291	Aromatic polyketide
18	*sav2465–2467*	3,007,876–3,012,729	Siderophore
19	*sav2835–2842 (spp)*	3,480,598–3,487,905	**Spore pigment**
20	*sav2890–2903 (olm)*	3,534,525–3,634,592	**Oligomycin**
21	*sav2989–2999 (ptl)*	3,744,875–3,757,141	**Neopentalenoketolactone**
22	*sav3031–3032 (ezs)*	3,788,761–3,791,219	**Albaflavenol (12), albaflavenone**
23	*sav3155–3164*	3,930,088–3,942,062	Non-ribosomal peptide
24	*sav3193–3202*	3,977,231–3,994,940	Non-ribosomal peptide
25	*sav3636–3651*	4,494,250–4,526,990	Non-ribosomal peptide
26	*sav3653–3667*	4,527,901–4,541,568	Aromatic polyketide
27	*sav3704, sav3706*	4,583,057–4,587,741	**Avenolide (autoregulator)**
28	*sav5149 (hpd)*	6,253,610–6,254,755	Ochronotic pigment
29	*sav5269–5274 (sid)*	6,383,181–6,386,774	**Nocardamine , deferrioxamine B**
30	*sav5361–5362*	6,500,109–6,501,345	Melanin
31	*sav5686–5689*	6,877,533–6,881,873	Microcin
32	*sav6395–6398 (ect)*	7,670,236–7,673,431	**Ectoine, 5-hydroxyectoine**
33	*sav6632–6633*	7,931,869–7,937,201	Non-ribosomal peptide
34	*sav7130–7131*	8,490,207–8,492,484	**Tetrahydroxynaphthalene**
35	*sav7161–7165*	8,522,760–8,530,697	Non-ribosomal peptide
36	*sav7184*	8,553,602–8,558,155	Polyketide
37	*sav7320–7323*	8,730,975–8,737,039	Vibrioferrin-like siderophore
38	*sav7360–7362*	8,777,769–8,789,766	Polyketide

[a]Products observed are indicated in bold

The completed nucleotide sequence of ivermectin published in the early 2000s revealed that the linear genome has 9,025,608 base pairs (bp) and encodes 7,582 protein (117). *S. avermitilis* also has two linear plasmids, SAP1 (94,287 kb) and SAP2 (approx. 200 kb) (23, 117). Before the availability of the genome sequences, only avermectin and oligomycin had been identified (104). The genome sequence revealed a total of 38

secondary metabolism biosynthetic gene clusters (63, 104). By genome mining and/or heterologous expression and manipulation of cultivation condition, approx. 22 secondary metabolites had been identified from 16 biosynthetic gene clusters (104). The remaining clusters are still cryptic until nowadays.

In addition, the analysis of *S. avermitilis* genome sequence revealed the presence of clustered putative autoregulatory locus *avaR*, far away from the secondary biosynthetic gene clusters. This locus contains three homologues of autoregulator receptor genes (*avaR1*, *avaR2*, and *avaR3*) together with *aco* and *cyp17* genes encoding a putative acyl-coA ligase and a putative cytochrome p450 monooxygenase for autoregulator biosynthesis (58). The AvaR1 had been established as the receptor for avenolide and regulates the production of avenolide by controlling the expression on *aco* gene (118).

In 2011, the avenolide was identified as new autoregulator signaling molecule or *Streptomyces* hormone for avermectin biosynthesis. Like other autoregulators, avenolide is also effective at nanomolar concentrations to elicit avermectin production (58). In the same year as the discovery of avenolide, the function of the autoregulator receptor homologue AvaR3 was clarified. The AvaR3 is an autoregulator receptor protein having an extended of amino acid residues that are absent in others autoregulator receptors (119). AvaR3 serves as a global regulator that governs secondary metabolites' production and morphological development. Disruption of *avaR3* caused in a remarkable reduction of avermectins, most likely because of the late expression of avermectin biosynthetic genes and an increased production of filipin due to precursor flux. Moreover, the *avaR3* mutant has fragmented mycelia in liquid culture and sporulation defect on solid medium (119).

1.7.Overview and objective of the study

As mentioned above, the deletion of autoregulator receptors or their homologues is an effective strategy to improve the titer of *Streptomyces* secondary metabolites production. The cryptic secondary metabolite biosynthetic gene clusters several of which produce new chemical entities had been activated using this strategy.

In most cases of deregulation of autoregulator signaling cascades, genes that encode the autoregulator receptors or receptor homologues are found adjacent to the target biosynthetic gene clusters, so that the product of the deletion mutant can be readily expected.

In *Streptomyces avermitilis*, the elucidation of the avenolide signaling cascade has just begun, and a similar complicated regulatory network cascades as in the well-known γ-butyrolactones has been observed. However, unlike other autoregulator receptors in *Streptomyces* spp., AvaR3 controls the production of avermectin and filipin, which are encoded by gene clusters approx. 4.0 Mb away from the *avaR* locus. This feature indicated that AvaR3 may also have the capacity to regulate other secondary metabolites (dubbed as cryptic secondary metabolites) whose biosynthetic gene are in the distal region of the *avaR* locus.

The aims of this research were to further assess the effects of the deregulation of AvaR3 on the activation of cryptic secondary metabolite gene clusters in *S. avermitilis*, further extend the regulatory *S. avermitilis* butenolide-system, to connect the activated secondary metabolites with their corresponding biosynthetic gene clusters, and to propose the biosynthetic pathway of the metabolites based on bioinformatics analyses.

Chapter II describes the investigation of the secondary metabolite profile of *avaR3* mutant and provides a detailed characterization of the remarkable peak at 33.9 min which

is observed only in the *avaR3* mutant, resulting in the identification of phthoxazolin A, an inhibitor of cellulose biosynthesis. The bioactivity of phthoxazolin A against oomycetes is also presented. The role of avenolide in the production of phthoxazolin A in *S. avermitilis* is described, suggesting that avenolide represses the production of phthoxazolin A through the function of AvaR3.

Chapter III describes the identification and characterization of phthoxazolin A gene cluster in *S. avermitilis*. The genetic differences between two strains of *S. avermitilis* are highlighted, and the efforts to identify biosynthetic gene clusters are presented. Finally, based on the findings of bioinformatics analyses, the biosynthetic pathway of phthoxazolin A is proposed.

Chapter IV summarizes the results of this thesis and provides conclusions.

Chapter 2

Activation of cryptic phthoxazolin A production in *Streptomyces avermitilis* by the disruption of autoregulator-receptor homologue AvaR3

2.1. Introduction

The sequencing of the massive genome streptomycetes has uncovered the huge collection of predicted secondary metabolite biosynthetic gene clusters which outnumbered the currently characterized natural compounds (23, 62-64). The gene clusters are most likely cryptic biosynthetic pathways since they are not related to any reported natural compound, they either not produce or produce in an extremely low quantity of secondary metabolites under routine fermentation conditions, indicating that many novel and/or functional secondary metabolites encoded in the genome are remaining to be characterized in streptomycetes (65-68). Consequently, these cryptic biosynthetic pathways need to be activated to get new/functional compounds and interesting biosynthetic pathways.

The production of secondary metabolites in *Streptomyces* is regulated by intricate regulatory systems in a ranked way: high-level regulators that react to various environmental and cellular factors stimulate the expression of low-level regulators, which are located within the secondary metabolite biosynthetic gene clusters, whereas the low-level regulators direct the expression of the biosynthetic gene clusters (18,19,36). Autoregulator signaling cascades are the well-known regulatory systems for secondary metabolite production in streptomycetes (19,53). Deregulation of an autoregulator

receptor or pseudoreceptor regulator within the secondary metabolite biosynthetic gene cluster causes the boosting titer of secondary metabolites (53).

The avenolide, a new type of autoregulator (termed as a *Streptomyces* hormone), initiates the production of avermectin, an important drug to treat roundworms and other parasitic infestation (58). The roles of *avaR* locus in the production of avermectin and avenolide had been studied: AvaR1 is an avenolide receptor that regulates the avenolide biosynthesis (118); AvaR3 is an AvaR1 homologue that positively regulates production of avermectin (119); Aco and Cyp17 are avenolide biosynthetic enzymes (58); and whereas the function of AvaR2, a homologue of AvaR1 is remain obscured. The AvaR3 is remarkably interesting since this homologue is the only autoregulator receptor which contains an additional extension of amino acid residues, and has multiple roles in the secondary metabolism and the morphological development (119). In addition, AvaR3 controls the production avermectin and filipin, whose biosynthetic gene are distant from the *avaR* locus, and controls the unknown genes required for the formation of mycelial clumps and aerial mycelia (119). These features guided me to investigate the prospect of the *avaR3* mutant to produce cryptic secondary metabolites whose gene cluster is situated in the region far from *avaR* locus. The activation of cryptic secondary metabolite gene cluster is important to optimize the biosynthetic potential of *Streptomyces avermitilis*.

2.2. Materials and Methods

2.2.1. Bacterial strains, plasmids, and growth conditions

S. avermitilis KA-320 was from the culture collection of the Kitasato Institute, the *avaR3* mutant and the *aco* mutant were from in-house laboratory culture collection as described elsewhere (58,119). The *S. avermitilis* strains are grown on YMS medium

(0.4% of Bacto™ Yeast Extract (Becton and Dickinson, Sparks, MD USA), 1% of malt extract (Becton and Dickinson, Sparks, MD USA), 0.4% of soluble starch and 2% of agar pH 7.5) supplemented with 10 mM of $MgCl_2$ and 10 mM of $CaCl_2$ (YMS-MC medium) for sporulation (119). *Escherichia coli* DH5α was used for general DNA cloning, and *E. coli* F⁻*dcm* Δ(*srl-recA*)*306*::Tn*10* carrying pUB307-*aph*::Tn*7* was obtained from Kitasato Institute and used for *E. coli*/*Streptomyces* intergeneric conjugation. pKU451, pKU479, and pKU250 (Appendix 5) were obtained from Kitasato Institute and used to construct a vector for deletion of the avermectin biosynthetic gene cluster. They were grown in 2x yeast extract-tryptone (YT) (1.6% of Bacto™ Tryptone (Becton and Dickinson, Sparks, MD USA),1% of Bacto™ Yeast Extract, 0.05% of NaCl) and supplemented with chloramphenicol (30 μg/ml) , kanamycin (50 μg/ml) and streptomycin (25 μg/ml) when necessary. The ISP4 agar (Becton and Dickinson, Sparks, MD USA) was used for *E. coli* and *Streptomyces* conjugation.

For analysis of secondary metabolites, the *S. avermitilis* strains were grown in APM medium (4.5% of glucose, 4.5% of peptonized milk (OXOID, Basingstoke, UK), 2.4% of Bacto™ Yeast Extract pH 7.5) (100), in synthetic production medium containing per liter glucose (60 g),$(NH4)_2SO_4$ (2 g), $MgSO_4 \cdot 7H_2O$ (0.1 g), K_2HPO_4 (0.5 g), NaCl (2 g), $FeSO_4 \cdot 7H_2O$ (0.05 g), $ZnSO_4 \cdot 7H_2O$ (0.05 g), $MnSO_4 \cdot 4H_2O$ (0.05 g), $CaCO_3$ (5 g), and Bacto™ Yeast Extract (2 g), pH 7.0 (101), on APM medium supplemented with 1.5% of agar (solid APM), and on yeast extract malt extract dextrin medium (YMD) (0.4% of Bacto™ Yeast Extract, 1% of Bacto™ Malt Extract (Becton and Dickinson, Sparks, MD USA), 0.4% of dextrin, and 2 % of agar pH 7.5). Spores (1.0 X 10^8 CFU) of the *S. avermitilis* strains were inoculated into 70 mL APM medium in a 500-mL baffled flask, and incubated at 28ºC, 160 rpm for 48 hours The mycelia were washed with fresh APM

twice, resuspended in fresh APM medium and stored at -80°C until use as a seed culture. All reagents used in this study were from Wako Pure Chemical Industries (Osaka, Japan), otherwise, they were stated. All the primers are listed in Table 2.1.

Table 2.1. Oligonucleotides used in this study

Primer	Sequence (5' – 3')*
For construction of *ave* mutant	
ave-up-Fw	GCCAGAAAGCTTCTGCTGAACCGCGACTGCCGGGTC
ave-up-Re	GGACTAGTGGTGGTGGTCAGCCCCTGCCGTCCGAC
ave-dw-Fw	GCACTAGTCTCCACCGGCGTATCGACCCCTACACCG
ave-dw-Re	CATAGTAAGCTTCAGTGCCCGTCGCTGTCCCCGTGGC
sav926-tFw	CGTTCGGCGCACAGGTGATGCCGGG
sav954-tRe	CCTACAGTGCCCATGCACACACCGAG
aph-Fw	CTCGAGACTAGTCAGTGAGTTCGAGCGACTCGAGT
aph-Re	CTCGAGACTAGTCTGGTACCGAGCGAACGCGTT
aveR-Fw	TGCTCGAAGAGCACAGCGAGGC
aveR-Re	CCGGTCAATTCTCCTTCCCGCA
aveA1-Fw	CCGTTACCGCCGAGGCTTCTGTC
aveA1-Re	CGCCTGACAGGCCAGATGCAAAG
aveA4-Fw	CAAGCGCGTTACTGCCGATCTC
aveA4-Re	CGCGTAGTCCTGGGACATGAGG
aveB1-Fw	CGCTTCTCCACGATGCAGTCGG
aveB1-Re	GCGTGCAGTGCCTCCATCACAC
aveD-Fw	ACCGGGTCGTGTTCACCCGTGC
aveD-Re	CATAGCCGATGTCCGGCGTCCA
aveBIII-Fw	CGAACGGTACGGAGTCGGAGAG
aveBIII-Re	GCTTCCGCCGCAATACTCATCA
aveBVIII-Fw	ACAGCAGTGCTCCCCTCCACAC
aveBVIII-Re	CCTGCGTGATGAGCAGGTCCAT
aveG-Fw	CGCCTACTTCCACGGTGTTTCC
aveG-Re	CCGGTTGGTAGCGGTACGTCTC

Table 2.1. Continued

Primer	Sequence (5' – 3')*
For semi-quantitative RT- PCR	
avaR3 Fw	TTCCATTTCCCCAGCAAGGCCG
avaR3 Rv	CCCACTCCTGCCATCTGCGGTA
rpoD Fw	ACTCGCTGTCACCGTCCTCAC
rpoD Re	CGCGCCAAGAACCACCTCCT

*Restriction sites are underlined

2.2.2. Analysis of *S. avermitilis* secondary metabolites

The 2.5 mL solid medium in a 12-well plate (Costar^{TM}, Corning Inc, Kennebunk, ME, USA) were inoculated with seed culture, followed by incubation at 28^{o}C for 3 days. Whereas, seed culture also was inoculated on 70 ml liquid medium (in 500-ml baffled flask followed by incubation at 28^{o}C 160 rpm for 3 days. The diced-agar culture or liquid culture were extracted with an equal volume of MeOH. The MeOH-extract was analyzed by Agilent 1200 HPLC-DAD system (Waldbronn, Germany) using a Capcell-Pak C_{18} column (UG 80; 5 µm, 4.6 i. d. x 250 mm; Shiseido, Tokyo, Japan) eluted with a linear gradient system [eluents: H_2O containing trifluoroacetic acid (TFA) 0.01% (A) and MeOH containing TFA 0.075% (B); 0 to 5 min 10% B and 5 to 55 min 10% B to 100% B; flow rate, 1 mL/min.

Production of phthoxazolin A was analysed using HPLC system described above and UV detection at 275 nm was chosen for phthoxazolin A analysis and the authentic sample of phthoxazolin A was used to quantify the amount of phthoxazolin A.

Avermectins in MeOH-extract was analyzed by Hitachi La Chrom 7300 HPLC system (Tokyo, Japan) on reversed-phase Mightysil RP-18GP column (4.6 by 250 mm;

Kanto Chemical, Tokyo, Japan) with solvent (MeOH:CH_3CN:H_2O=18:62:20) and detection at 246 nm (50). The authentic sample of avermectins was used to quantify the amount of avermectins.

2.2.3. Isolation and structural elucidation of phthoxazolin A (1)

The YMD medium was inoculated with seed culture and incubated for 4 days at 28°C. The 5 L of *avaR3* mutant culture in YMD medium was cut into cubes and extracted with twice volumes of ethyl acetate, after which the ethyl-acetate layer was evaporated to dryness. The crude extract (3.78 g) was applied to reversed-phase open column chromatography using a COSMOSIL 140 C18-OPN column (Nacalai Tesque, Kyoto, Japan) with a MeOH-H_2O step gradient system (20%, 40%, 50%, 80%, 100% v/v). The 50% MeOH fraction was evaporated to dryness to give 92.4 mg of yellow-brownish oil. The last step purification was completed by preparative reversed-phase HPLC (JASCO, Tokyo, Japan) using an XTerra RP18 column (5 μm; 10 i. d. x 150 mm; Waters, MA, USA) with 25% CH_3CN at 3 mL/min and detection at 275 nm to get 5.5 mg of pure compound as a pale yellow oil.

The UV spectra were obtained from a Hitachi U-3210 spectrophotometer (Tokyo, Japan) and IR spectra were recorded on an FTIR-8400S spectrometer (Shimadzu, Kyoto, Japan). Measurement of optical rotation was accomplished on a P-1020 polarimeter (JASCO, Tokyo, Japan). HRCIMS was measured on JEOL JMS-700 spectrometer (Tokyo, Japan). The Varian Inova 600 MHz NMR system (Palo Alto, CA, USA) was used to record the NMR spectra (^{1}H, 600 MHz; ^{13}C, 150 MHz) and the solvent signal ([MeOH]-d_4:δ_C 49.1, δ_H 3.31; [chloroform]-d:δ_H 7.24) were used as reference signal to the ^{1}H and ^{13}C chemical shifts.

2.2.4. Physico-chemical properties of phthoxazolin A (1)

Pale yellow oil; UV (MeOH) λ_{max} (log ε): 204 (3.94), 265 (4.14), 275 (4.21), 285 (4.11), 331 (3.01) nm; IR (film) ν_{max} 3371, 2935, 1658, 1653, 1511 cm^{-1}; $[\alpha]^{25}_{D}$ +15.7 (*c* 0.18, CH_2Cl_2); HRCIMS *m/z* 291.1684 $[M + H]^+$ (calculated for $C_{16}H_{23}N_2O_3$, 291.1709); ^1H and ^{13}C NMR data, see Table 2.2.

2.2.5. Biological assays

2.2.5.1. Anti-oomycetes assay

The biological activity of phthoxazolin A was evaluated in agar diffusion susceptibility testing against *Aphanomyces cochlioides* Cel1 and *Phytophthora sojae* P6497. *Aphanomyces cochlioides* Cel1 was obtained from the NARO Gene Bank in Tsukuba, Japan (stock number MAFF305845) (120). *A. cochlioides* cultured for 3 days on a Corn Meal Agar (Becton and Dickinson, Sparks, MD USA) plate containing 0.4% (w/v) Bacto™ Yeast Extract (Becton and Dickinson, Sparks, MD USA) and 50 mM phosphate buffer (pH 6.6) at 25°C in the dark. The *Phytophthora sojae* P6497 were grown at 25ºC on V8-agar (20% of V-8 vegetable juice (Campbell's Soup Company, NJ, USA), 2% of $CaCO_3$, 1.8% of agar).

The active growing mycelia of *P. sojae* and *A. cochlioides* were punched using sterile cork borer (8.0 mm in diameter) to obtain mycelial plugs, these plugs were placed on new medium and was incubated at 25ºC for 3-5 days until the diameter of mycelial lawn reached approximately 2 cm. For agar diffusion susceptibility test, several amounts of phthoxazolin A were loaded on the sterile paper disks (φ = 9.0 mm; Advantec, Japan) and placed around 3 cm apart from the edge of indicator strain. The inhibitory activity was measured after incubation at 25ºC for 2-5 days.

2.2.5.2. Antibacterial assay and anti-yeast assay

Bioactivity of phthoxazolin A was evaluated against *Bacillus subtilis* PCI 219, *Escherichia coli* ATCC 25922 and *Saccharomyces cerevisiae* ATCC 9804 using agar diffusion susceptibility test. *B. subtilis* was grown in 3 ml of liquid medium containing Bacto™ Casitone (Becton and Dickinson, Sparks, MD USA) 0,5% and Bacto™ Beef Extract (Becton and Dickinson, Sparks, MD USA) 0.3% PH 6.5 for overnight at 30ºC 120 spm. A portion of this pre-culture (2%) was inoculated to the solid medium with the same composition as described above with addition 1.5% of agar. For agar diffusion susceptibility test, several amounts of phthoxazolin A were loaded on the sterile paper disks (φ = 9.0 mm; Advantec, Japan) and placed on the solid media which had been inoculated with *B. subtilis*. Incubation was performed at 30ºC for 16 hours. Bioactivity was determined by the presence of clear zone inhibition.

Meanwhile, *Escherichia coli* was inoculated into Luria-Bertani (LB) liquid medium containing Bacto™ Tryptone (Becton and Dickinson, Sparks, MD USA) 1%, Bacto™ Yeast Extract (Becton and Dickinson, Sparks, MD USA) 0.5% NaCl 1% pH 7.0 or LB agar (LB liquid medium supplemented with 1.5% agar) for bioassay at 37ºC with the similar procedure as for *B. subtilis*. Furthermore, *S. cerevisiae* was inoculated into Yeast Peptone Dextrose (YPD) medium containing Bacto™ Yeast Extract 1%, Bacto™ Peptone (Becton and Dickinson, Sparks, MD USA) 2% and dextrose 2% and YPD agar (YPD supplemented with agar 1.5%) at 30ºC followed with agar diffusion method as described above.

2.2.5.3. Antifungal activity

Antifungal activity of phthoxazolin A was evaluated against *Aspergillus oryzae*

RIB40 using agar diffusion assay as described by Espinel-Ingroff with some modifications (121). The surface of Muller Hinton Agar (Becton and Dickinson, Sparks, MD, USA) was inoculated with spore suspension (OD600 nm = 0.09 – 0.017) of *A. oryzae* using a sterile cotton swab. The media were allowed to dry for 30 minutes in the clean bench before application of paper disks impregnated with phthoxazolin A. The plates were further incubated at 35ºC for 24-48 hours. Bioactivity was determined by the presence of clear zone inhibition.

2.2.5.4. Anti- *Ralstonia* activity

Phthoxazolin A was evaluated using *Ralstonia solanacearum* RS1000 (which is isogenic to MAFF7301030) (122). *R. solanacearum* was maintained with Kelman's yeast extract agar medium (Bacto™ Pepton (Becton and Dickinson, Sparks, MD USA) 1%, Casamino Acids (Becton and Dickinson, Sparks, MD USA) 0.1%, glucose 0.5%, Bacto™ Yeast Extract 0.5%, Bacto™ Agar (Becton and Dickinson, Sparks, MD USA) 1.5%), supplemented with tetrazolium chloride 50 ug /ml (123) and nalidixic acid 30 ug/ml, followed by incubation at 30ºC for 24-48 hours. A single colony from this plate was transferred into 3 ml of Kelman's yeast extract liquid medium and incubated at 30ºC for overnight 120 spm. A portion of this pre-culture (1%) was inoculated into 50 ml of Kelman's yeast extract liquid medium (main culture), followed by incubation at 30ºC for overnight 120 spm.

After incubation, cells from the main cultivation was harvested by centrifugation and washed with sterile water twice. The pellet was resuspended in sterile water to give OD600nm =2,0 (124). A 250 µl of cell suspension was mixed with 25 ml of Kelman's yeast extract agar medium for agar diffusion susceptibility test (124) as described above,

with incubation at 30^{o}C for 24 hours.

2.2.5.5. Anti-mycobacterial activity

The anti-mycobacterial assay was performed by colorimetric assay using 3-(4, 5-dimethylthiazol-2-yl)-2, 5-diphenyltetrazolium bromide (MTT) method (125) with *Mycobacterium smegmatis* mc2155 and *Mycobacterium bovis* Bacille de Calmette et Guérin (BCG) Pasteur as indicator strains. The *M. smegmatis* was maintained in Middlebrook 7H9 medium (Becton and Dickinson, Sparks, MD, USA), supplemented with 0.2% glycerol, 0.04% NaCl, 0.2% glucose and 0.05% Tween80, at 37^{o}C 95 rpm, for 36 hours. Whereas, the *M. bovis* BCG was maintained in Middlebrook 7H9 supplemented with 0.2% glycerol, 10% OADC (Becton and Dickinson, Sparks, MD, USA) and 0.05%Tween80 at 37^{o}C 95 rpm for 1 week.

The *Mycobacterium* culture broth was diluted to get a concentration of 1x10^{5} CFU/ml for *M. smegmatis*, and 1x10^{6} CFU/ml for M. bovis BCG. Both diluted cultures were inoculated into 96-well plate, and then a serially diluted sample was added to the 96-well plate, isoniazid was used as positive control. The bacteria were incubated at 37 °C for 36 hours (for *M. smegmatis)* or for 7 days (for *M. bovis* BCG Pasteur). After incubation, 10 µl of MTT (Sigma-Aldrich, St Louis MO, USA) solution (5 mg/ml) was added into each well and incubated at 37 °C for additional 12 h-24 hours. After incubation 50 µl of sodium dodecyl sulfate-dimethylformamide (SDS-DMF) was added to each well and mixed. The optical density at 560 nm was measured to determine MIC value. The MIC value was expressed as the lowest concentration that inhibited visible growth of organisms on the well plate after incubation.

2.2.6. Deletion of the avermectin biosynthetic gene cluster

A fragment upstream (1,116,642-1,118,780 nt) of the avermectin biosynthetic gene cluster (*sav935-sav953*) (*ave*) was PCR-amplified by the ave-up-Fw/ave-up-Re primer pair, and a fragment downstream of *ave* (1,211,842 -1,213,686 nt) was PCR-amplified by the ave-down-Fw/ave-down-Re primer pair. These fragments were cleaved by *Hind*III and *Spe*I and cloned into the *Hind*III site of pKU451. The subsequent plasmid was cleaved with *Spe*I and connected with a kanamycin-resistant (*aphII*) fragment derived from PCR-amplification of pKU479 with the aph-Fw/aph-Re primer pair, to create pLT138. The pLT139 was constructed by ligation of a 5.7 kb *HindIII* fragment obtained from pLT138 with pKU250 at the HindIII site. This pLT139 was put into *E. coli F-dcm* Δ(*srl-recA*)306::*Tn10* carrying pUB307-*aph::Tn7* (the donor *E. coli*) by electroporation and further used for conjugation with *S. avermitilis*.

The donor *E. coli* containing pLT139 was grown in 3 ml liquid 2xYT at 37º C, 140 spm for approximately 2 hours until the optical density at 600nm (OD_{600}) = 0.1, the culture was centrifuged and the cells were washed twice with fresh 2xYT, and resuspended in 110 μl of 2xYT. The spores of *S. avermitilis* recipient (10^{-9} CFU) were mixed with the donor *E.coli* cells in ratio 1:10 and 1:100 (v/v) and spread into ISP4 agar plates. After incubation at 28ºC for 18 hours, each plate was overlaid using 1 ml sterile water containing 250 μg of kanamycin and 250 μg of nalidixic acid, and the incubation was continued at 28ºC for 3 days. The *ave* biosynthetic gene cluster was substituted with the disrupted allele by a homologous recombination event. The candidate strains for the *ave*-deletion mutant were verified the genotype by PCR analysis using aveR, aveA1, aveA4, aveB1, aveD, aveBIII, aveBVIII, AveG primer pairs and followed by DNA sequencing. The *S. avermitilis ave*-deletion mutant was termed as Δ*ave*.

2.2.7. Transcription analysis of *avaR3* gene

A portion of the mycelia harvested from 70 ml of synthetic media at 28ºC at the indicated cultivation times was used for RNA extraction by an RNeasy Mini Kit (QIAGEN Sciences, Germantown, MD, USA) and 23 μg of RNA were further treated with 20 unit of DNase I (Takara Bio. Inc, Shiga, Japan) at 37ºC for 1 hour. The complementary DNA was synthesized using SuperScript III RNase H-reverse transcriptase (Invitrogen, Carlsbad, CA, USA) and random primers (Invitrogen) from 2 μg of RNA-treated DNAse as a template. The amplification of the *avaR3* and *rpoD* genes transcription was performed by PCR using GoTaq Green Master Mix (Promega, Madison, WI, USA) under condition 97ºC for 3 min, followed by discrete cycle at 97ºC for 30s, 60ºC for 30s, and 72ºC for 1 min. The absence of DNA impurity was confirmed by RT-PCR without reverse transcriptase.

2.3. Results

2.3.1. Secondary metabolites analysis of Δ *avaR3* mutant

To examine the possibility of AvaR3 affects the production of other secondary metabolites, the metabolite profiles of the *avaR3* mutant were analyzed by HPLC with a diode array detector. The metabolite profiles between the wild-type strain and the *avaR3* mutant are almost identical when they cultivated in media for avermectin production (liquid APM medium or solid APM medium) (Figure 2.1).

One noticeable large peak (33.9 min) was observed only in culture of the *avaR3* mutant grown on YMD medium (Figure 2.2) and synthetic production medium (Figure 2.3), indicating that AvaR3 represses the production of an uncharacterized compound which was eluted at 33.9 min, in addition to AvaR3 function in controlling the production of avermectin/filipin

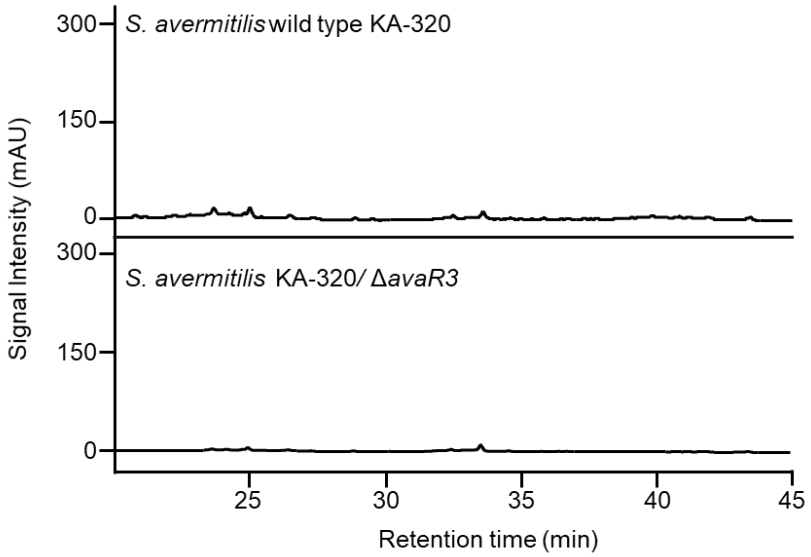

Figure 2.1. HPLC analysis of MeOH extracts from the wild-type strain (WT) and the *avaR3* mutant (Δ*avaR3*) cultivated in APM medium. mAU, milliabsorbance units at 275 nm.

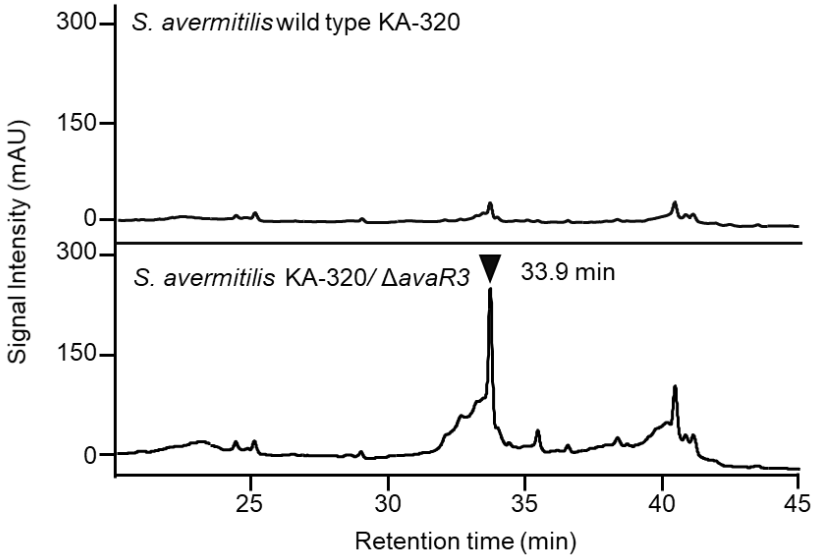

Figure 2.2. HPLC analysis of MeOH extracts from the wild-type strain (WT) and the *avaR3* mutant (Δ*avaR3*) cultivated in YMD medium. mAU, milliabsorbance units at 275 nm. The peak of phthoxazolin A is indicated by a black inverted triangle.

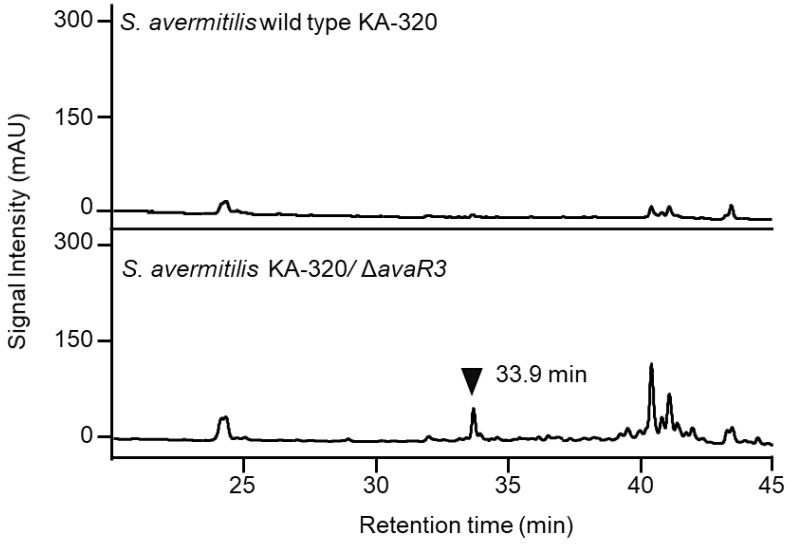

Figure 2.3. HPLC analysis of MeOH extracts from the wild-type strain (WT) and the *avaR3* mutant (Δ*avaR3*) cultivated in synthetic production medium. mAU, milliabsorbance units at 275 nm. The peak of phthoxazolin A is indicated by a black inverted triangle.

2.3.2. Isolation and structure elucidation of phthoxazolin A (1) from the Δ*avaR3* mutant

To elucidate the structure of the emerging peak, the ethyl acetate crude extract from the 5 L of YMD agar culture of the Δ*avaR3* mutant was subjected to an ODS open column chromatography and preparative HPLC purification. These purification procedures yielded 5.5 mg of the pure compound **1** which its purity was confirmed by HPLC as shown in Figure 2.4.

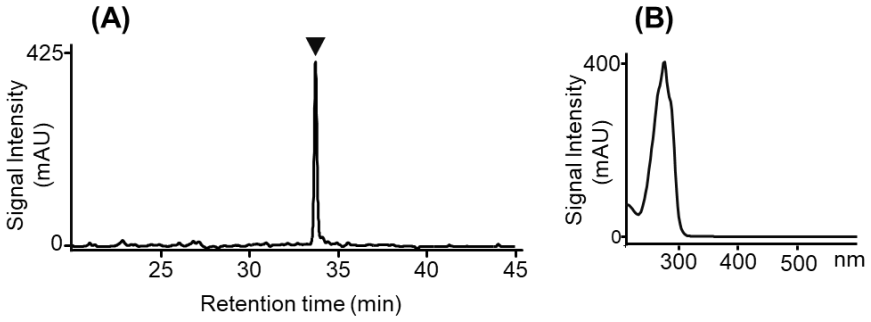

Figure 2.4. (A) HPLC chromatograms of purified phthoxazolin A (1), (B) UV spectrum of purified phthoxazolin A. mAU, milliabsorbance units at 275 nm. The peak of phthoxazolin A is indicated as a black inverted triangle.

The HRCIMS measurement (positive ion mode) exhibited a molecular ion peak at *m*/*z* 291.1684 $[M + H]^+$ (calculated for $C_{16}H_{23}N_2O_3$, 291.1709) accordingly, the molecular formula was determined to be $C_{16}H_{22}N_2O_3$. Compound (**1**) has a UV absorption maximum at 275 nm with two shoulders at 265 and 285 nm (as described in physicochemical properties in Material and Methods), indicating that conjugated triene moiety are present in the structure.

The structure of compound **1** was deduced by NMR spectra (Table 2.2). The ^{1}H-^{1}H COSY correlations showed the coupling among close aliphatic methine protons (H-5 to H-9) and methylene protons (H2-10), signifying the presence of the triene moiety, which well corresponded with the UV spectrum observation.

In contrast, the HMBC signals showed correlations from two methyl protons (H_3-2-CH_3) linked to C-2 (δ_C 46.6), to a carbonyl carbon C-1 (δ_C 183.3) and a hydroxy methine C-3 (δ_C 75.5) indicated the partial structure (C-1-C-2-C-3 with 2-CH_3) (Figure 2.5).

Table 2.2. NMR spectroscopic data of **1** in methanol-d_4.

Position	δ_H (mult, *J* in Hz)	δ_C	HMBC[a]
1		183.3	
2		46.6	
2-Me	1.06 (s)	22.0	1, 2, 2-Me, 3
2-Me	1.27 (s)	26.4	1, 2, 2-Me, 3
3	4.71 (s)	75.5	1, 2, 2-Me, 3, 4,
4		140.1	
4-Me	1.85 (s)	20.0	3, 4, 5, 7
5	6.47 (d, 12.6)	125.7	3, 4-Me, 6, 7
6	6.30 (t, 11.4)	129.2	4, 8, 9
7	5.97 (t, 11.4)	129.0	8
8	6.73 (dd,15.0, 12.6)	129.5	10
9	5.80 (dt,15.0, 7.2)	129.7	7, 10, 11
10	3.57 (d, 7.2)	29.6	8, 11, 12
11		153.1	
12	6.86 (s)	122.7	10, 13
13	8.10 (s)	152.8	11, 12

[a] HMBC correlations are from proton(s) to the indicated carbon.

The methyl proton (H_3-4-CH_3) linked to an aliphatic methine carbon C-4 (δ_C140.1) displayed HMBC correlations to C-3 and an aliphatic carbon C-5 (δ_C 125.7), whereas the methine proton at C-3 connected to the C-5 carbon, indicating an association between the triene group and C-1-C-2-C-3 with 2-CH_3 through the aliphatic carbon C-4. The presence of a primary amide was indicated by IR absorption bands (Appendix 4) of compound **1** in the carbamoyl group (1,653 and 1,658 cm^{-1}), implying that the carbonyl group at carbon

C-1 was attached to an amide group. The monosubstituted oxazole group was deduced from one quaternary carbon (C-11) which was coupled to an aliphatic carbon C-10 (δ_C 29.6) and two methine carbons (C-12 and C-13), based on the HMBC signals from H-10 to C-11 and C-12. A hydroxy absorption at 3,371 cm^{-1} was observed by IR spectrum of compound **1** (Appendix 4) and a hydroxyl group was proposed to be coupled to the hydroxy methine carbon C-3.

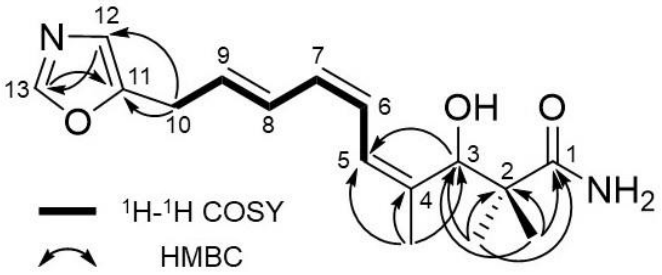

Figure 2.5. ^1H-^1H COSY and key HMBC correlations of phthoxazolin A (**1**)

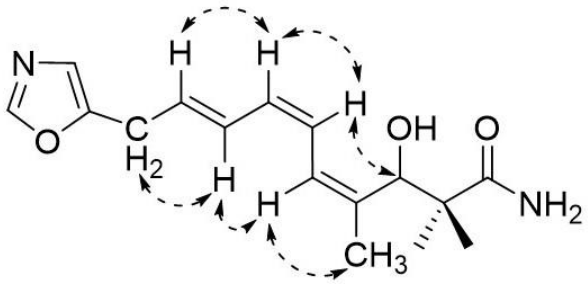

Figure 2.6. Key NOESY correlations of phthoxazolin A (**1**)

Based on the vicinal coupling constants ($J_{6,7}$ = 11.4 Hz and $J_{8,9}$ = 15.0 Hz) (Table 2.2) and NOESY correlations for H-3/H-6 and H3-4-CH3/H-5 (Figure 2.6), the conformation of the conjugated triene moiety was designated as 6*Z*, 8*E*, and 4*Z* respectively. Consequently, the one dimensional structure of compound **1** was deduced as (4*Z*,6*Z*,8*E*)-3-hydroxy-2,2,4-trimethyl-10-(oxazol-5-yl)deca-4,6,8-trienamide.

To evaluate the absolute configuration of compound **1** at C-3, the optical rotation of compound **1** was determined, and indicating that the $[\alpha]_D$ value of compound **1** was positive. Similarly, phthoxazolin A and inthomycin also have the positive $[\alpha]_D$ value; {$[\alpha]^{21}_D$ +37.4 (*c* 1.0, $CHCl_3$)}, {$[\alpha]^{20}_D$ +28.7 (*c* 1.40, CH_2Cl_2) } for inthomycin A and phthoxazolin A respectively, showing the R the configuration at C-3 (126, 127).

Table 2.3. ^{1}H NMR data of **1** and phthoxazolin A in $CDCl_3$.

Position	**1**	**Phthoxazolin A**[a]
	δ_H (mult, *J* in Hz)	**δ_H (mult, *J* in Hz)**
1-NH_2	5.50 (br s), 6.23 (br s)	5.70 (br s), 6.33 (br s)
2	-	-
2-Me	1.08 (s)	1.08 (s)
2-Me	1.32 (s)	1.35 (s)
3	4.63 (d, 5.6)	4.64 (d, 5.8)
3-OH	4.03 (d, 5.6)	4.02 (d,5.8)
4-Me	1.83 (s)	1.84 (s)
5	6.41(d, 12.0)	6.41 (d,11.5)
6	6.18 (t, 11.4)	6.10 (dd, 11.5, 11.5)
7	5.94 (t, 11.1)	5.95 (dd, 11.5, 11.5)
8	6.63 (dd, 15.3, 11.7)	6.64 (dd, 15.0, 11.5)
9	5.77(dt, 15.0, 7.2)	5.77(dt,15.0, 7.0)
10	3.50 (d,7.0)	3.51 (d,7.0)
11	-	-
12	6.79 (s)	6.80 (s)
13	7.78 (s)	7.79 (s)

[a] Data from Tanaka *et al.* (128)

The compound **1** has the absolute configuration of 3*R* since the positive value of [α]D which is similar to inthomycin A/phthoxazolin A. The ^{1}H-NMR analysis of compound **1** in $CDCl_3$ showed reasonably identical spectrum to that of phthoxazolin A (Table 2.3), and thus I considered that compound **1** was phthoxazolin A/inthomycin A.

2.3.4. The biological activity of phthoxazolin A (1).

Phthoxazolin A has been reported to have a cellulose synthesis inhibitor activity (128-130). In this research phthoxazolin A (**1)**, showed effective inhibitory activity against plant pathogenic oomycetes from the different taxonomic order; *P. sojae* with a MIC value of 5 µg disk^{-1} (Figure 2.7A) and *A. cochlioides* with a MIC value of 3.1 µg disk^{-1} (Figure 2.7B).

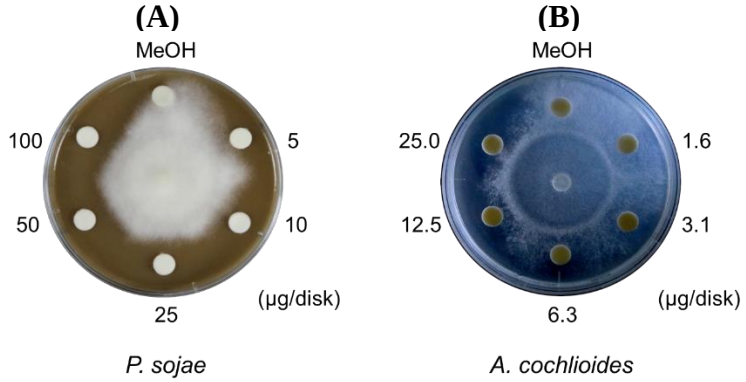

Figure 2.7. Disk diffusion assays of phthoxazolin A against *P. sojae* (A) and *A. cochlioides* (B). Methanol was used as a negative control. Inhibitory activity was observed after incubation at 25^{o}C for 4 days *P. sojae* and for 7 days *A. cochlioides*, and the plates were photographed from the top.

Even though phthoxazolin A showed growth-inhibitory activity against a broad range of plant pathogenic oomycetes, phthoxazolin A was deficient of growth-inhibitory activity against *A. oryzae*, *B. subtilis*, *E. coli*, *R. solanacearum*, and *Saccharomyces cerevisiae* at the 500 µg/disk level, and *M. smegmatis* and *M. bovis* BCG up to at least 50 µM.

2.3.5. Regulation of phthoxazolin A production by *Streptomyces* hormone

The *avaR3* mutant displayed 79% decreasing production of avermectin in the liquid APM medium (119), with no detectable production of phthoxazolin A (**1**). Whereas, the *aco* mutant which was deficient of avenolide production also displayed low production of avermectin by 94% in the liquid APM medium (58). To confirm the response of *S. avermitilis* in the YMD medium, from which phthoxazolin A (**1**) was isolated, the *avaR3* mutant and the *aco* mutant were cultivated in the YMD medium and the production of avermectin was evaluated.

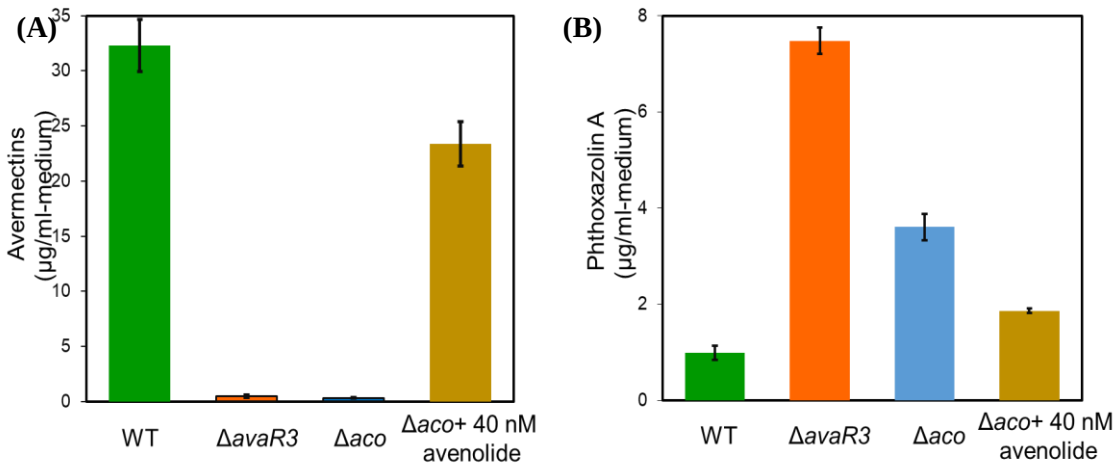

Figure 2.8. Production of avermectin (A) and phthoxazolin A (B). Δ*avaR3*, *avaR3* mutant; Δ*aco*, *aco* mutant. Synthetic avenolide was added to the YMD medium at 40 nM concentration. Data shown represent mean +/- standard error of triplicate experiments.

The production of avermectin reduced to only 2% and 1% of that by the wild-type strain, respectively (Figure 2.6A), suggesting that the *avaR3* and *aco* mutants displayed a serious defect in the production of avermectin. These results implied that the avenolide may regulate the production of avermectin and phthoxazolin A (**1**).

The *aco* mutant and the *avaR3* mutant produced phthoxazolin A around 3.6-fold and 7.6-fold of that by the wild-type strain, respectively (Figure 2. 6B). Furthermore,

supplementation of avenolide to the *aco* mutant resumed the production of phthoxazolin A (**1**) to that of the wild-type and enhanced production of avermectin to 72% of that in the wild-type strain. These results signified that avenolide has the capacity to not only triggers production of avermectin but also suppresses the production of phthoxazolin A.

2.3.6. Production of phthoxazolin A (1) in the avermectin non-producer mutant

The use of excess precursors from the avermectin assembly line is favourable and can provoke the superior production of phthoxazolin A (1) in the low-avermectin producers (*avaR3* and *aco* mutants) since the phthoxazolin A and avermectin are derived from the polyketide synthase assembly line. I assessed the production of phthoxazolin A in the avermectin-deficient mutant (Δ*ave*) (Figure 2.7) to investigate the possibility that precursor preference might account for the elevated production of phthoxazolin A in both mutants. The production of avermectin from Δ*ave* mutant on the YMD medium was abolished and production of phthoxazolin A showed a slight increase (1.5-fold relative to the wild-type strain) (Figure 2.8).

The disruption of the avermectin pathway merely acted a small role in the enhancement of phthoxazolin A (**1**) in comparison to that examined in the *avaR3* mutant (7.6-fold) and *aco* mutants (3.6-fold) (Figure 2.6B). This result indicated that the excess precursor from the low production of avermectin provides only partially to the enhancement of the phthoxazolin A (**1**). Consequently, the superior phthoxazolin A production (**1**) in the *avaR3* mutant can be assigned to the regulatory function of AvaR3, rather than an effect of the low production of avermectin.

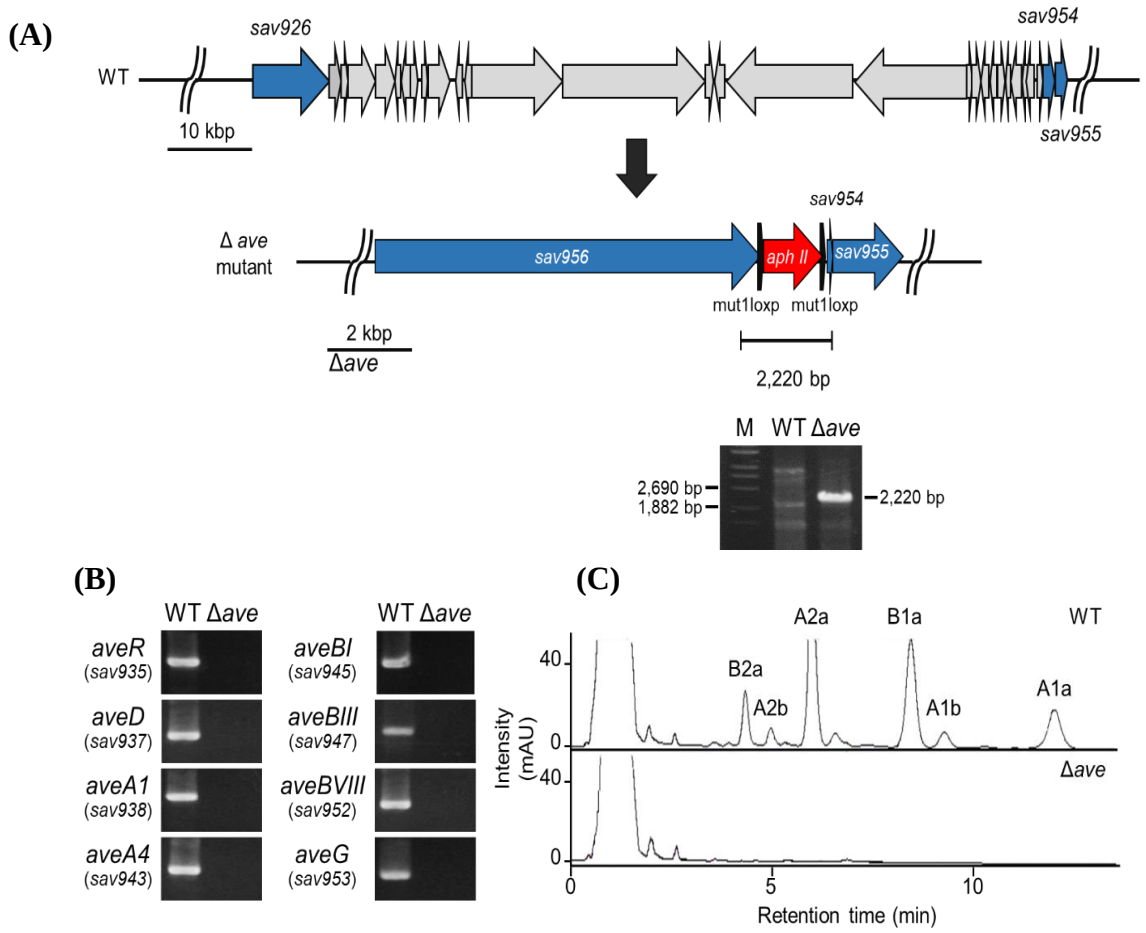

Figure 2.9. *Streptomyces avermitilis ave*-deletion mutant. (A) Graphic representation for the genotype of the *ave*-deletion mutant. With the primer pair sav926-tFw/sav954-tRe, a fragment (2,220 bp) containing the mut1loxP-*aphII*-mut1loxP cassette was amplified with PCR. (B) PCR analysis to confirm the *ave*-deletion. Internal fragments of the individual *ave* genes were detected by PCR using the primer described in Material and Methods. (C) HPLC chromatograms of avermectin production in the *ave*-deletion mutant. mAU, milliabsorbance units at 246 nm. Peaks eluted at 4.5, 5.2, 6.2, 8.7, 9.5, and 12.3 min are avermectin (AVM) derivatives, such as AVM B2a, AVM A2b, AVM A2a, AVM B1a, AVM A1b, and AVM A1a, respectively.

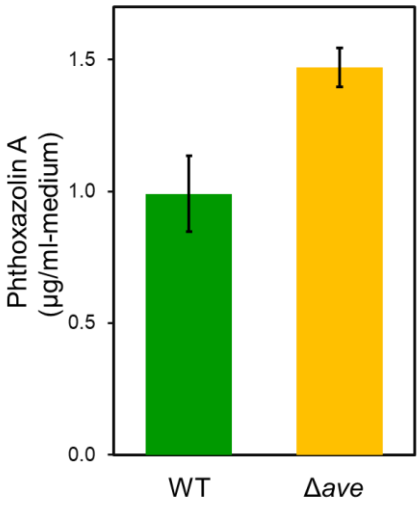

Figure 2.10. Production of phthoxazolin A (**1**) WT (A) and the avermectin non-producer mutant (B). WT, wild-type strain. Data shown represent mean +/- standard error of triplicate experiments.

2.3.7. Transcriptional analysis of *avaR3* in Δ*aco* mutant.

The *avaR3* transcript level in the *aco* mutant cultivated in synthetic production medium was lower than that in the wild-type strain. This transcriptional pattern with the dropped production of phthoxazolin A was resumed to that of the wild-type strain by the supplementation of avenolide (Figure 2.9), suggesting that the boost of phthoxazolin A production in *aco* mutant was due to the low expression of *avaR3*.

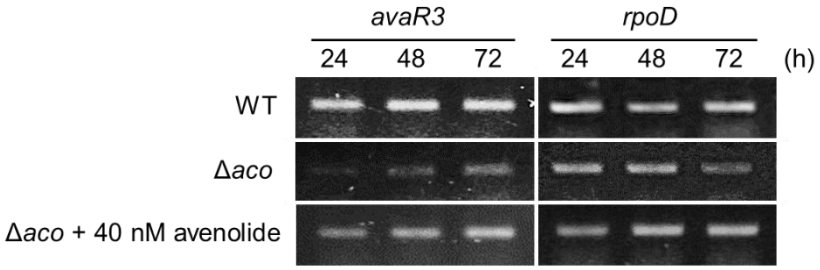

Figure 2.11. Gene expression analysis of the *avaR3* gene by RT-PCR. Total RNAs were prepared from mycelium at the indicated times. The *rpoD* gene was used as an internal control.

2.4. Discussion

The abundance of biosynthetic pathways for new secondary metabolites showing notable biological activities was observed in the genome of actinomycetes. Most of those pathways had been indicated as cryptic biosynthetic pathways, due to poor expression during cultivation. In this study, I have shown that deletion of AvaR3, an autoregulator homologue in *S. avermitilis* led to the exceptionally increasing production of cryptic phthoxazolin A.

The deletion of a transcriptional regulator situated in cryptic gene cluster had enabled the production of an adequate quantity of compound for structure elucidation (89, 93 94). Nevertheless, the adjacent region of the *avaR3*/*aco* locus (*sav3703*/*sav3706*) has plausible gene cluster for aromatic polyketide (*sav3653*-*sav3667*) and ochronotic pigment (*sav5149*), which seem to have different module organization than that for the biosynthesis of phthoxazolin A. This signifies that AvaR3 controls the expression of gene cluster required for a phthoxazolin A biosynthetic which is situated at a far position. This is the first report in *Streptomyces*, in which the alteration of an autoregulator receptor homologue in a far position leads to the activation of cryptic secondary metabolism. Numerous genes encoding autoregulator receptor homologues are present in the actinomycetes genomes. Consequently, genetic alteration of an autoregulator receptor or its homologue is a valuable strategy for acquiring new secondary metabolites and new biosynthetic pathways.

The conventional fermentation and /or genetic modification of the biosynthetic genes in *S. avermitilis* has led to identification only about 22 secondary metabolites from 38 gene clusters (104). This information indicates that many metabolites still await to be characterized. Phthoxazolin A is a polyketide compound showing a 5-substituted oxazole

ring and a (*Z, Z, E*)-triene moiety, and its structure is similar to the substructure of oxazolomycin from *Streptomyces albus* JA3453 (131). The hybrid non-ribosomal peptide synthetases (NRPSs) and polyketide synthases (PKSs) is responsible for the production of oxazolomycin (132). Especially, OzmO (an NRPS enzyme) from *Streptomyces albus* JA3453 possesses a formylation domain and an adenylation domain to activate glycine and is vital for generation of the oxazole ring structure. But, the *S. avermitilis* genome database (strain number K139) lacks an OzmO orthologue and has no biosynthetic gene cluster similar to that for the biosynthesis of oxazolomycin. So I have no hint to identify the biosynthetic gene cluster of phthoxazolin A.

The features of an avenolide receptor (AvaR1), its homologue (AvaR**3**), and avenolide biosynthetic enzymes (Aco and Cyp17) had been established, and the involvement of the avenolide-signaling cascade in the production of avermectin had been progressively uncovered (58,118,119). In this study, it was shown that unlike in the avermectin production, avenolide has an antagonistic effect for the production of phthoxazolin A, because the supplementation of avenolide into the avenolide-deficient mutant (Δ*aco* strain) decreases the production of phthoxazolin A.

Furthermore, transcriptional analysis revealed that the low transcript of *avaR3* in Δ*aco* mutant can be restored by addition of avenolide. These results suggested that avenolide triggers the expression of AvaR3 that suppresses the production of phthoxazolin A. A considerable boost in the production of phthoxazolin A was observed in *avaR3* deletion mutant, whereas it was an only slight increase in the avermectin-deficient mutant. Thus, substrates/precursors competitiveness in avermectin and phthoxazolin A biosynthetic pathways provides moderate impacts to the fundamental mechanism for the boost in the production of phthoxazolin A in the *avaR3* mutant. As a

result, production of phthoxazolin A is suppressed by AvaR3, which is under the control of avenolide. In summary, avenolide shows distinctive actions: to not only stimulates the production of avermectin but also suppresses the production of phthoxazolin A. Only IM-2, a γ-butyrolactone-type *Streptomyces* hormone exerts bifunctional characteristics like avenolide (133). The further study on the relationship between the avenolide-signaling cascade and the production of phthoxazolin A will provide new and interesting knowledge on the regulatory mechanisms for secondary metabolism in streptomycetes.

2.5. Summary

Investigation of the metabolite profiles of AvaR3 (an autoregulator receptor homologue) deficient mutant in *Streptomyces avermitilis* had been carried out. Unlike the wild-type strain, the *avaR3* mutant produces a notable quantity of phthoxazolin A in the culture. The phthoxazolin A showed potent growth inhibitory activity against *Aphanomyces cochlioides* and *Phytophthora sojae*. Moreover, the production of phthoxazolin A is suppressed by avenolide controlled-AvaR3, indicating that avenolide is the first butenolide-type of *Streptomyces* hormone showing unique functions, it not only elicits the production of secondary metabolite (avermectin) but also suppresses the production of secondary metabolite (phthoxazolin A). These results suggest that the genetic alteration of autoregulator receptor homologues is a beneficial tool to activate cryptic bioactive secondary metabolism.

Chapter 3

Characterization of phthoxazolin A biosynthetic gene cluster in *Streptomyces avermitilis*

3.1. Introduction

Oxazole-containing polyketides belong to the hybrid PKS/NRPS group of secondary metabolites and have numerous therapeutic activities such as antibacterial, antifungal, antiviral, and antitumor. The secondary metabolites in this group are included oxazolomycin produced by *Streptomyces albu*s JA3453 (131), rhizoxin which possesses a methyl-oxazole and macrocyclic lactone structure produced by the bacterial endosymbiont *Burkholderia rhizoxina* (134), conglobatin which has a rare symmetrical oxazole-macrocyclic lactone structure produced by *Streptomyces conglobatus* (135), chivosazol which has glycosylated oxazole-macrocyclic structure produced by myxobacteria *Sorangium cellulosum* SOce56 (136), and rhizopodin produced by *Stigmatella aurantiaca* Sga15 (137). Among these oxazole-containing polyketides, conglobactin is the only metabolite biologically synthesized by the *cis*-AT type I PKS – NRPS hybrid system (135), whereas the rest of them are likely to be produced by *trans*-AT type I PKS-NRPS hybrid system (131,134,136,137).

In Chapter II, I have shown that *Streptomyces avermitilis* has the ability to produce phthoxazolin A, a secondary metabolite which also belongs to oxazole-containing polyketides group. Phthoxazolin A is a heterocyclic aromatic oxazole linked to a triene moiety, showing a cellulose biosynthesis inhibitor (129,130) and a broad spectrum of oomycetes growth inhibitor, the chemical structure matches perfectly to the partial

structure of oxazolomycin. The biosynthetic gene cluster of phthoxazolin A has not yet been identified, even though it was discovered 27 years ago.

The genome of *S. avermitilis* shows 38 gene clusters for secondary metabolisms, yet, the similar cluster to that for oxazolomycin biosynthesis was not present. Hence, the location of phthoxazolin A biosynthetic gene cluster is concealed someplace in the *S. avermitilis* genome

3.2. Materials and Methods

3.2.1. Bacterial strains, plasmids, and growth conditions

S. avermitilis KA-320, K139, and SUKA22 strains were obtained from the culture collection of Kitasato Institute, *S. avermitili*s KA-320 Δ*avaR3* was from in-house library culture collection (119) and the *S. avermitilis* strains were grown on Yeast-Malt Extract Soluble Starch (YMS) medium (0.4% of Bacto™ Yeast Extract (Becton and Dickinson, Sparks, MD USA), 1% of Bacto™ Malt Extract (Becton and Dickinson, Sparks, MD USA), 0.4% of soluble starch and 2% of agar pH 7.5), supplemented with 10 mM of $MgCl_2$ and 10 mM of $CaCl_2$ (YMS-MC medium) for spore formation (119). *Escherichia coli* DH5α was obtained from Kitasato Institute and used for general DNA manipulation, and *E. coli* F$^-$*dcm* Δ(*srl-recA*) *306*::Tn*10* carrying pUB307-*aph*::Tn*7* was used for *E. coli/Streptomyces* conjugation. The plasmids pKU451, pKU470, pKU479, pKU480, and pKU250 (Appendix 5) were obtained from Kitasato Institute and used to construct vectors for genes deletion, pKU 470 (Appendix 5) was used for Cre recombination. The *E. coli* was grown in liquid 2xYeast Extract-Tryptone (YT) (1.6% of Bacto ™ Tryptone (Becton and Dickinson, Sparks, MD USA), 1% of Bacto ™ Yeast Extract (Becton and Dickinson, Sparks, MD USA), 0.05% of NaCl pH 7.0) or Luria - Bertani (LB) Agar (1% of Bacto ™

Tryptone (Becton and Dickinson, Sparks, MD USA), 0.5% of Bacto ™ Yeast Extract (Becton and Dickinson, Sparks, MD USA), 1% of NaCl , 1.5% of agar, pH 7.0), and supplemented with chloramphenicol (30 μg/ml), kanamycin (50 μg/ml), hygromycin B (100 μg/ml), ampicillin (50μg/ml), and streptomycin (25μg/ml), when necessary. The ISP4 agar (Becton and Dickinson, Sparks, MD USA) was used for *E. coli* and *Streptomyces* conjugation.

Spores (1.0 X 10^8 CFU) of the *S. avermitilis* strains were inoculated into 70 mL Avermectin Production Medium (APM) (4.5% of glucose, 4.5% of peptonized milk (OXOID, Basingstoke, UK), 2.4% of Bacto ™ Yeast Extract (Becton and Dickinson, Sparks, MD USA) pH 7.5) in a 500-mL baffled flask, and mycelia were harvested after 48 hours of cultivation. The mycelia were washed, re-suspended in fresh APM and stored at -80°C until use as a seed culture. All reagents used in this study were from Wako Pure Chemical Industries (Osaka, Japan), otherwise, they were stated. All the primers are listed in Table 3.1.

3.2.2. Analysis of phthoxazolin A production

The seed culture was inoculated on 2.5 mL Yeast-Malt Extract Dextrin (YMD) medium (0.4% of Bacto ™ Yeast Extract (Becton and Dickinson, Sparks, MD USA), 1% of Bacto ™ Malt Extract (Becton and Dickinson, Sparks, MD USA), 0.4% of dextrin, and 2 % of agar, pH 7.5) in 12-well plate (Costar™, Corning Inc, Kennebunk, ME USA) followed by incubation at 28°C for 3 days. The agar culture was cut into cubes and extracted with an equal volume of MeOH. The MeOH-extract was analyzed by Agilent 1200 HPLC-DAD system (Waldbronn, Germany) using a Capcell-Pak C18 column (UG 80; 5 μm, 4.6 i. d. x 250 mm; Shiseido, Tokyo, Japan) eluted with a linear gradient system

(eluents: H_2O containing trifluoroacetic acid (TFA) 0.01% (A) and MeOH containing TFA 0.075% (B); 0 to 5 min 10% B and 5 to 55 min 10% B to 100% B; flow rate, 1 mL/min, with UV detection at 275 nm)

Table 3.1. Oligonucleotides used in this study

Primer	Sequence (5' – 3')*
For construction of large-deletion mutants	
aphII Fw	ATGGATTGCACGCAGGTTCTCC
aphII Re	GCGGCGATACCGTAAAGCACGA
sav68-up-Fw	ATCATGAAGCTTATCCTCGTCCGGCTGCCCTGGTGGTGCGAG
sav68-up-Re	CCACTAGTGATATCGACGGTCTCCACCAGTGATGCGGACACAC
sav68-up test Fw	GGTCTCGGTCCTGACGGGGATGTCCACCC
sav71-dw Fw	GCACTAGTTGGGCACTGTGGAGCGACGTGAGCCGGTG
sav71-dw-Re	ATCAGTAAGCTTTACACCAGACGCCGGTTCACGTTCCCCGCC
sav432-up-Fw	GAATTCAAGCTTCCCCCTGTCTCCGCACCGGCATCAGGAGGA
sav434-up-Re	GGACTAGTGGTGGTGACCAGGTACCTGTACAGGAAGCGCTCGC
sav434-up test Fw	TTCGCCCGCGCTCACTCCCCGTACTACC
sav434-dw test Re	GGCTCTCGTTGCAGCCGTAGGTGTTGACCAC
sav434-dw-Fw	GAATTCAAGCTTCCCCCTGTCTCCGCACCGGCATCAGGAGGA
sav434-dw-Re	TAATTCAAGCTTCTGAGGTCCGCAGGCGGGGCGGAGGTTCCG
sav845-up-Fw	ATGCAAAGCTTACGACGGAAGGAGCTGACCGCATG
sav845-up-Re	GGACTAGTGTAATAGGGGTCGTCCACCAGGTCTCGGC
sav845-up test-Fw	GCTGCGACAGTGAAGGACGATCAGTGA
sav845-dw-test-Re	GTCGGCGGAGAAGAAGAACAAGCTGAC
sav845-dw-Fw	GCACTAGTCGAGCTGGAAGGAGGACACCGGCGGCATGGAC
sav845-dw-Re	CTGTCCAAGCTTACTGTTGCTCCCGAACGGCAGGTCCC
sav1007-up-Fw	GCATTCAAGCTTATGCTTTCGCACTCCATCGAGCAC
sav1007-up-Re	GGACTAGTGGTGATTGTCATCGACAGTTTCACCGTG
sav1007-up-test-Fw	GGCCATGCGATCCACACACAGATGAGAC
sav1007-dw-test-Re	GTCATTCCGGTGCTGGAACGGTTTTAGG
sav1007-dw-Fw	CGACTAGTTCGAGCCGACCTGGCTGACCACCCAGC

Table 3.1. Oligonucleotides used in this study (continued)

Primer	Sequence (5' – 3')*
sav1007-dw-Re	GTGCAGAAGCTTGGCGCGGCTGGTGTAGATCCAGTTG
sav1286-up-Fw	CACTTCAAGCTTCCTTCCGGCATTTCGATGTGCCGCCC
sav1286-up-Re	GGACTAGTGATCATGGTCTTGTCGCCGGGCGCGGCTC
sav1286-dw-test-Re	GCGAGACCAGCACGATGCCGACGAG
sav1286-dw-Fw	CGACTAGTCGACGCGCTCAGTGACTCGTTCGCCGC
sav1286-dw-Re	GAATTCAAGCTTACCTTCGGGCCCCCGGACACCTGG
wo-mutloxP-SpeI-Fw	GCACTAGTGCTCATTTAAATCCGTTGGATACACCAAG
wo-mutloxP-SpeI-Re	GGACTAGTTTAGACATTATTTGCCGGACTACCTTGGTGATCT CGCTTTCACGTAG
mutloxP-SpeI-Fw	GGACTAGTGAGCGACTCGAGTACCGTTCGTATAGCATACATT ACGAAGTTATACGCG
mutloxP-SpeI-Re	CTCGAGACTAGTCTGGTACCGAGCGAACGCGTT
For construction of *ptxA* deletion	
ptxA-up-Fw	CGATCCAAGCTTAACGACTGCGTGTGCAGGTCGCCGCG
ptxA-up-Re	GCACTAGTCTGGAGGGCGCAGCCGCACACCTCATGGAG
ptxA-dw-Fw	CAATTCAAGCTTGCTCACCGACCGGCAGGGCCTCGACC
ptxA-dw-Re	GGACTAGTGAACATGAACACGACGGGGAGGGAATCGGTG
ptzA-tFw	CAGTGTGTACGTCCAGACGGTCAGCG
ptzA-tRe	GCTCGAACTCAAGGCCGTGGAGTCG
hph-Fw	CTCGAGACTAGTCAGTGAGTTCGAGCGACTCGAGT
hph-Re	CTCGAGACTAGTCTGGTACCGAGCGAACGCGTT
ptzA-Fw	GCATCTCCTCGCGGGACTGCCTGCG
ptzA-Re	GGCAGGTTGCCGCGTGCGAAGTTG
For *ptxA* complementation	
ptxA-comp-Fw	GTGCCGGTTGGTAGTGGGAGGTGAATGAGGGCGCCAAGGG
ptxA-comp-Re	CTTTAGATTCTAGAGCCCGGGCAGGTGCGGTCAGCGGAAG
apr-Fw	CCCCGGCGGTGTGCTG
apr-Re	GACGTCGCGGTGAGTTCAGGC

*) Restriction sites are underlined.

3.2.3. *E. coli* and *Streptomyces* intergeneric conjugation

The donor *E. coli* (*E. coli* F$^-$*dcm* Δ(*srl-recA*) *306*::Tn*10* carrying pUB307-*aph*::Tn*7*) with particular vector for gene deletion or gene expression was grown in 3 ml liquid 2xYT at 37^{o}C 140 spm for approximately 2 hours until the optical density at 600nm (OD_{600}) = 0.1, the cells were washed with fresh 2xYT twice, and resuspended in 110 μl of 2xYT. The spores of *S. avermitilis* KA-320 Δ*avaR3* recipient (10^{-9}CFU/ml) were mixed with the donor *E.coli* cells in ratio 1:10 and 1:100 (v/v) and spread into ISP4 agar plates. After incubation at 28^{o}C for 18 hours, each plate was overlaid using 1 ml sterile water supplemented with kanamycin (625 μg) or hygromycin B (500 μg) or thiostrepton (250 μg) or apramycin (500 μg) in combination with 250 μg of nalidixic acid, and the incubation was continued at 28^{o}C for 3 days. The transformants were further used for genotype analysis by PCR.

3.2.4. Construction of *Streptomyces avermitilis* large-deletion (SALD) mutant strains.

The Cre-*loxP*-mediated recombination system was applied for construction of large-deletion mutant strains. The recombination between two specific DNA sequences termed *loxP* sites was activated by the Cre recombinase (138). The *loxP* site contains two sets of 13-bp inverted repeats as Cre binding sites, an unequal main spacer of 8 bp which determines the direction of the *loxP* sequence and involves in the exchange of DNA strand throughout recombination. A nucleotide sequence located between two *loxP* would be deleted when the *loxP* sites are in the same direction, but the nucleotide sequence would be inverted when the *loxP* sites are in the opposite direction (138). The variation of the inverted repeats termed as mutant *loxP* allows reiterated gene deletion in one host (139).

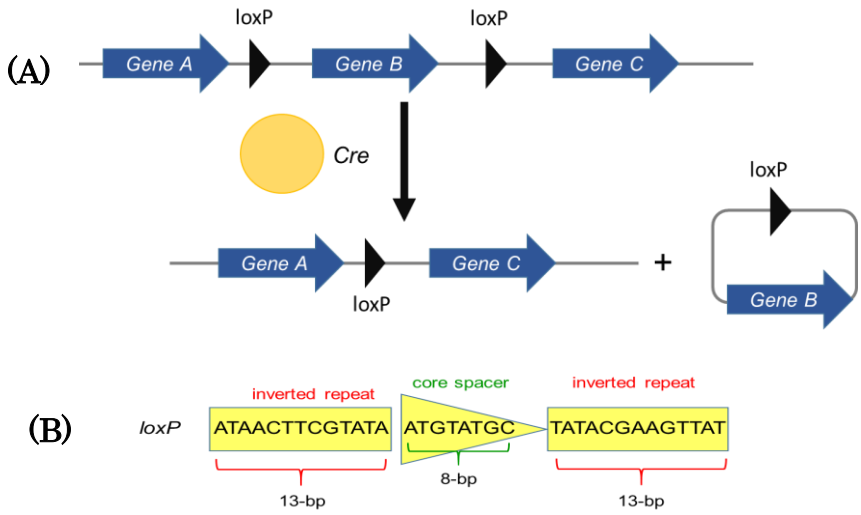

Figure 3.1. (A) Schematic representation of Cre-*loxP* recombination system for gene deletion. (B) *LoxP* sequence representing the core spacer and the flanking inverted-repeats.

The *S. avermitilis* KA-320 Δ*avaR3* mutant contains kanamycin-resistant gene flanked by two *loxP* sites as a consequence of the kanamycin resistance cassette amplification from pKU 474 during vector construction as described in previous research (119). Removal of kanamycin resistance gene in the *S. avermitilis* KA-320 Δ*avaR3* mutant by the Cre expression was necessary so that the kanamycin resistant gene could be reused in further constructions. The plasmid pKU470 for Cre expression was introduced into the *S. avermitilis* KA-320 Δ*avaR3* strains using intergeneric conjugation followed by overlay using thiostrepton and nalidixic acid. The progenies from *S. avermitilis* KA-320 Δ*avaR3* mutant were selected based on their ability to grow in the YMS-MC medium supplemented with thiostrepton. To further induce the Cre recombination, the selected *S. avermitilis* KA-320 Δ*avaR3* progenies showing thiostrepton resistance were further inoculated into 3 ml of Tryptone Soya Broth (TSB)(OXOID, Basingstoke, UK) -Yeast Extract Malt Extract medium (YEME) (0.3% of Bacto ™ Yeast Extract (Becton and Dickinson, Sparks, MD USA), 0.5% of Bacto ™

Peptone (Becton and Dickinson, Sparks, MD USA), 0.3% of Bacto ™ Malt Extract (Becton and Dickinson, Sparks, MD USA), 1% of Glucose, 34% of sucrose) ratio 1:1 (v/v) supplemented with thiostrepton 10 μg /ml. This culture was incubated at 28°C 120 spm for 5 days, followed by inoculation on YMS-MC medium and further incubation at 28°C for 4-6 days. The single colonies obtained from YMS-MC medium were assessed their sensitivity to kanamycin, and the absence of kanamycin gene was confirmed by PCR analysis using aphII-Fw/aphII-Re. The selected progeny (Δ*avaR3* marker-less) was further used for construction large-deletion mutant strains.

The generation of large deletion mutants was also based on the temporal Cre-expression toward two variants of mutant *loxP*, *lox66* (*loxP*-mut1L) and *lox71* (*loxP*-mut1R) which led to their recombination into a double-mutant *loxP* site termed *lox72* and deletion of genomic region between *lox66* and *lox71*. Plasmids either of which having mutant *loxP* (*lox66)* connected with hygromycin (*hph*) resistant gene (*lox66-hph*) or *lox71* connected with kanamycin (*aphII*) resistant gene (*aphII*-lox71) flanking by homologous target regions were constructed. The plasmids were introduced into *S. avermitilis* Δ*avaR3* marker-less one at a time. The double-crossover strains were simply selected based on their ability to grow in YMS-MC medium supplemented with kanamycin and hygromycin. The desirable mutants had the *lox66-hph* cassette in the left flank of the target regions and the *aphII-lox71* cassette in the right flank of the target region. The Cre recombinase expression in the double-crossover strains led to recombination of those two *loxP* sites and deletion of target region as shown in Figure 3.2.

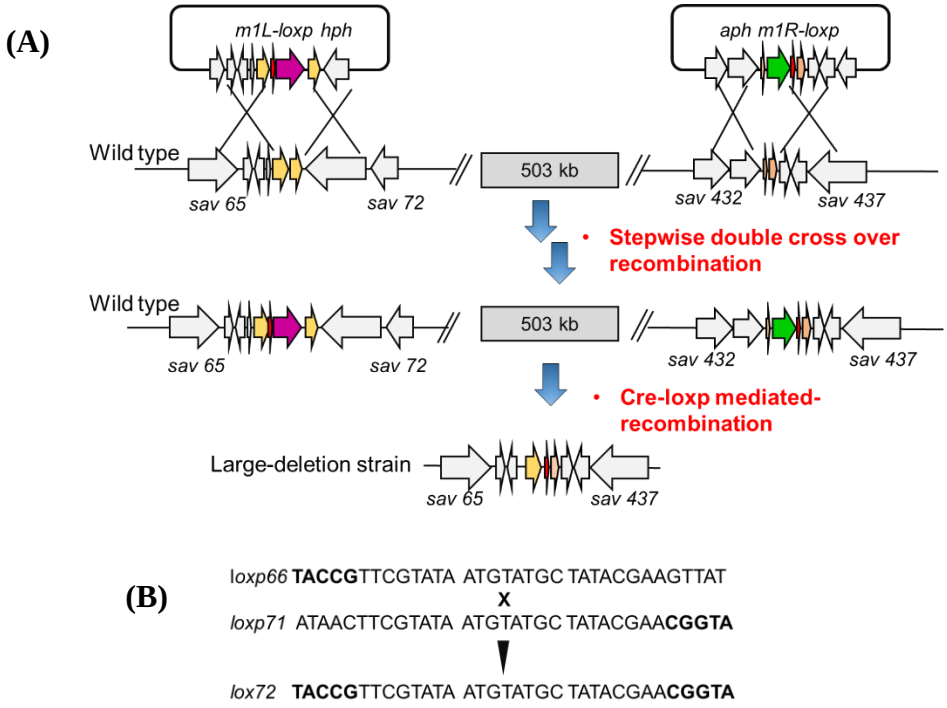

Figure 3.2. (A) Schematic representation of Cre-*loxP* recombination system for gene deletion in *Streptomyces avermitilis* Δ*avaR3* mutant (B). Representation of mutant *lox66* and *lox71* sites, which after Cre recombination result in a double-mutant *lox72* site. *loxP*, native *loxP* sequences.

To construct SALD-1 mutant, two fragments (77,219-79,457 nt and 79,479-81,744 nt) were PCR-amplified by primers sav68-up-Fw/sav68-up-Re and sav71-dw-Fw/sav71-dw-Re. The fragments were treated with *Hind*III/*Spe*I and ligated to pKU451 to get pLT143. The plasmid pLT 143 was cut with *Spe*I and cloned together with a *lox 66-hph* fragment (PCR-amplified from pKU480 as a template using the mutloxP-SpeI-Fw/wo-mutloxP-SpeI-Re primer pair) to create pLT144. The pLT145 was generated by ligation of a 6.6 kb *Hind*III fragment, obtained from pLT144 with pKU250 at the *Hind*III site. The intergeneric conjugation method described above was used to introduce the pLT145 to *S. avermitilis* KA-320 Δ*avaR3* marker-less, followed by overlay using 500 µg of hygromycin B and 250 µg of nalidixic acid. Resultant transformants resistant to hygromycin B was termed as *S. avermitilis* KA-320 Δ*avaR3*/*sav71*::*lox66-hph* mutant.

Others two fragments (582,859-584,876 nt and 584,906-587,127 nt) were amplified by PCR using the primer pairs (sav432-up-Fw/sav434-up-Re and sav434-dw-Fw/sav434-dw-Re). These fragments were digested with *Hind*III/*Spe*I, and cloned to pKU451 to generate pLT146. A fragment contains kanamycin-resistant gene (*aphII*) with mut-*loxP* (*aphII-lox71*) was PCR-amplified from pKU479 with the primer pair wo-mutloxP-SpeI-Fw/mutloxP-SpeI-Re and cloned into the *Spe*I site of pLT146 to get pLT147. The pLT148 was constructed by ligation of a 6.0 kb *Hind*III fragment obtained from the plasmid pLT147, with pKU250 at the *Hind*III site. The conjugation method as described above was used to introduce the pLT148 to *S. avermitilis* KA-320 Δ*avaR3*/*sav71*::*lox66-hph* mutant, followed by overlay using 625 μg of kanamycin and 250 μg of nalidixic acid per plate. Resultant transformants resistant to both hygromycin and kanamycin termed *S. avermitilis* KA-320 Δ*avaR3*/*sav71*::*lox66-hph* /Δ*sav434*::*aphII-lox71* mutant. This strain was used for further Cre expression with the protocol described above. The single colonies obtained from YMS-MC medium were assessed their sensitivity to hygromycin and kanamycin, and the deletion of a 0.51 Mb region from *sav71* to *sav434* was confirmed by PCR using primer pair sav68-up test Fw / sav434-dw test Re and DNA sequencing.

To construct SALD-2 mutant, the *aphII* gene of pLT148 was excised with *SpeI* and replaced with the *lox66-hph* fragment, resulting in pLT149. The intergeneric conjugation method described above was used to introduce pLT149 to *S. avermitilis* KA-320 Δ*avaR3* marker-less to generate *S. avermitilis* KA-320 Δ*avaR3*/*sav434*::*lox66-hph* mutant. Two fragments (999,468-997,573 nt and 1,004,009-1,002,110 nt) were PCR-amplified by the primer pairs (sav845-up-Fw/sav845-up-Re and sav845-dw-Fw/sav845-dw-Re), and cloned into pKU451 to generate pLT150. The pLT150 was cloned with the *aphII-lox71* fragment to get pLT151. The pLT152 was constructed by ligation of a 5.4 kb *Hind*III

fragment obtained from pLT151, with pKU250 at the *Hind*III. The intergeneric conjugation method described above was used to introduce the pLT152 to *S. avermitilis* KA-320 Δ*avaR3*/*sav434*::*lox66-hph* mutant, the resultant transformants were termed as *S. avermitilis* KA-320 Δ*avaR3*/*sav434::lox66-hph* /Δ*sav845::aphII-lox71*. The intergeneric conjugation method described above was used to introduce the pKU470 into the double-mutant strain and followed by Cre recombination method for deletion of a 0.42 Mb region from *sav434* to *sav845*. The candidates of SALD-2 were confirmed by PCR using primer pair sav434-up-test Fw/sav845-dw-test-Re and DNA sequencing.

To construct the SALD-3 mutant, the *aphII* gene of pLT152 was excised with *SpeI* and replaced with the *lox66-hph* fragments to get pLT153. The intergeneric conjugation method described above was used to introduce the pLT153 into *S. avermitilis* KA-320 Δ*avaR3* marker-less, to generate *S. avermitilis* KA-320 Δ*avaR3*/sav845::*lox66-hph* mutant. Two fragments (1,271,761-1,273,916 nt and 1,273,956-1,276,187 nt) were PCR-amplified by the primer pairs (sav1007-up-Fw/sav1007-up-Re and sav1007-dw-Fw/sav1007-dw-Re), and cloned into pKU451 to generate pLT154. This plasmid was ligated with the *aphII-lox71* fragment to produce pLT155. The pLT156 was constructed by ligation of a 6.0 kb *Hind*III fragment obtained from pLT155, with pKU250 at the *Hind*III. The intergeneric conjugation method described above was used to introduce the pLT156 to *S. avermitilis* KA-320 Δ*avaR3*/*sav845::lox66-hph* mutant, to generate *S. avermitilis* KA-320 Δ*avaR3*/*sav845::lox66-hph*/Δ*sav1007::aphII-lox71* mutant. The intergeneric conjugation method described above was used to introduce the pKU470 into the double-mutant strain and followed by Cre recombination method for deletion of a 0.28 Mb region from *sav845* to *sav1007*. The candidates of SALD-3 were confirmed by PCR using primer pair sav845-up-test Fw/sav1007-dw-test-Re and DNA sequencing.

To construct SALD-4 mutant, the *aphII* gene of pLT156 was excised with *SpeI* and replaced with the *lox66-hph* fragment to get pLT157. The intergeneric conjugation method described above was used to introduce the pLT157 into *S. avermitilis* KA-320 Δ*avaR3* marker-less to generate *S. avermitilis* KA-320 Δ*avaR3*/*sav1007::lox66-hph* mutant. Two fragments (1,593,533-1,595,311 nt and 1,595,580-1,597,661 nt) were PCR-amplified by the primer pairs (sav1286-up-Fw/sav1286-up-Re and sav1286-dw-Fw/sav1286-dw-Re), and cloned into pKU451 to generate pLT158. The pLT158 was ligated with the *aphII-lox71* to produce pLT159. The pLT160 was constructed by ligation of a 5.5 kb *Hind*III fragment obtained from pLT159 with pKU250 at the *Hind*III site. The pLT160 was transferred to *S. avermitilis* KA-320 Δ*avaR3*/*sav1007::lox66-hph* mutant by intergenic conjugation, to get *S. avermitilis* KA-320 Δ*avaR3*/*sav1007::lox66-hph* mutant/Δ*sav1286::aphII-lox71*. The intergeneric conjugation method described above was used to introduce the pKU470 into the double-mutant strain and followed by Cre recombination method for deletion of a 0.32 Mb region covering from *sav1007* to *sav1286*. The candidates of SALD-4 were confirmed by PCR using primer pair sav1007-up-test Fw/sav1286-dw-test-Re and DNA sequencing.

3.2.5. Genome sequencing and bioinformatics analyses

The nucleic acid sequence of *S. avermitilis* KA-320 was achieved by connecting data obtained from the MEGABACE 1000 DNA sequencer and the high-throughput DNA sequencer (Illumina). Around 21 contigs were produced and used for screening of plausible gene cluster for phthoxazolin A. Annotation of open reading frames (ORFs) and gene functions were accomplished manually by using the FramePlot 4.0 beta program (http://nocardia.nih.go.jp/fp4/), the 2ndFind program (http://biosyn.nih.go.jp/2ndfind/),

the BLAST algorithm, antiSMASH (http://antismash.secondarymetabolite.org/), and the web-based PKS/NRPS analysis program (http://nrps.igs.umaryland.edu/nrps/). The plausible gene cluster for biosynthesis of phthoxazolin A was located in a contig (ca. 164 kb) and the nucleic acid sequence in this gene cluster and the flanking regions had been deposited in the DDBJ; accession number LC315614.

3.2.6. Phylogenetic tree analysis of *trans*-AT domains

The amino acid sequences of *trans*-AT domains (Appendix 6) were retrieved from NCBI database and aligned using ClustalW (http://www.genome.jp/tools/clustalw/). The unrooted phylogenetic tree was also generated by the same software and edited in Genetyx-Tree (Genetyx version 10).

3.2.7. Deletion of the *ptxA* gene in the *avaR3* mutant

Two 2.0 kb fragments upstream and downstream of the *ptxA* gene were amplified by PCR using the primer pairs (ptxA-up-Fw/ptxA-up-Re and ptxA-dw-Re/ptxA-dw-Fw). These fragments were treated by *Hind*III and *Spe*I, and cloned into pKU451, to generate pLT140. A hygromycin-resistant gene (hph) (PCR-amplified with pKU480 and the hph-Fw/hph-Re primer pair) was ligated with *Spe*I–treated the pLT140 to produce pLT141. The pLT142 was constructed by ligation of a 6.2 kb *Hind*III fragment obtained from pLT141 with pKU250 at *Hind*III site. By intergeneric conjugation, the pLT142 was transferred into the *S. avermitilis* KA-320 Δ*avaR3* mutant, and the wild-type *ptxA* gene was exchanged with the mutant allele by a homologous recombination event. The transformants for the *ptxA* deletion was verified by PCR analysis using ptzA-tFw/ptzA-tRe, ptzA-Fw/ptzA-Re primer pairs and DNA sequencing. The *S. avermitilis* KA-320

avaR3/*ptxA* double mutant was named as Δ*avaR3* Δ*ptxA*.

3.2.8. Complementation of the *avaR3/ptxA* double mutant

The intact *ptxA* gene around 3.2 kb was PCR-amplified by using the primer pair ptxA-comp-Fw/ptxA-comp-Re, and ligated to the BamHI site of pLT101 (Appendix 5) (140) utilizing GeneArt Seamless Cloning and Assembly Kit (Life Technologies). The subsequent plasmid was introduced into the *S. avermitilis* KA-320 Δ*avaR3*/*ΔptxA* double mutant by intergeneric conjugation with overlay using apramycin and nalidixic acid. Integration of the plasmid was verified by apramycin resistance and PCR analysis using apr-Fw/apr-Re and ptzA-Fw/ptzA-Re.

3.3. Results

3.3.1. Phthoxazolin A production in the *S. avermitilis* progeny

S. avermitilis strain KA-320, the original culture stock isolated in the 1970s, has inferior production of avermectin and unstable sporulation properties. One progeny (strain K139) was selected by morphological selection of strain KA-320 without any mutagenesis, showed excellent production of avermectin and stable sporulation (141). The genome sequencing of *S. avermitilis* had been accomplished using strain K139 (H. Ikeda, personal communication).

S. avermitilis K139 and KA-320 were both reported as isogenic to MA-4680, ATCC 31267, and NRRL 8165 in several publications (50,105,108,109,142). Metabolite profile of *S. avermitilis* KA-320 showed production of phthoxazolin A (Figure 3.3B). Whereas, SUKA22 is genetically created by deleting the 1.5 Mb left the chromosomal region of *S. avermitilis* K139 (98,101,105), and metabolite profile of SUKA 22 showed

no production of phthoxazolin A (Figure 3.3B), this result suggested that the deleted-chromosomal region could have phthoxazolin A biosynthetic gene cluster.

Since KA-320 and K139 are presumed to have identical genotype as mentioned above, I made several series of large-deletion mutants (SALD mutants) from the *S. avermitilis* KA-320 Δ*avaR3* mutant and examined the production of phthoxazolin A in these mutants (Figure 3.4B). Unexpectedly, the SALD-1, SALD-2, SALD-3 and SALD-4 strains showed production of phthoxazolin A at an equivalent quantity to the Δ*avaR3* mutant strain.

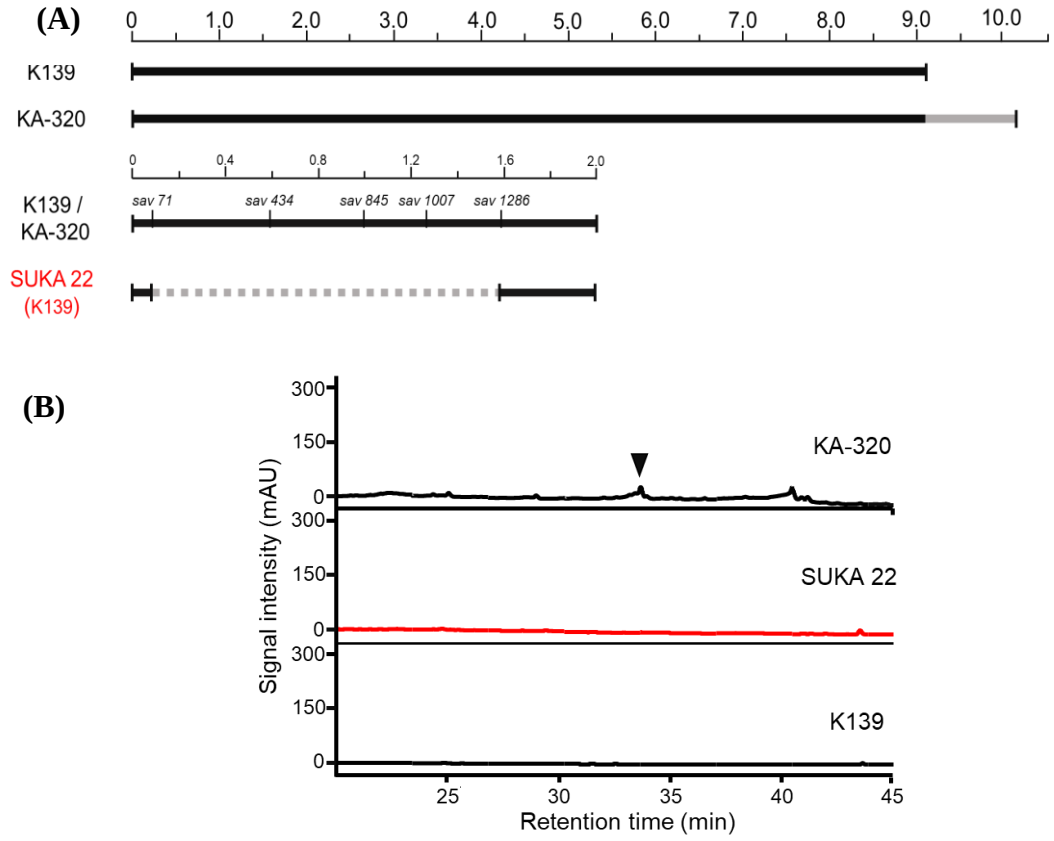

Figure 3.3. (A) Graphic depiction of *Streptomyces avermitilis* SUKA 22. Gray solid line indicates the extrachromosomal region of *S. avermitilis* KA-320, and gray dashed lines indicate the deleted-chromosomal region of K139. KA-320, *S. avermitilis* KA-320; K139, *S. avermitilis* K139; SUKA22, *S. avermitilis* SUKA22 (K139) as a genetic background). (B) Production of phthoxazolin A in the *S. avermitilis* progenies. mAU, milliabsorbance units at 275 nm. Phthoxazolin A is represented by a black inverted triangle.

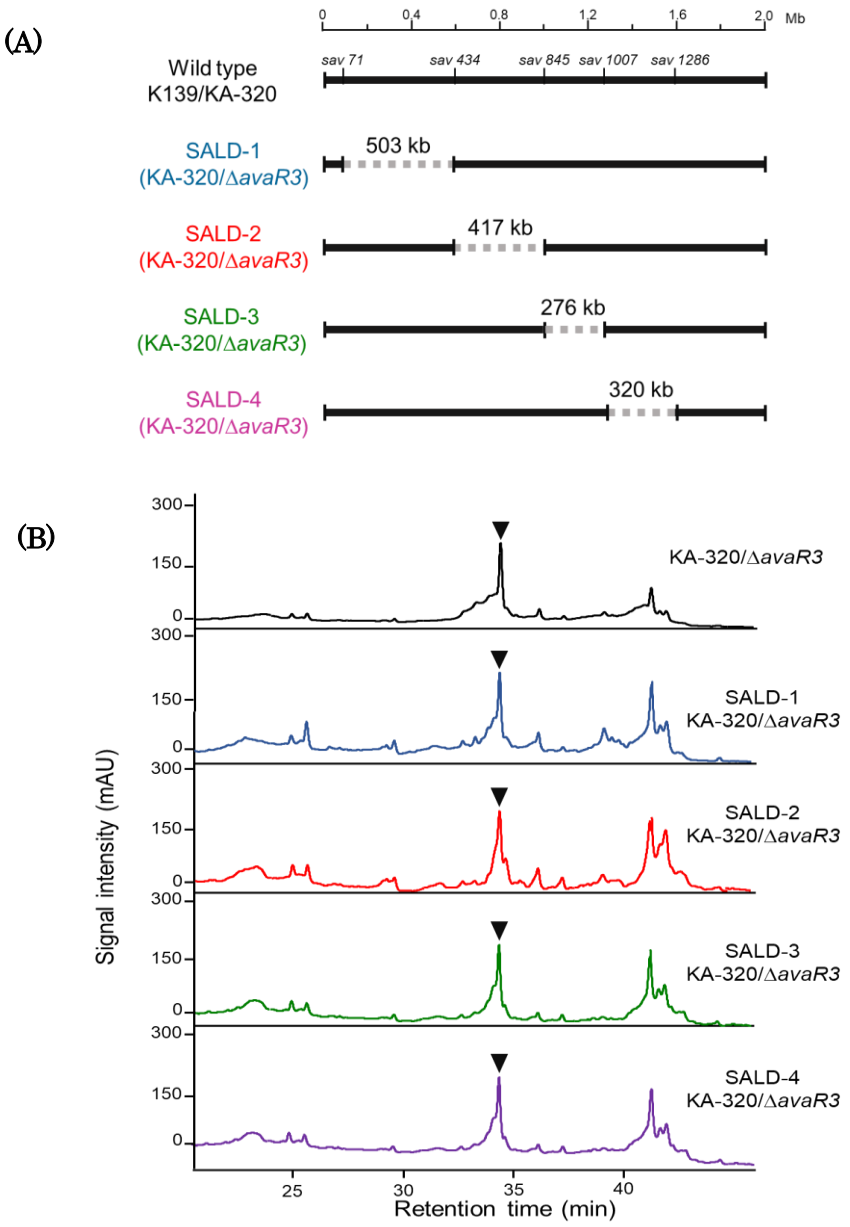

Figure 3.4. (A) Schematic representation of *Streptomyces avermitilis* large-deletion (SALD) mutant strains. Gray dashed lines indicates the deleted-chromosomal region. Wild-type, *S. avermitilis* KA-320 or K139; (B) Production of phthoxazolin A in the *S. avermitilis* SALD mutants. mAU, milliabsorbance units at 275 nm. Phthoxazolin A is represented by an inverted triangle

Because of this contradictive result, I finally obtained strain K139 and analyzed its metabolite profile. It became apparent that production of phthoxazolin A was not observed in the strain K139 (Figure 3.3B), suggesting that genetic disparities between *S.*

avermitilis KA-320 and K139 were bigger than that I expected to give capability for the biosynthesis of phthoxazolin A

3.3.2. Identification of the phthoxazolin A biosynthetic gene cluster

The Contour-clamped Homogeneous Electric Field (CHEF) electrophoresis of the chromosomes showed that the strain KA-320 has longer linear chromosome (about 800-1,000 kb) than that of strain K139, and the extrachromosomal region of strain KA-320 seems to be found at nearby AseI-T or AseI-D fragments at the right-hand region of the K139 linear chromosome (H. Ikeda, personal communication). It was hinted that the extrachromosomal region of strain KA-320 might have biosynthetic gene cluster for phthoxazolin A. Thus, the genome of strain KA-320 was sequenced and bioinformatics analyses were performed using the genomic sequence. Indeed, a plausible biosynthetic gene cluster of phthoxazolin A that spanned 99.9 kb was found in the extrachromosomal region of KA-320 (Figure 3.5). Assessment of sequences with genes in the publicly available databases and annotation analysis showed that this cluster has 43 ORFs. The genetic organization and proposed functions are shown in Figure 3.5 and Table 3.2, respectively.

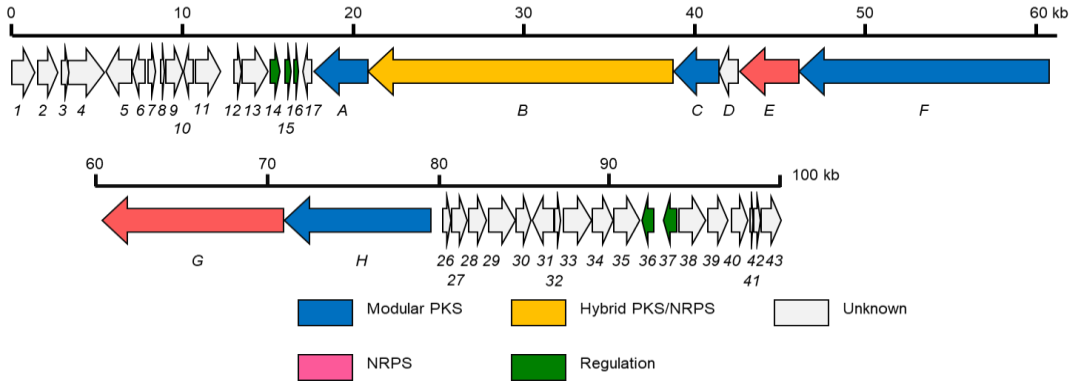

Figure 3.5. Biosynthesis gene cluster of phthoxazolin A. ORFs expected to contribute in phthoxazolin A biosynthesis are colored.

Table 3.2. Deduced functions of ORFs in the phthoxazolin A biosynthetic gene cluster.

Gene	Size[a]	Homolog[b] and origin	Identity/ similarity (%)	Proposed function
orf1	539	OK006_RS37135(WP_054234754.1) *Actinobacteria bacterium* OK006	70/81	Copper oxidase
orf2	359	ASC56_RS00960(WP_055489610.1) *Streptomyces* sp. TP-A0356	86/91	Serine/threonine phosphatase
orf3	83	B0183_RS05155 (WP_078208448) *Haemophilus parasuis*	55/37	Hypothetical protein
orf4	705	BLU79_RS13920(WP_093906007.1) *Streptomyces* sp. cf386	82/89	Histidine kinase
orf 5	504	GlpK (WP_015654981), *S. davawensis* JCM 4913	91/95	Glycerol kinase
orf 6	255	ASC56_RS09905 (WP_055490882), *Streptomyces* sp.TP-A0356	92/96	IclR-family transcriptional regulator
orf 7	142	ADL25_RS11400 (WP_059127556), *Streptomyces* sp. NRRL F-5122	67/76	Histidine kinase
orf 8	80	IQ62_RS20385 (WP_037697207), *S. scabiei* NCPPB 4086	85/91	Hypothetical protein
orf 9	333	Ppk2 (WP_007385561), *S. sviceus* ATCC 29083	88/93	Polyphosphate kinase
orf 10	180	SAMN05216482_0059 (SEB58800), *Streptomyces* sp. PAN_FS17	78/87	Hypothetical protein
orf 11	481	G412_RS0110405 (WP_02881204), *S. flavidovirens* DSM 40150	96/98	Glyceraldehyde 3-phosphate dehydrogenase
orf 12	137	NF37_RS0107960 (WP_032755078), *S. alboviridis* NRRL B-1579	81/91	Integrase
orf 13	501	AWV61_RS50755(WP_060880896), *S. scabiei* 95-18	83/85	Transposase
orf 14	188	AVL59_RS26005 (WP_067308799), *S. griseochromogenes* ATCC 14511	81/86	Two-component system sensor kinase
orf 15	113	CCN44_RS40620 (WP_086704188), *S. tricolor* NRRL B-16925	86/86	Two-component system response regulator
orf 16	94	IG08_RS0113085 (WP_030600335), *S. fulvoviolaceus* NRRL B-2870	87/88	LuxR-family transcriptional regulator
orf 17	169	BIV24_RS13170 (WP_071366454), *Streptomyces* sp. MUSC 93	74/82	Polyketide cyclase

Table 3.2. (Continued)

Gene	Size[a]	Homolog[b] and origin	Identity/ similarity (%)	Proposed function
ptxA (orf 18)	1065	OzmM (ABS90474), *S. albus* JA3453	57/68	Acetyl transferase
ptxB (orf 19)	5939	OzmH (ABS90470), *S. albus* JA3453	53/62	Hybrid NRPS-PKS
ptxC (orf 20)	877	OzmQ (ABS90478), *S. albus* JA3453	67/76	Type I PKS
ptxD (orf 21)	362	OzmP (ABS90477), *S. albus* JA3453	77/88	Hypothetical protein
ptxE (orf 22)	1154	OzmO (ABS90476), *S. albus* JA3453	53/62	NRPS
ptxF (orf 23)	4885	OzmN (ABS90475), *S. albus* JA3453	51/60	Type I PKS
ptxG (orf 24)	3542	NRPS (OMI35273), *S. sparsogenes* DSM 40356	65/74	NRPS
ptxH (orf 25)	2860	PKS 1-1 (ADI03434), *S. bingchenggensis* BCW-1	63/72	Type I PKS
orf 26	155	SibV (ACN39745), *Streptosporangium sibiricum* DSM 44039	66/77	Dioxygenase
orf 27	306	BZL62_RS04865 (WP_086716558), *Streptomyces sp.* NRRL B-2347	68/78	Hypothetical protein
orf 28	347	AOK13_RS10670 (WP_055559528), *S. luridiscabiei* NRRL B-24455	81/87	IMP dehydrogenase
orf 29	517	BZL62_RS04825 (WP_086716551), *S. angustmyceticus* NRRL B-2347	79/86	Acetolactate synthase
orf 30	295	SAMN05444920_109123 (SEG95653), *Nonomuraea solani*, CGMCC 4.7037	55/70	Hydroxyacid dehydrogenase
orf 31	410	BR98_RS37570 (WP_083976095), *Kitasatospora azatica* KCTC 9699	70/82	Cytochrome P450
orf 32	71	WT80_RS35315 (WP_081087741) *Burkholderia stagnalis* MSMB774WGS	43/56	Hypothetical protein
orf 33	526	KCH_RS21250 (WP_084223811), *Kitasatospora cheerisanensis*	66/77	Fatty acid Co A ligase
orf 34	409	SAMN05216533_5065 (SEF00159), *Streptomyces* sp. Ag109_O5-10	85/92	5-Aminolevulinate synthase

Table 3.2. (Continued)

Gene	Size[a]	Homolog[b] and origin	Identity/ similarity (%)	Proposed function
orf 35	509	Ann2 (AGY30678), *S. calvus* ATCC 13382	67/81	5-Aminolevulinate synthase
orf 36	225	ColR1 (AIL50186), *S. aureus* SOK1/5-04	50/62	LuxR-family transcriptional regulator
orf 37	248	IF01_RS0119920 (WP_051755722), *S. purpeofuscus* NRRL B-1817	75/83	TetR-family transcriptional regulator
orf 38	516	OO66_RS31780 (WP_051763676), *S. virginiae* NRRL B-8091	74/83	Multidrug MFS transporter
orf39	218	SMCF_RS43270 (WP_086014295), *S. coelicoflavus* ZG0656	80/87	4'phospho-pantetheinyl transferase
orf40	166	AQI88_RS03055 (WP_066991659), *S. cellostaticu*s DSM40189	87/91	Hypothetical protein
orf41	99	AVL59_RS13665 (WP_067303421), *S. griseochromogenes* ATCC 14511	87/94	Hypothetical protein
orf42	117	AQI88_RS03065(WP_066991232.1) *S. cellostaticus* DSM 40189	89/92	Hypothetical protein
orf43	272	OO69_RS22260(WP_033282486.1), *Streptomyces* sp. NRRL F-525	76/84	Hypothetical protein

[a] Numbers refer to amino acid residues.
[b] Parenthetical codes are National Center for Biotechnology Information accession numbers.

Hybrid PKS/NRPS system was shown in phthoxazolin A cluster. PKS genes (*ptxC*, *ptxF,*and *ptxH*), one hybrid NRPS/PKS gene (*ptxB*), two NRPS genes (*ptxE* and *ptxG*), and a gene for acyltransferase activity (*ptxA*) were identified (Table 3.3). The contribution of PtxA in the biosynthesis machinery of phthoxazolin A was assessed by deletion of *ptxA* in *S. avermitilis* KA-320 Δ*avaR3* genetic background (Figure 3.6A and 3.6B).

Table 3.3. The PKS/NRPS modules and domains from 7 genes in *ptx* cluster

Genes	Function	Modules	Domains
ptxA	Acyltransferase	-	AT1-AT2-Ox
ptxB	Hybrid PKS-NRPS	Module 5	KS-KR-MT-ACP
		Module 6	C-A-PCP
		Module 7	KS-DH-KR-ACP
		Module 8	KS-KR-ACP
		Module 9	KS^0
ptxC	PKS	Module 1	KS-ACP
ptxE	NRPS	Loading Module	F-A-PCP
ptxF	PKS	Module 2	KS-DH-KR-ACP
		Module 3	KS-DH-KR-ACP
		Module 4	KS-DH-KR-MT-ACP
ptxG	NRPS	Module 12	C-A-PCP
		Module 13	C-A-MT-PCP-C-Cyp
ptxH	PKS	Module 9	DH-ACP-ACP
		Module 10	DH-KS-KR-ACP
		Module 11	KS^0-ACP

The production of phthoxazolin A in the Δa*vaR3* Δ*ptxA* strain was abolished (Figure 3.6C middle panel) and complementation with intact *ptxA* gene resumed the production of phthoxazolin A to the level of that in the parental strain (Δ*avaR3*) (Figure 3.6C, lower panel). These results suggested that the *trans*-AT (PtxA) is vital for the biosynthesis of phthoxazolin A. Hence, the biosynthesis of phthoxazolin A by PKS genes and the hybrid NRPS/PKS needs the enzymatic activity of PtxA.

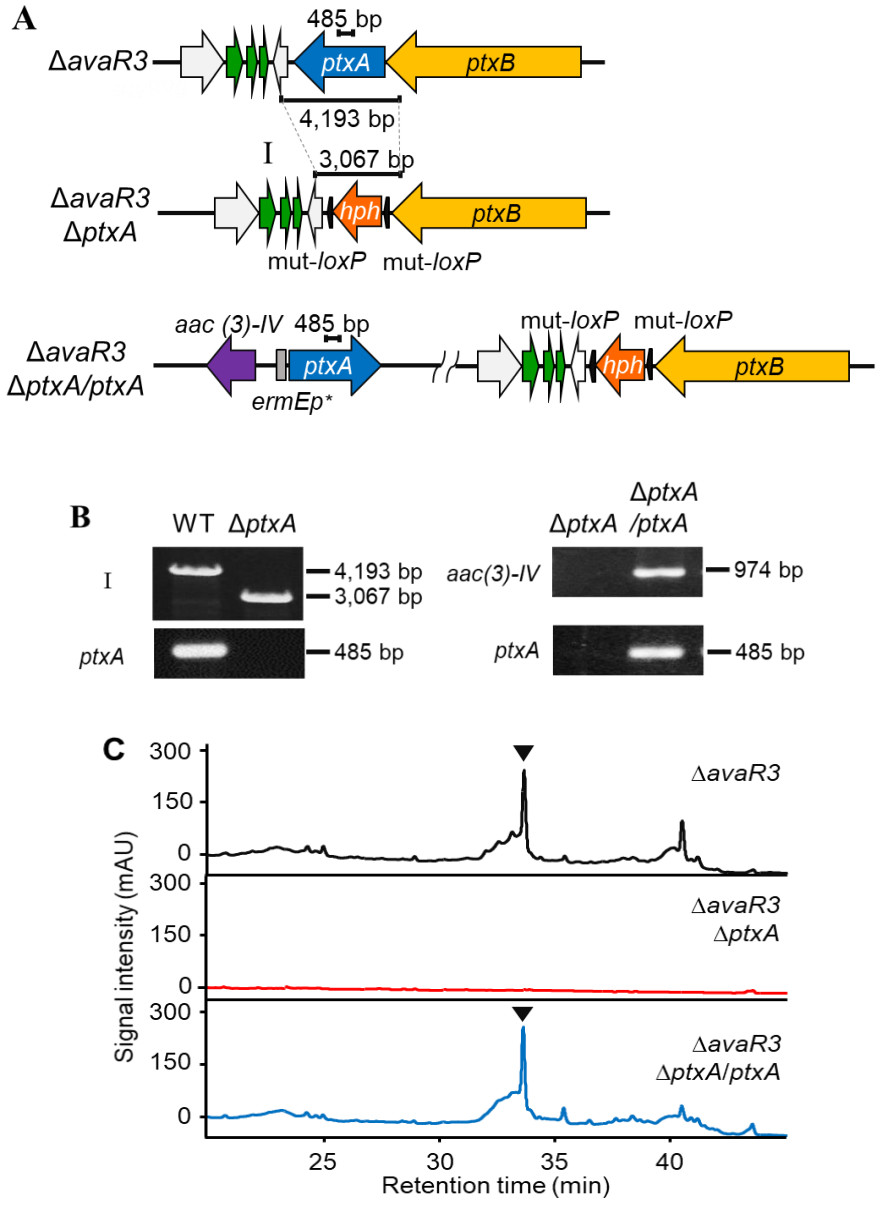

Figure 3.6. (A) General scheme of the *ptxA* gene disruption. Δ*avaR3*, *avaR3* mutant; Δ*avaR3* Δ*ptxA*, *avaR3*/*ptxA* double mutant; Δ*avaR3* Δ*ptxA*/*ptxA*, *ptxA*-complemented *avaR3*/*ptxA* double mutant. (B) Genetic verification of *ptxA* gene-disruption and its complementation by PCR The primer pair ptzA-tFw/ptzA-tRe, a fragment (4,193 bp) containing the entire *ptxA* gene or a fragment (3,067 bp) containing the mut-loxP (L)-hph-mut-loxP (R). The primer pair ptzA-Fw/ptzA-Re for the internal *ptxA* gene (485 bp), the primer pair apr-Fw/apr-Re for internal region of *aac(3)IV* gene (974 bp) (C) Production of phthoxazolin A. mAU, milliabsorbance units at 275 nm. Phthoxazolin A is represented by an inverted triangle.

3.3.3. A gene encoding a discrete AT

In the *ptx* cluster, ten PKS modules (modules 1 to 5 and 7 to 11) are encoded by three PKS genes (*ptxC*, *ptxF*, and *ptxH*) and a hybrid NRPS/PKS gene (*ptxB*). All the PKS modules are deficient of AT domains, indicating the AT activity is provided by PtxA protein. The PtxA showed two AT domains connected with an oxidoreductase domain. (Figure 3.7). It was previously reported that between two AT domains in OzmM, only second domain (OzmM-AT2) is essential for oxazolomycin biosynthesis and the first AT domain (OzmM-AT1) is redundant (132). Further analysis of the amino acid sequences of two AT domains from PtxA (PtxA-AT1 and PtxA-AT2) with other *trans*-AT enzymes showed that the PtxA-AT2 falls into the same clade as Ozm-AT2 and KirC1-AT2 distinct from PtxA-AT1. The KirC1-AT2 had been proven by biochemical analysis to load malonyl-CoA extender units to the ACPs in the kirromycin biosynthesis (143). In addition, some critical amino acid residues for acyltransferase activity are likely missing in the PtxA-AT1 (144) (substitution of Glu^{63} and His^{91} with His and Ser, respectively), this similar feature also can be observed in OzmM-AT1(132) and KirC1-AT1 (143). In conclusion, only PtxA-AT2 might provide malonyl-CoA units to the Ptx PKS modules.

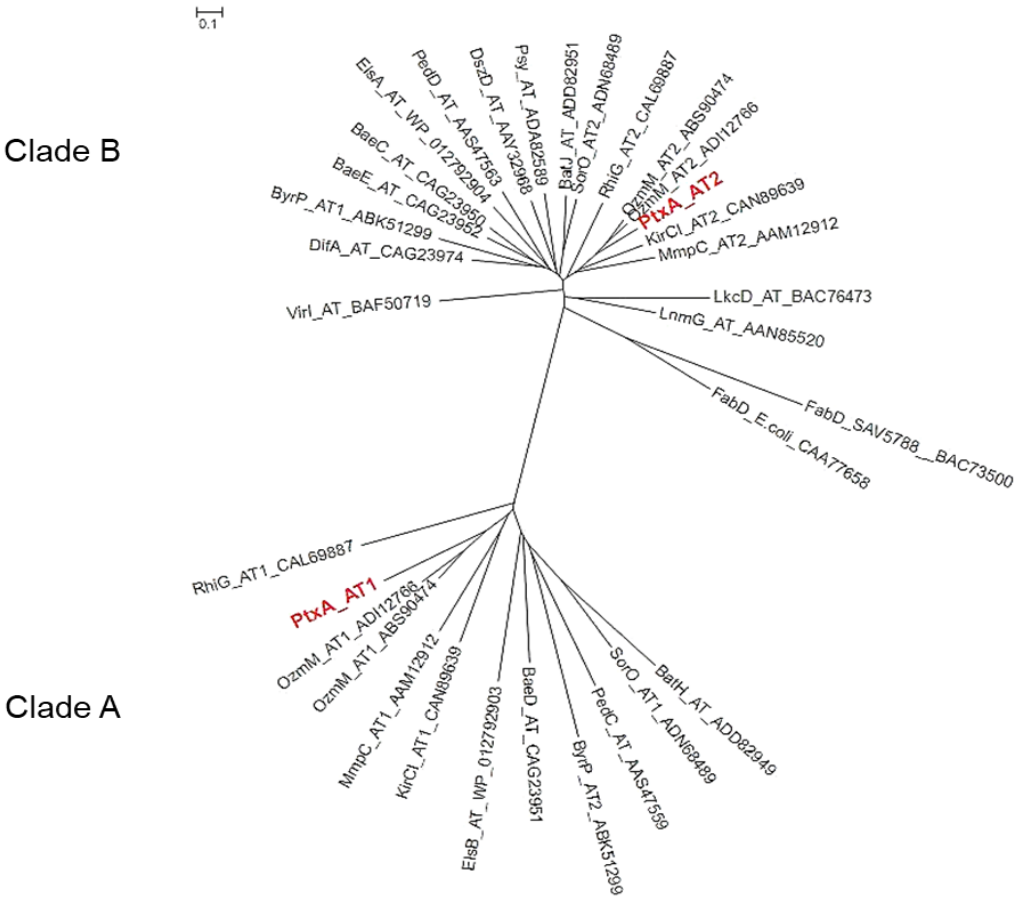

Figure 3.7. Phylogenetic analysis of AT domains of the *trans-AT* PKS system. The origin of *trans*-AT domains and their NCBI accession numbers are listed in Appendix 6

3.3.4. Genes for the assembly of polyketide

The products of PKS genes, PtxC and PtxF have high homology to OzmQ (67% identity) and OzmN (51% identity). The OzmQ and OzmN are represented by PKS modules 2, 3, 4 and necessary for generation of a triene moiety in the oxazolomycin biosynthetic machinery (132). The incorporation of a methyl group at C-2 of phthoxazolin A is due to the action of methyltransferase (MT) in PKS module 4 of PtxC, whereas the geminal methyl groups are likely incorporated by single methyltransferase domain in PKS module 5 of PtxB.

The amino acids alignment of KS domains core regions in the *ptx* cluster revealed

the presence of signature motifs and their active sites (145) (Cys-His-His, marked with asterisks) in almost all KS domains except in KS9 and KS11 which showed a mutation in the second His of active sites (substitution of His to Asn and His to Ala respectively) (Figure 3.8A). This His residue in HTGTG motif is required for decarboxylative condensation of malonyl CoA to growing PKS chain (30,145). The mutation in the KS9 and K11 indicated that those two KS domains might be non-functional; these domains were termed as non-elongating KS domains or KS^0 (30). Whereas in the ACP domains, the Ser residue in the signature motif plays an essential function as the 4'-phosphopantetheine attachment site (146), but the ACP9a of module 9 showed substitution of Ser to Trp (Figure 3.8B), indicating that this domain might be non-functional. The Rossmann fold for NADP (H)-binding (147) was observed in all seven KR domains (Figure 3.8D). In addition, a conserved catalytic triad (Ser-Tyr-Asn) (147) was observed in almost KR domain, except in KR4 and KR5 which have an atypical arrangement (Ser-Tyr-Cys for KR4 and Ser-Tyr-Ser for KR5). These alterations in the active sites have also been observed in KR domains of other *trans*-AT types I PKSs, such as those in OocL and OocR in the oocydin A biosynthesis (148), indicated that all KR domains in Ptx cluster are functional. In regard to the DH domains, the important His residue in the signature motif HXXXGXXXXP is present in all DH domains (149) (Figure 3.8C), signifying that the dehydratase (DH) domains are functionally working, and are accountable for the formation of conjugated double bonds in triene structure. In conclusion, the modules 1 to 5 of PKS appear to be involved for generating the polyketide structure of phthoxazolin A and the last PKS modules (modules 7, 8, 9, 10, and 11) might be responsible for generating an extra triene moiety.

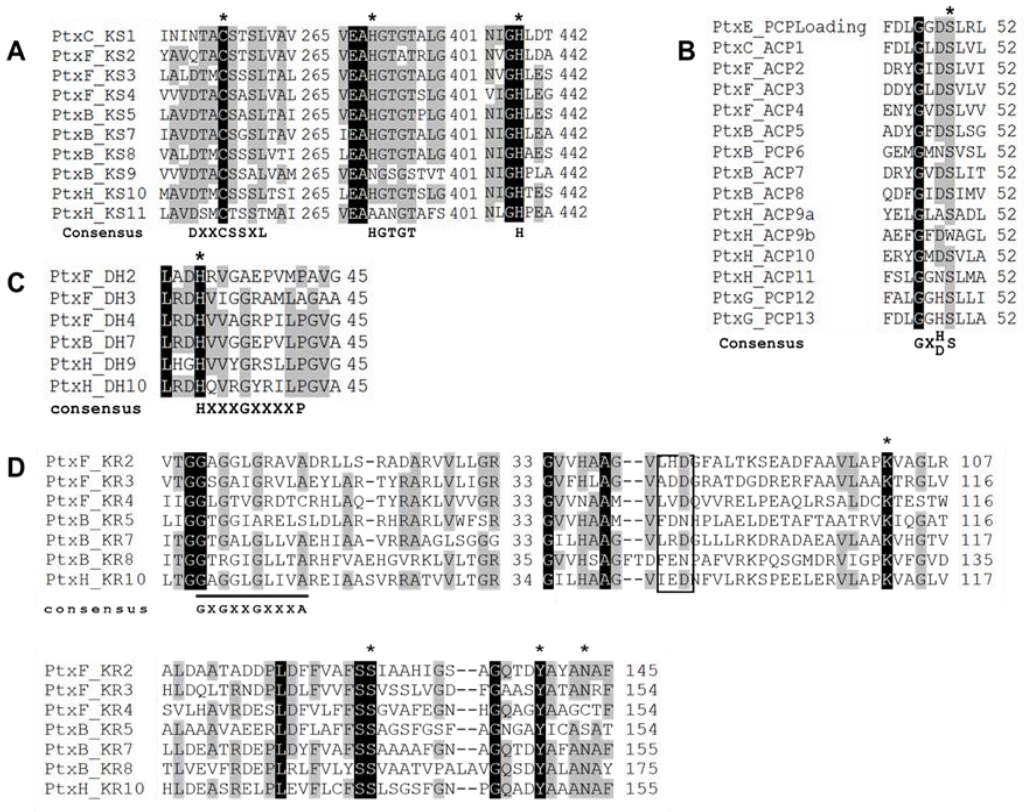

Figure 3.8. Alignment of core regions of PKSs and NRPSs domains in phthoxazolin A cluster. (A) The core regions of KS domains from PKSs (B). The core regions of ACP/PCP domains from PKSs and NRPSs (C). The core regions of DH domains from PKSs, (D) The core regions of KR domains from PKSs The catalytic residues are denoted with asterisks. The core regions for the Rossmann-binding motif in KR domains are underlined. The numbers indicate amino acid positions in each domain. The "LDD" motif for B-type KR domains is shown in a box.

3.3.5. Genes for the formation of an oxazole ring

The NRPS encoded by *ptxE* contains a formylation (F) domain, an adenylation (A) domain, and a PCP domain, which performs as loading modules to add the first amino acid into the biosynthetic machinery. Based on antiSMASH analysis (99), the A domain of PtxE is predicted to specifically activate glycine, subsequently, the PtxE-A domain loaded the activated-glycine (glycyl-S-PCP) onto the PtxE-P domain. The unique F domain in the loading module has been found in the biosynthesis of gramicidin (150), oxazolomycin (132), rhizopodin, (137), and conglobatin (135). The formylation of

glycyl-S-PCP is likely catalyzed by PtxE-F domain based on the same process in the biosynthesis of gramicidin (150).

The *ptxD* gene (Figure 3.5) shows high homology with *ozmP* from *ozm* cluster for oxazolomycin biosynthesis and *congE* for conglobatin biosynthesis, *ptxD* is located in the downstream region of the *ptxE* gene. The setup of *ptxD-ptxE* is the same as to those of *ozmO-ozmP* for oxazolomycin biosynthesis and *congA-congE* for conglobatin biosynthesis. In addition, PtxD, CongE, and OzmP possess a signature motif SGGKDS in the N-terminal which represents ATP-pyrophosphatase domain for ATP binding activity (151). The CongE had been shown to activate the amide oxygen by transferring adenyl from ATP for the formation of oxazole ring moiety in the conglobactin biosynthesis (135). Consequently, PtxD is expected to be involved in cyclodehydration of the formyl-glycyl intermediate into the oxazole.

3.3.6. Genes for the assembly of the nonribosomal peptide

Four NRPS modules are present in the *ptx* gene cluster, one module is a loading module encoded by *ptxE*, module 6 in the PKS/NRPS hybrid protein PtxB, and two modules (module 12 and 13) are part of the PtxG protein. The amino acid specificity-conferring codes of the A domains showed that glycine, serine and tyrosine are activated by PtxB-A6, PtxG-A12 and PtxG-A13 respectively. PtxB-A6 might recognize and incorporate glycine residue to generate carbamoyl moiety of phthoxazolin A. A *N*-MT domain and a cytochrome P450 domain are part of the last NRPS module (module 13) of the PtxG protein. The MT domain is predicted responsible for methylation of the Tyr residue added by PtxG-A13. The contribution of the NRPS modules 12 and 13 in phthoxazolin A biosynthesis is difficult to foresee at present because apparently the NRPS

module 6 is a final module in the phthoxazolin A assembly line based on its chemical structure.

3.3.7. Hypothetical model for biosynthesis of phthoxazolin A

Based on the bioinformatics analyses of the Ptx proteins mentioned above, a hypothetical model for the biosynthesis of phthoxazolin A was proposed (Figure 3.9). The biosynthesis of phthoxazolin A begins with glycine activation and its the assembly to the PCP domain of PtxE, subsequently, a formyl-glycyl-*S*-PCP is generated by the action of the F domain. The condensation of a malonyl-CoA into the formyl-glycyl intermediate is performed by minimal PKS module encoded by PtxC. Subsequently, the PtxD catalyzes the cyclodehydration on the intermediate. The module 2 to 5 of PtxF and PtxB incorporate four malonyl-CoA units and three methyl groups.

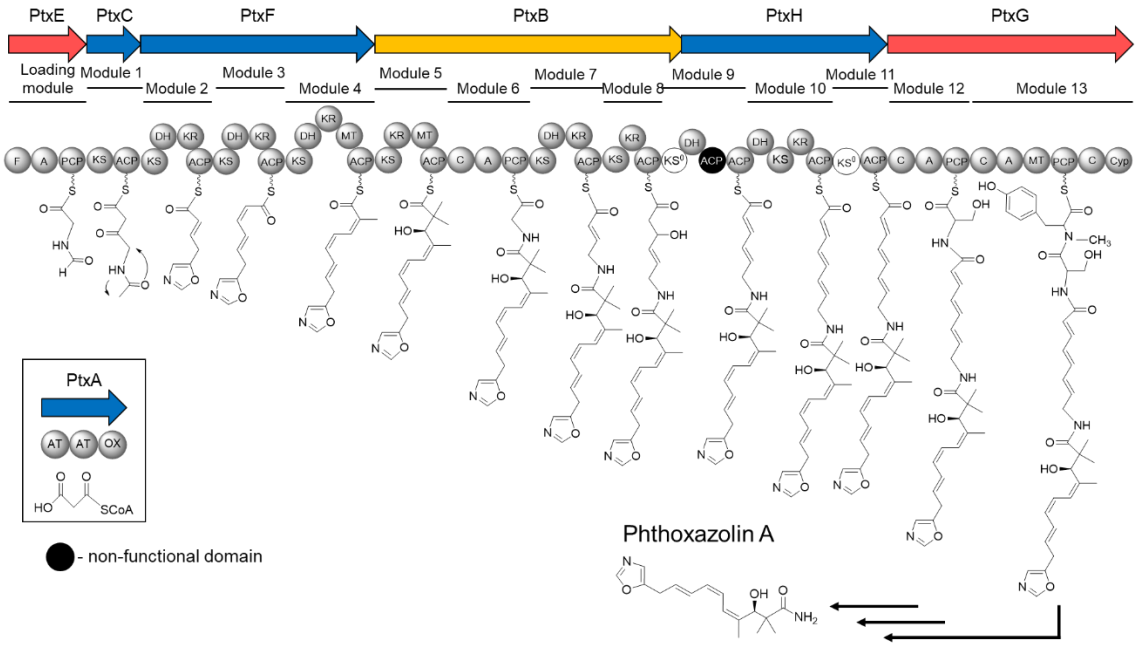

Figure 3.9. Hypothetical model for biosynthesis of phthoxazolin A. The predicted non-functional domain is shaded in black.

Three conjugated double bonds (C8-C9, C6-C7 and C4-C5) and their geometrical configuration are likely to be generated by the KR-DH domain pair in the modules 2, 3 and 4. The KR5 of PKS module 5 could be categorized as a KR domain of the partially reducing PKS due to less conserved LDD motif and lack of tryptophan residue after Ser active site (152), thus it is predicted to establish a hydroxyl group at C-3 of the phthoxazolin A in the *R* configuration. To conclude phthoxazolin A biosynthesis, a glycine residue is activated and loaded onto the polyketide intermediate to produce a carbamoyl moiety by NRPS module 6.

The PKS module 7 to 11 might generate a triene moiety, and the last two NRPS modules (module 12 and 13) might add two amino acids (Ser and *N*-Tyr) into the machinery. Nevertheless, these parts of the structures are excessive for the biosynthesis of phthoxazolin A. The release of complete chain of PKS/NRPS products from the machinery is unclear because thioesterase (TE) domain is absent in the *ptx* cluster. At last, the product produced by the *ptx* machinery should be treated by some enzymes to finalize the biosynthesis of phthoxazolin A. So far, the candidate enzyme has not been spotted in the *ptx* gene cluster or its flanking regions.

3.4. Discussion

The oxazole-containing polyketides are characterized by an oxazole-moiety connected with a polyketide structure or a hybrid peptide-polyketide structure. Only a handful biosynthetic machinery of this group of natural product had been characterized (131-137) showing the intricate pathways for the formation of heterocycles and consecutive elongation by PKSs or PKS/NRPSs. In Chapter 2, I described the activation

and the structure elucidation of a cryptic oxazole-polyketide compound, phthoxazolin A, from the original avermectin producer *S. avermitilis* KA-320. In this chapter, I have presented that strain KA-320 harbors an extrachromosomal region, which is absent in strain K139 (the genome is publicly available). Furthermore, the biosynthetic gene cluster for phthoxazolin A (*ptx* cluster) is located in the extrachromosomal of strain KA-320. The *ptx* gene cluster can be categorized as *trans*-AT type I PKS system that employs a discrete AT enzyme to provide a malonyl-CoA unit into each PKS module, unlike to the *cis*-acting AT enzyme in which a malonyl–CoA units is provided by AT domain attached to each PKS module (29-31).

The structure of phthoxazolin A is similar to the substructure of oxazolomycin. The analysis of domain function in the gene clusters showed almost identical framework with the *ozm* PKS-NRPS clusters over the first eight modules, with the exception of PKS module 7 for the phthoxazolin A biosynthesis. The Ptx proteins and their orthologue in the *ozm* cluster are 51%-71% identical. The biosynthesis of phthoxazolin A is started by formylation of the glycine residue, followed by elongation by a malonyl-CoA unit and cyclodehydration to produce an oxazole ring structure. The completion of phthoxazolin A biosynthesis requires three more malonyl-CoA units to generate a triene moiety and glycine to produce a carbamoyl moiety as the final substructure. The configuration of the conjugated triene of phthoxazolin A is designated as 4*Z*,6*Z*,8*E*. Alignment of the KR core regions in the *ptx* cluster showed that KR2, KR3, and KR4 have the signature "LDD" motif for B-type KR domains (153,154) even though their motifs diverge among each KR domains. The B-type KR domain in combination with a DH domain usually generates *trans* (*E*) double bond configuration of polyketide chain extension intermediates (147). Thus, three *trans* conjugated double bonds are estimated in the polyketide intermediate,

but they are evidently absent in phthoxazolin A structure. The foundation to alter the double bond configuration is unclear. Yet, this paradoxical aspect for the establishment of conjugated double bonds has also been spotted in oxazolomycin and chivosazol biosynthetic machinery (132, 136).

The loading module to NRPS module 6 is essential for the phthoxazolin A biosynthesis, but the *ptx* cluster has six extra modules (PKS module 7 to NRPS module 13) which might generate unknown compound and they are predicted serving as a precursor of phthoxazolin A. The PKS modules 8 and 9 contain KS-KR-ACP-KS^0 domains followed by DH-ACP domains, non-elongating KS (KS^0) domain in pair with DH domain are termed as type A bimodules for dehydration (31,155). The domain pair of KS^0-ACP as a non-elongating module is also located in PKS module 11. These kinds of A bimodule and the domain pair of KS^0-ACP are widely distributed in *trans*-AT type I PKS system (31,155). A polyketide chain extension and a condensation of amino acids are likely to be performed by modules 10 and 11, and NRPS modules 12 and 13, indicating that a larger structure than that of phthoxazolin A can be generated by *ptx* gene cluster; i.e. phthoxazolin A is a cleaved product of the unknown precursor compound. Several others metabolites in the parental strain are also abolished in the *avaR3*/*ptxA* double mutant, (Figure 3.6C): any of those metabolites can be the precursor for phthoxazolin A. The oxidative cleavage of the final product by a putative FAD-dependent monooxygenase (PedG) had been proposed to generate a pederin precursor in pederin biosynthetic pathway (156). In contrast, the *ptx* gene cluster and its adjacent regions show the absence of a FAD-dependent monooxygenase, indicating that the synthesis of phthoxazolin A may use another cleavage mechanism.

3.5. Summary

In this chapter, I found that *Streptomyces avermitilis* KA-320, the original avermectin producer, has an extrachromosomal region which contains a distinctive *trans*-AT type I PKS system for the biosynthesis of phthoxazolin A. The gene cluster extents around 99.9 kb and consists of 43 ORFs. The complete loss of phthoxazolin was observed in the Δ*ptxA* mutant, it suggests that the gene cluster involves in the biosynthesis of phthoxazolin A. Consequently, eight genes can be ascribed to the roles in phthoxazolin A biosynthesis including polyketide synthases (*ptxB*, *ptxC*, *ptxF*, and *ptxH*) with *ptxA* gene encodes acyltransferase for all PKS modules, together with nonribosomal peptide synthetase (*ptxE* and *ptxG*), hybrid polyketide synthase and nonribosomal peptide synthetase *(ptxB*) and a gene with unknown function but conserved in the oxazole-polyketide biosynthetic cluster, *ptxD*. The *ptx* assembly line shows additional PKS/NRPS modules, suggests that *S. avermitilis* is able to produce a larger compound than phthoxazolin A, thus the phthoxazolin A may be a cleaved product from the PKS/NRPS machinery.

Chapter IV

Conclusions

Streptomyces species are known as a reliable source of bioactive natural products that have shown enormous potential for the discovery of lead molecules for pharmaceutical and agricultural applications. Moreover, recently published *Streptomyces* genome sequences have revealed a much bigger biosynthetic capacity of secondary metabolites than previously understood, elevating the expectation to find a novel structure of natural products with valuable biological activities.

However, the use of this biosynthetic potential has been hampered since most of the products are not sufficiently produced under laboratory conditions. The reality that many streptomycetes possess cryptic secondary metabolite biosynthetic gene clusters has inspired the development of methods to activate and identify the products of these clusters. Thus, genome mining strategies using bioinformatics tools, molecular genetics, and analytical chemistry have been a powerful tool to facilitate the activation of cryptic secondary metabolites in the postgenomic era.

The complex regulation of secondary metabolisms in *Streptomyces* has been one of the advantages that can be manipulated to increase the titers of metabolic products in genetically amenable strains. The autoregulator signaling cascades have been a prominent regulatory mechanism for secondary metabolites' production in *Streptomyces*. Studies of the autoregulator signaling cascade for avermectin production in *Streptomyces avermitilis* led to the identification of the global regulator AvaR3, a pseudo-autoregulator receptor, which controls not only the production of avermectin but also the production of filipin

and colony development.

Given the important role of AvaR3 in secondary metabolisms, I investigated whether AvaR3 also regulates other secondary metabolites, i.e., cryptic secondary metabolites. A comparative metabolic profiling of Δ*avaR3* mutant and wild-type strain revealed that a distinct metabolite was detected clearly only in Δ*avaR3* mutant, which indicates the AvaR3 regulation on the distinct cryptic secondary metabolite (Chapter II). This metabolite was identified as phthoxazolin A, which showed broad-spectrum anti-oomycetes. The identification of phthoxazolin A from Δ*avaR3* mutant confirmed that the deletion of an autoregulator receptor homologue is indeed an effective tool to activate cryptic secondary metabolite production in *Streptomyces* species.

Unlike the production of avermectin, production of phthoxazolin A is suppressed by avenolide, a new type of *Streptomyces* hormone, via the action of AvaR3 (Chapter II). This result highlights the uniqueness of avenolide as a novel class of *Streptomyces* hormone which functions not only to elicit but also to repress secondary metabolism, similarly to IM-2, a γ-butyrolactone-type autoregulator.

During the efforts to link the production of phthoxazolin A with its corresponding biosynthetic gene cluster, the genetic differences between two wild-type strains of *Streptomyces avermitilis* (KA-320 and K139) were revealed. The KA-320 strain was sequenced and used as a template for bioinformatics analyses, which led to the identification of a plausible biosynthetic gene cluster of phthoxazolin A (*ptx* cluster) that covers a 99.9-kb DNA region encoding 43 open reading frames that are located in an extrachromosomal region of the KA-320 strain. Eight genes can be given roles in the biosynthesis of phthoxazolin A, including in polyketide assembly and nonribosomal peptide assembly for oxazole moiety and a terminal amide group, as well as several

putative regulatory functions.

The disruption of a gene encoding acyltransferase (AT), *ptxA*, caused in the total loss of phthoxazolin A production, indicating that the discreet acyltransferase is indispensable for phthoxazolin A production. Thus, the *trans*-AT PKS/NRPS-hybrid cluster is involved in the biosynthesis of phthoxazolin A (Chapter III). Consequently, based on the bioinformatics analyses described above and some relevant references, a hypothetical model for the biosynthesis of phthoxazolin A is proposed. An additional substructure which is predicted being generated from ptx cluster i.e. a bigger compound than that of phthoxazolin A is unnecessary for phthoxazolin A structure.

However, the mechanism underlying how phthoxazolin A is generated from that ancestral compound remains ambiguous (Chapter III). The identification of the phthoxazolin A gene cluster increases our understanding of the diversity and complexity of the *trans*-AT-type I PKS machinery and provides interesting perspectives for the engineering of PKS/NRP biosynthetic pathways.

The identification of phthoxazolin A is the first successful example on activation of secondary metabolism in a streptomycete by the manipulation of an autoregulator receptor homologue gene (*avaR3*) located far from the biosynthetic gene cluster of the corresponding metabolite. With the increasing numbers of *Streptomyces* genome sequences, the alteration of an autoregulator or its homologue can be applied to all streptomycetes and even beyond the genus. Thus, awakening the cryptic gene clusters is a promising establishment for the discovery of numerous novel secondary metabolites and the development of novel biosynthetic pathways.

In addition, further insights into the relationship between avenolide-signaling cascades and the biosynthesis of phthoxazolin A will advance our knowledge in the

regulation of secondary metabolite production in streptomycetes.

References

1. Wright, F. and Bibb, M. J.: Codon usage in the G+C-rich *Streptomyces* genome, Gene, 113, 55-65 (1992).
2. Chandra, G and Chater, K. F.: Developmental biology of *Streptomyces* from the perspective of 100 actinobacterial genome sequences, FEMS Microbiol. Rev., 38, 345–379 (2014).
3. Chater, K. F., Biro, S., Lee, K. J., Palmer, T., and Schrempf, H.: The complex extracellular biology of *Streptomyces*, FEMS Microbiol. Rev., 34, 171–198 (2010).
4. Yamada, Y., Kuzuyama, T., Komatsu, M., Shin-Ya, K., Omura, S., Cane, D. E., and Ikeda, H.: Terpene synthases are widely distributed in bacteria. Proc. Natl. Acad. Sci. USA, 112, 857–862 (2015).
5. Seipke, R. F., Kaltenpoth, M., and Hutchings, M. I.: *Streptomyce*s as symbionts: an emerging and widespread theme? FEMS Microbiol. Rev., 36, 862–876, (2012).
6. van der Meij, A., Worsley, S. F., . Hutchings, M. I., and van Wezel, G. P.: Chemical ecology of antibiotic production by actinomycetes. FEMS Microbiol. Rev., 41, 392–416 (2017).
7. Loria, R., Bukhalid, R. A., Fry, B. A., and King, R. R.: Plant pathogenicity in the genus *Streptomyces*, Plant Dis., 81, 836-846 (1997).
8. Kirby, R., Sangal, V., Tucker, N. P., Zakrzewska-Czerwinska, J., Wierzbicka, K., Herron, P.R., Chu, C. J., Chandra, G., Fahal, A. H., Goodfellow, M., and Hoskisson, P. A.: Draft genome sequence of the human pathogen *Streptomyces somaliensis*, a significant cause of actinomycetoma, J. Bacteriol., 194, 3544-3545(2012).
9. Quintana, E. T., Wierzbicka, K., Mackiewicz, P., Osman, A., Fahal, A. H., Hamid, M.E., Zakrzewska-Czerwinska, J., Maldonado, L. A., and Goodfellow, M.: *Streptomyces sudanensis* sp. nov., a new pathogen isolated from patients with actinomycetoma, Antonie Van Leeuwenhoek, 93,305–313 (2008).
10. Kofteridis, D. P., Maraki, S., Scoulica, E., Tsioutis, C., Maltezakis, G., Gikas, A.: *Streptomyces* pneumonia in an immunocompetent patient: a case report and literature review *Streptomyces* pneumonia in an immunocompetent patient: a case report and literature review, Diagn. Microbiol. Infect. Dis., 59,459-462(2007).

11. Berdy, J.: Thoughts and facts about antibiotics: Where we are now and where we are heading, J. Antibiot. (Tokyo), 65, 385–395 (2012).
12. Katz, L. and Baltz, R.H: Natural product discovery, J. Ind. Microbiol. Biotchnol., 43, 155-176 (2016).
13. Flärdh, K., and Buttner. M. J.: *Streptomyces* morphogenetics: dissecting differentiation in a filamentous bacterium, Nat Rev Microbiol, 7:36–49 (2009).
14. Kiesser, T. Bibb, M. J., Buttner, M. J., Charter, K. F., and Hopwood, D. A.: Practical *Streptomyces* Genetics, The John Innes Foundation (2000).
15. Miguélez, E. M, García M, Hardisson, C, Manzanal, M. B.: Autoradiographic study of hyphal growth during aerial mycelium development in *Streptomyces antibioticus*. J. Bacteriol., 176, 2105-2107(1994).
16. Miguélez, E. M, Hardisson, C, Manzanal, M. B.: Streptomycetes: a new model to study cell death, Int. Microbiol., 3,153-158(2000).
17. Jones, S. E., Ho, L., Rees, C. A., Hill, J. A., Nodwell, J. R., and Elliot, M. A.: *Streptomyces* exploration is triggered by fungal interactions and volatile signals. eLife 6:e21738. DOI: 10.7554/eLife.21738 (2017).
18. Bibb, M.: The regulation of antibiotic production in *Streptomyces coelicolor* A3(2), Microbiology, 142, 1335-1334(1996).
19. Bibb, M. J.: Regulation of secondary metabolism in streptomycetes, Curr. Opin. Microbiol., 8, 208-215 (2005).
20. Challis, G.L. and Hoopwood, D.A.: Synergy and contingency as driving forces for the evolution of multiple secondary metabolite production by *Streptomyces* species. Proc. Natl. Acad. Sci. USA, 100, 14555-14561(2003).
21. Niu, G, Chater, C. F, Tian, Y., Zhang, J. and Tan, H.: Specialised metabolites regulating antibiotic biosynthesis in *Streptomyces* spp., FEMS Microbiol. Rev., 40, 554–573 (2016).
22. Tribewal, N., and Tang, Y.: Biocatalyst for natural product biosynthesis, Annu Rev Chem Biomol Eng.,5,347-66 (2014).
23. Nett, M., Ikeda, H., and Moore, B. S.: Genomic basis for natural product biosynthetic diversity in the actinomycetes, Nat. Prod. Rep., 26, 1362–1384 (2009).
24. Fisch, K. M.: Biosynthesis of natural products by microbial iterative hybrid PKS–NRPS, RSC Adv., 3, 18228-18247(2013).

25. Weissman, K.: Introduction to polyketide biosynthesis, in Method of Enzymology vol 259, 3-16 ed. D.Hoopwood.(2009)
26. Shen, B.: Polyketide biosynthesis beyond the typeI, II and III polyketide synthase paradigms.Curr. Opin. Chem. Biol., 7, 285-295 (2003).
27. Hertweck, C.: The biosynthetic logic of polyketide diversity, Angew. Chem. Int. Ed., 48, 4688 – 4716 (2009).
28. Olano, C., Mendez, C, Salas, J. A.: Post-PKS tailoring steps in natural product-producing actinomycetes from the perspective of combinatorial biosynthesis, Nat. Prod. Rep., 27, 571–616 (2010).
29. Cheng, Y. Q., Coughlin, J. M., Lim, S. K., and Shen, B.: Type I polyketide synthases that require discrete acyltransferases, pp. 165-186 in D. A. Hopwood (Ed), Methods in Enzymology, vol. 459, Elsevier Inc. (2009).
30. Helfrich E. J. N. and Piel, J.: Biosynthesis of polyketides by *trans*-AT polyketide synthases, Nat. Prod. Rep., 33, 231-316 (2016).
31. Hertweck, C: Decoding and reprogramming complex polyketide assembly lines: prospects for synthetic biology, Trends in Biochem. Sci.,40,189-199 (2015).
32. Condurso, H. L. and Bruner, S. D.: Structure and non-canonical chemistry of nonribosomal peptide biosynthetic machinery, Nat. Prod. Rep., 29, 1099-1110 (2012).
33. Stachelhaus, T., Mootz, H. D., and Marahiel, M. A.: The specificity-conferring code of adenylation domains in nonribosomal petide synthetases, Chemistry and Biology, 6, 493-505 (1999).
34. Marahiel, M. A.: Working outside the protein-synthesis rules: insight into non-ribosomal peptide synthesis, J. Pept. Sci., 15, 799-807 (2009).
35. Walsh, C. T., Chen, H., Keating, T. A, Hubbard, B. K., Losey,H. C., Luo, L., Marshall, C. G., Miller, D. A, and Patel, H. M.: Tailoring enzymes that modify nonribosomal peptides during and after chain elongation on NRPS assembly lines, Curr. Opin. Chem. Biol., 5, 525–534 (2001).
36. Van Wezel, G. P and McDowall, K.: The regulatory of the secondary metabolism of *Streptomyces* : new links and environmental advances, Nat. Prod. Rep., 28, 1311-1333 (2011).
37. Ruiz, B, Chávez, A, Forero, A., García-Huante, Y., Romero, A., Sánchez, M., et al:

Production of microbial secondary metabolites: Regulation by the carbon source, Critical Rev. in Microbiol., 36, 146–167(2010).

38. Rigali, S., Titgemeyer, F., Barends, S., Mulder, S., Thomae, A.W., Hopwood, D.A., and van Wezel, G.P.: Feast or famine: the global regulator DasR links nutrient stress to antibiotic production by Streptomyces, EMBO Rep., 9, 670-675 (2008).
39. Hesketh, A., Sun, J., and Bibb, M.J.: Induction of ppGpp synthesis in *Streptomyces coelicolor* A3(2) grown under conditions of nutrional sufficiency elicits *actII-ORF4* transcription and actinorhodin biosynthesis, Mol. Microbiol., 39, 136-144, (2001).
40. Martin, J. F., Sola-Landa, A., Santos-Beneit, F., Fernandez-Martinez, L. T., Prieto, C., and Rondriguez-Garcia, A.: Cross-talk global nutritional regulator in control of primary and secondary metabolism in *Streptomyces*, Microb. Biotechnol., 4, 165-174 (2011).
41. Borodina, I., Siebring, J., Zhang, .J, Smith, C. P., van Keulen, G., Dijkhuizen, L., and Nielsen, J., Antibiotic overproduction in *Streptomyces coelicolor* A3 (2) mediated by phosphofructokinase deletion, J. Biol. Chem., 283, 25186-25199 (2008).
42. Rodríguez, H., Rico, S., Díaz, M., and Santamaría, R. I.: Two-component systems in *Streptomyces*: key regulators of antibiotic complex pathways, Microbial Cell Factories, 12, 127 (2013).
43. Anderson, T. B., Brian, P., and Champness, W. C.: Genetic and transcriptional analysis of *absA*, an antibiotic gene cluster-linked two-component system that regulates multiple antibiotics in *Streptomyces coelicolor*, Mol Microbiol., 39, 553-66 (2001).
44. Floriano, B., Bibb. M.: afsR is a pleiotropic but conditionally required regulatory gene for antibiotic production in *Streptomyces coelicolor* A3(2), Mol. Microbiol. 21, 385–396, (1996).
45. Horinouchi S.: AfsR as an integrator of signals that are sensed by multiple serine/threonine kinases in *Streptomyces coelicolor* A3(2), J. Ind. Microbiol. Biotechnol., 30, 462- 467 (2003).
46. Wietzorreck, A and Bibb, M.: A novel family of proteins that regulates antibiotic production in streptomycetes appear to contain an OmpR-like DNA-binding fold, Mol. Microbiol., 25, 1181–1184 (1997).
47. Liu, G.,Charter, K. F., Chandra, G.,Niu, G, and Tan , H.: Molecular regulation of

antibiotic biosynthesis in *Streptomyces*, Microbiol Mol Biol Rev., 77, 112–143 (2013).

48. Martin, J. F., and Liras, P.: Engineering of regulatory cascades and networks controlling antibiotics biosynthesis in *Streptomyces*, Curr. Opin. Microbiol., 13, 263-273 (2010).
49. Wilson, D.J., Xue, Y., Reynolds, K.A., and Sherman, D.H.: Characterization and analysis of the PikD regulatory factor in the pikromycin biosynthetic pathway of *Streptomyces venezuelae*, J. Bacteriol., 183, 3468-3475 (2001).
50. Kitani, S., Ikeda, H., Sakamoto, T., Noguchi, S., and Nihira, T.: Characterization of a regulatory gene, *aveR*, for the biosynthesis of avermectin in *Streptomyces avermitilis*, Appl. Microbiol. Biotechnol., 82, 1089-96 (2009).
51. Kuscer, E., Coates, N., Challis, I., Gregory, M., Wilkinson, B., Sheridan, R., Petković, H.: Roles of rapH and rapG in positive regulation of rapamycin biosynthesis in *Streptomyces hygroscopicus*, J .Bacteriol., 189, 4756-4763 (2007).
52. Zhang, Y., He, H., Liu, H., Wang, H., Wang, X., and Xiang, W.: Characterization of a pathway-specific activator of milbemycin biosynthesis and improved milbemycin production by its overexpression in *Streptomyces bingchenggensis*, Microbial Cell Factories, 52, 1-15 (2016).
53. Takano, E.: γ-Butyrolactones: *Streptomyces* signaling molecules regulating antibiotic production and differentiation, Curr. Opin. Microbiol., 9, 287-294 (2006).
54. Willey, J. M., and Gaskell, A. A: Morphogenetic signaling molecules of the streptomycetes, Chem. Rev., 111, 174-187 (2011).
55. Sidda, J. D., Poon, V., Song, L., Wang, W., Yang, K., and Corre, C.: Overproduction and identification of butyrolactones SCB1-8 in the antibiotic production superhost *Streptomyces* M1152, Org. Biomol. Chem., 14, 6390-6393 (2016).
56. Thao, N. B., Kitani, S., Nitta, H., Tomioka, T., Nihira, T.: Discovering potential *Streptomyces* hormone producers by using disruptant of essential biosynthetic gene as indicator strains, J. Antibiot. (Tokyo), http//doi:10.1038/ja.2017.85
57. Corre, C., Song, L., O'Rourke, S., Chater, K. F., Challis, G. L.: 2-Alkyl-4-hydroxymethylfuran-3-carboxylic acids, antibiotic production inducers discovered by *Streptomyces coelicolor* genome mining, Proc. Natl. Acad. Sci. USA. ,105, 17510-17515(2008).

58. Kitani, S., Miyamoto, K. T., Takamatsu, S., Herawati, E., Iguchi, H., Nishitomi, K., Uchida, M., Nagamitsu, T., Omura, S., Ikeda, H., and Nihira, T.: Avenolide, a *Streptomyces* hormone controlling antibiotic production in *Streptomyces avermitilis*, Proc. Natl. Acad. Sci. USA, 108, 16410-16415 (2011).
59. Arakawa, K., Tsuda, N., Taniguchi, A, and Kinashi, H.: The butenolide signaling molecules SRB1 and SRB2 induce lankacidin and lankamycin production in *Streptomyces rochei*, ChemBioChem, 13, 1447-1457 (2012).
60. Xu, G., Wang, J., Wang, L., Tian, X., Yang, H., Fan, K., Yang, K., and Tan, H.: "Pseudo" gamma-butyrolactone receptors respond to antibiotic signals to coordinate antibiotic biosynthesis, J. Biol .Chem., 285,27440-27448 (2010).
61. Ohnishi, Y., Yamazaki, H., Kato, J.Y., Tomono, A., and Horinouchi, S.: AdpA, a central transcriptional regulator in the A-factor regulatory cascade that leads to morphological development and secondary metabolism in *Streptomyces griseus*, Biosci. Biotechnol .Biochem., 69,431-439 (2005).
62. Bentley, S. D., Chater, K. F., Cerdeño-Tárraga, A. M., Challis, G. L., Thomson, N. R., James, K. D., Harris, D. E., Quail M. A., Kieser, H., Harper, D., and other 33 authors: Complete genome sequence of the model actinomycete *Streptomyces coelicolor* A3(2), Nature, 417, 141-147 (2002).
63. Omura, S., Ikeda, H., Ishikawa, J., Hanamoto, A., Takahashi, C., Shinose, M., Takahashi, Y., Horikawa, H., Nakazawa, H., Osonoe, T., Kikuchi, H., Shiba, T., Sakaki, Y., and Hattori, M.: Genome sequence of industrial microorganism *Streptomyces avermitilis*: deducing ability of producing secondary metabolites, Proc. Natl. Acad. Sci. USA, 98, 12215–12220 (2001).
64. Ohnishi, Y., Ishikawa, J., Hara, H., Suzuki, H., Ikenoya, M., Ikeda, H., Yamashita, A., Hattori, M., and Horinouchi, S.: Genome sequence of the streptomycin-producing microorganism *Streptomyces griseus* IFO 13350, J. Bacteriol., 190, 4050-4060 (2008).
65. Craney, A., Ahmed, S, and Nodwell, J.: Towards a new science of secondary metabolism, J. Antibiot. (Tokyo), 66, 387-400 (2013).
66. Baltz, R. H.: Gifted microbes for genome mining and natural product discovery, J. Ind. Microbiol. Biotechnol., 44, 573-588 (2017).
67. Scherlach, K. and Hertweck, C.: Triggering cryptic natural product biosynthesis in

microorganisms, Org. Biomol. Chem., 87, 1753–1760 (2009).

68. Rutledge, P. J. and Challis, G. L.: Discovery of microbial natural products by activation of silent biosynthetic gene clusters, Nat. Rev. Microbiol., 13, 509–523 (2015).
69. Medema, M. H. and Fischbach, M. A.: Computational approaches to natural product discovery, Nat. Chem. Bio., 11,639-648 (2015).
70. Bode, H. B., Bethe, B., Hofs, R., and Zeeck, A.: Big efffects from small changes: possible ways to explore nature's chemical diversity, ChemBioChem., 3, 619 -627 (2002).
71. Schiewe, H. J and Zeeck, A.: Cineromycins, gamma-butyrolactones and ansamycins by analysis of the secondary metabolite pattern created by a single strain of *Streptomyces*, J Antibiot (Tokyo), 52, 635-642 (1999).
72. Rateb, M. E., Houssen, W. E., Harrison, W. T. A. Deng, H. Okoro, C. K., and Asenjo,J. A. et al: Diverse metabolic profiles of a *Streptomyces* strain isolated from a hyper-arid environment molecules J. Nat. Prod., 74, 1965–1971 (2011).
73. Hoz, J. F, Méndez, C., Salas, J. A, and Olano, C.: Novel bioactive paulomycin derivatives produced by *Streptomyces albus* J1074, Molecules, 22, (2017) doi: 10.3390/molecules22101758
74. Tanaka, Y., Hosaka, T., and Ochi, K.: Rare earth elements activate the secondary metabolite-biosynthetic gene clusters in *Streptomyces coelicolor* A3(2), J Antibiot (Tokyo), 63,477-481 (2010).
75. Shi, Y., Pan, C., Auckloo, B. N., Chen, X., Chen, C. A, Wang, K., Wu, X., Ye, Y., Wu, B.: Stress-driven discovery of a cryptic antibiotic produced by *Streptomyces* sp. WU20 from Kueishantao hydrothermal vent with an integrated metabolomics strategy, Appl. Microbiol. Biotechnol., 101,1395-1408 (2017).
76. Craney, A., Ozimok, C., Pimentel-Elardo, S.M, Capretta, A., Nodwell, J. R.: Chemical perturbation of secondary metabolism demonstrates important links to primary metabolism, Chem. Biol., 19, 1020-1027 (2012).
77. Onaka, H., Mori, Y., Igarashi, Y., and Furumai, T.: Mycolic acid-containing bacteria induce natural-product biosynthesis in *Streptomyces* species, Appl. Environ. Microbiol., 77, 400-406 (2011).
78. Ochi, K: From microbial differentiation to ribosome engineering, Biosci.Biotechnol.

Biochem., 71, 1373-1386 (2007).

79. Wang, G., Hosaka, T., and Ochi, K.: Dramatic activation of antibiotic production in *Streptomyces coelicolor* by cumulative drug resistance mutations, Appl. Environ. Microbiol., 74, 2834-2840 (2008).
80. Ochi, K. and Hosaka, T.: New strategies for drug discovery: Activation of silent or weakly expressed microbial gene clusters. Appl. Microbiol. Biotechnol., 97,87–98. (2013).
81. Hosaka, T., Ohnishi-Kaneyama, M., Muramatsu, H., Murakami, K., Tsurumi, Y., Kodani, S., Yoshida, M., Fujie, A. and Ochi, K.: Antibacterial discovery in actinomycetes strains with mutations in RNA polymerase or ribosomal protein S12, Nature Biotechnol., 27, 462-464 (2009).
82. Hosaka, T, Xu, J, and Ochi, K., Increased expression of ribosome recycling factor is responsible for the enhanced of protein synthesis during the late growth phase in antibiotic–overproducing *Streptomyces coelicolor* ribosomal *rpsL* mutant. Mol. Microbiol., 61, 883-897 (2006).
83. Hu, H., Zhang, Q., and Ochi, K., Activation of antibiotic biosynthesis by specified mutations in the *rpoB* gene (encoding the RNA polymerase β Subunit) of *Streptomyces lividans*, J. Bacteriol., 184, 3984-399 (2002).
84. Gomez-Escribano, J. P., Song, L., Fox, D. J., Yeo, V., Bibb, M. J., and Challis, G. J.: Structure and biosynthesis of the unusual polyketide alkaloid coelimycin P1, a metabolic product of the *cpk* gene cluster of *Streptomyces coelicolor* M145, Chem. Sci., 3, 2716-2720 (2012).
85. McKenzie, N. L., Thaker, M., Koteva, K., Hughes, D.W., Wright, G.D., Nodwell, J.R.: Induction of antimicrobial activities in heterologous streptomycetes using alleles of the *Streptomyces coelicolor* gene *absA1*, J. Antibiot (Tokyo), 63, 177-182 (2010).
86. Kalan, L., Gessner, A., Thaker, M. N., Waglechner, N., Zhu, X., Szawiola, A., Bechthold, A., Wright, G. D., and Zechel, D. L.: A cryptic polyene biosynthetic gene cluster in *Streptomyces calvus* is expressed upon complementation with a functional *bldA* gene, Chem. Biol., 20, 1214-1224 (2013).
87. Ohnishi, Y., Yamazaki, H., Kato, J., Tomono, A, and Horinouchi, S.: AdpA, a central transcriptional regulator in A-factor regulatory cascade that leads to morphological

development and secondary metabolism in *Streptomyces griseus*, Biosci. Biotechnol. Biochem., 69, 431-439 (2005).

88. Xu, J., Zhang, J., Zhuo, J., Li, Y., Tian, Y., and Tan, H.: Activation and molecular mechanism of a cryptic oviedomycin biosynthetic gene cluster via the disruption of a global regulatory gene-adpA in *Streptomyces ansochromogenes*, J. Biol. Chem., 87, 19708-19720 (2017)
89. Laureti, L., Song, L., Huang, S., Corre, C., Leblond, P., Challis, G. L., and Aigle, B.: Identification of a bioactive 51-membered macrolide complex by activation of a silent polyketide synthase in *Streptomyces ambofaciens*, Proc. Natl. Acad. Sci. USA, 108, 6258-6263 (2011).
90. Olano, C., García, I., González, A., Rodriguez, M., Rozas, D., Rubio, J., et al : Activation and identification of five clusters for secondary metabolites in *Streptomyces albus* J1074, Microb Biotechnol., 7, 242-256 (2014).
91. Du, D., Katsuyama,Y,, Onaka, H., Fujie, M., Satoh, N., Shin-Ya, K., and Ohnishi, Y.: Production of a novel amide-containing polyene by activating a cryptic biosynthetic gene cluster in *Streptomyces* sp. MSC090213JE08, ChemBioChem, 17, 1464-1471(2016).
92. Sekurova, O. N., Pérez-Victoria, I., Martín, J., Degnes, K. F., Sletta, H., Reyes, F., and Zotchev, S. B.: New deferoxamine glycoconjugates produced upon overexpression of pathway-specific regulatory gene in the marine sponge-derived *Streptomyces albus* PVA94-07, Molecules, 21, doi:10.3390/molecules21091131 (2016).
93. Bunet, R., Song, L., Mendes M. V., Corre, C., Hotel, L., Rouhier, N., Framboisier, X., Leblond, P., Challis, G. L., and Aigle, B. : Characterization and manipulation of the pathway-specific late regulator AlpW reveals *Streptomyces ambofaciens* as new producer of kinamycins, J. Bacteriol., 193, 1142-1153 (2011).
94. Gottlet, M., Kol, S., Gomez-Escribano, J. P., Bibb, M., and Takano, E.: Deletion of a regulatory gene within *cpk* cluster reveals novel antibacterial activity in *Streptomyces coelicolor* A3 (2), Microbiology, 156, 2343-2353 (2010).
95. Kunitake, H., Hiramatsu, T., Kinashi, H., and Arakawa, K.: Isolation and biosynthesis of an azoxyalkene compound produced by a multiple gene disruptant of *Streptomyces rochei*. ChemBioChem., 16, 2237-2243 (2015).

96. Sidda, J. D., Song, L.,Poon, V., Al-Bassam, M., Lazos, O., Buttner, M. J., Challis, G. J., and Corre, C.: Discovery of a family of γ-aminobutyrate ureas via rational derepression of a silent bacterial gene cluster, Chem. Sci., 5, 86-89 (2014).
97. Aroonsri, A., Kitani, S., Ikeda, H., and Nihira, T.: Kitasetaline, a novel β-carboline alkaloid from *Kitasatospora setae* NBRC 14216T, J. Biosci. Bioeng., 114, 56 -58 (2012).
98. Aroonsri, A., Kitani, S., Hashimoto, J., Kosone, I., Izumikawa, M., Komatsu, M., Fujita, N., Takahashi, Y., Shin-ya, K., Ikeda, H., and Nihira, T.: Pleiotropic control of secondary metabolism and morphological development by KsbC, a butyrolactone autoregulator receptor homologue in *Kitasatospora setae*, Appl. Environ. Microbiol., 78, 8015-8024 (2012).
99. Weber, T., Blin, K., Duddela, S., Krug, D., Kim, H. U., Bruccoleri, R., Lee, S. Y., Fischbach, M. A.,Müller, R., Wohlleben, W., Breitling, R., Takano, E, and Medema, M. A.: antiSMASH 3.0 - a comprehensive resource for the genome mining of biosynthetic gene clusters, Nucleic Acids Res., 43, W237-W243 (2015).
100. Ziemert, N., Alanjary, M., and Weber, T.: The evolution of genome mining in microbes-a review, Nat. Prod. Rep., 33, 988-1005 (2016).
101. Komatsu, M., Uchiyama, T., Omura, S., Cane, D. E., and Ikeda, H.: Genome-minimized *Streptomyces* host for the heterologous expression of secondary metabolism, Proc. Nat., Acad. Sci. USA, 107, 7422 – 7427 (2010).
102. Gomez-Escribano, J. P., and Bibb, M. J.: Engineering *Streptomyces coelicolor* for heterologous expression of secondary metabolite gene clusters, Microbiol. Biotechnol., 4,207-215 (2011).
103. Nah, H. J., Pyeon, H. R, Kang, S. H., Choi, S. H.,and Kim, E. S., Cloning and heterologous expression of a large-sized natural product biosynthetic gene cluster in *Streptomyces* species, Front. Microbiol., doi.org/10.3389/fmicb.2017.0039415 (2017).
104. Ikeda, H., Shin-ya, K., and Omura, S.: Genome mining of *Streptomyces avermitilis* genome and development of genome-minimized host for heterologous expression of biosynthetic gene clusters, J. Ind. Microbiol. Biotechnol., 41, 233-250 (2014).
105. Komatsu, M., Komatsu, K., Koiwai, H., Yamada, Y., Kozone, I., Izumikawa, M., Hashimoto, J., Takagi, M., Omura, S., Shin-ya, K., Cane, D. E, and Ikeda, H.:

Engineered *Streptomyces avermitilis* host for heterologous expression of biosynthetic gene cluster for secondary metabolites, ACS Synth. Biol., 2, 384-96 (2013).

106. Gomez-Escribano, J. P., and Bibb, M. J.: Heterologous expression of natural product biosynthetic gene clusters in *Streptomyces coelicolor*: from genome mining to manipulation of biosynthetic pathways, J. Ind. Mocrobiol. Biotechnol., 41, 425-431 (2014).
107. Castro, J. F, Razmilic, V, Gomez-Escribano, J. P, Andrews, B., Asenjo, J.A., and Bibb M. J.: Identification and heterologous expression of the chaxamycin biosynthesis gene cluster from *Streptomyces leeuwenhoekii*, Appl Environ Microbiol., 81, 5820-5831 (2015).
108. Yamada, Y., Arima, S., Nagamitsu, T., Johmoto, K., Uekusa, H., Eguchi, T., Shin-ya, K., Cane, D. E., and Ikeda, H.: Novel terpenes generated by heterologous expression of bacterial terpene synthase genes in an engineered *Streptomyces* host, J Antibiot (Tokyo), 68,385-394 (2015).
109. Park, O. K., Choi, H. Y., Kim, G.W., and Kim, W. G.: Generation of new complestatin analogues by heterologous expression of the complestatin biosynthetic gene cluster from *Streptomyces chartreusis* AN1542, ChemBioChem., 17,1725-1731 (2016).
110. Saha, S, Zhang, W., Zhang, G., Zhu, Y., Chen, Y., Liu, W., Yuan, C., Zhang, Q., Zhang H.,, Zhang, L., Zhang, W., and Zhang, C.: Activation and characterization of a cryptic gene cluster reveals a cyclization cascade for polycyclic tetramate macrolactams, Chem. Sci.,8,1607-1612 (2017).
111. Pait, I.G.U, Kitani, S., Roslan, F.W., Ulanova, D., Arai, M., Ikeda, H., and Nihira, T.: Discovery of a new diol-containing polyketide by heterologous expression of a silent biosynthetic gene cluster from *Streptomyces lavendulae* FRI-5, J. Ind. Microbiol. Biotechnol., 45, 77-87 (2018).
112. Burg, R.W., Miller, B.M., Baker, E.E., Birnbaum, J., Currie, S. A., Hartman R. et al : Avermectins, new family of potent anthelmintic agents: producing organism and fermentation, Antimicrob. Agents Chemother., 15,361-367(1979).
113. Õmura, S. and Crump, A.: The life and times of ivermectin- a success story, Nat. Rev. Microbiol., 2, 984-989 (2004).
114. Chabala, J. C., Mrozik. H., Tolman, R.L., Eskola, P., Lusi, A., Peterson, L.H et al.:

Ivermectin, a new broad-spectrum antiparasitic agent, J. Med. Chem., 23,1134-1136 (1980).

115. Crump, A and Omura, S.: Ivermectin, 'Wonder drug' from Japan: the human use perspective, Proc. Jpn. Acad., Ser. B, 87,13-28 (2011).

116. Crump, A.: Ivermectin: enigmatic multifaceted 'wonder' drug continues to surprise and exceed expectations, J. Antibiot.(Tokyo) 70, 495–505 (2017).

117. Ikeda, H., Ishikawa, J., Hanamoto, A., Shinose, M., Kikuchi, H., Shiba, T. et al: Complete genome sequence and comparative analysis of the industrial microorganism *Streptomyces avermitilis*, Nat. Biotechnol., 21,526-531 (2003).

118. Sultan, S. P., Kitani, S., Miyamoto, K. T., Iguchi, H., Atago, T., Ikeda, H., and Nihira, T.: Characterization of AvaR1, a butenolide-autoregulator receptor for biosynthesis of a *Streptomyces* hormone in *Streptomyces avermitilis*, Appl. Microbiol. Biotechnol., 100, 9581-9591 (2016).

119. Miyamoto, K. T., Kitani, S., Komatsu, M., Ikeda, H., and Nihira, T.: The autoregulator receptor homologue AvaR3 plays a regulatory role in antibiotics production, mycelial aggregation and colony development of *Streptomyces avermitilis*, Microbiology, 157, 2266-2275 (2011).

120. Sakihama, Y., Shimai, T., Sakasai, M., Ito, T., Fukushi, Y., Hashidoko, Y., and Tahara, S.: A photoaffinity probe designed for host-specific signal flavonoid receptors in phytopathogenic Peronosporomycete zoospores of *Aphanomyces cochlioides*, Arch. Biochem. and Biophys., 432, 145-151 (2004).

121. Espinel-Ingroff, A.: Comparison of three commercial assays and a modified disk diffusion assay with two broth microdilution reference assays for testing *Zygomycetes*, *Aspergillus* spp., *Candida* spp., and *Cryptococcus neoformans* with posaconazole and amphotericin B, J. Clin. Microbiol., 40, 3616-3622 (2006).

122. Mukaihara, T., Tamura, N., Murata, Y., and Iwabuchi, M.: Genetic screening for Hrp type III-related pathogenicity genes controlled by HrpB transcriptional activator in *Ralstonia solanacearum*, Mol. Microbiol., 54, 863-875 (2004).

123. Kelman, A: The relationship of pathogenicity of *Pseudomonas solanacearum* to colony appearance in a tetrazolium medium. Phytopathology, 44, 693-695(1954).

124. Chen, Y., Yan, F., Chai, Y., Liu, H., Kolter, R., Losick, R.,and Guo, J.: Biocontrol of tomato wilt disease by *Bacillus subtilis* isolates from natural environments

depends on conserved genes mediating biofilm formation, Environ. Microbiol., 15(3), 848-864 (2013).

125. Arai, M., Sobou, M., Vilchéze, C., Baughn, A., Hashizume, H., Pruksakorn, P., Ishida, S., Matsumoto, M., Jacobs, W. R. Jr., and Kobayashi M.: Halicyclamine A, a marine spongean alkaloid as a lead for anti-tuberculosis agent, Bioorg. Med. Chem., 16, 6732—6736 (2008).
126. Yoshino, M., Eto, K., Takahashi, K., Ishihara, J., and Hatakeyama, S.: Organocatalytic asymmetric syntheses of inthomycins A, B and C, Org. Biomol. Chem., 10, 8164-8174 (2012).
127. Henkel, T. and Zeeck, A.: Sekundärstoffe aus dem chemischen screening, 16. Inthomycine, neue oxazol-triene aus *Streptomyces* sp., Liebigs Ann. Chem., 367-373 (1991).
128. Tanaka, Y., Kanaya, I., Shiomi, K., Tanaka, H., and Omura, S.: Phtoxazolin A, a specific inhibitor of cellulose biosynthesis from microbial origin: Isolation, physico-chemical properties, and structure elucidation, J. Antibiot. (Tokyo), 46, 1214-1218 (1993).
129. Tanaka, Y., Sugoh, M., Ji, W., Iwabuchi, J., Yoshida, H., and Omura, S.: Screening method for cellulose biosynthesis inhibitor with herbicidal activity, J. Antibiot. (Tokyo), 48, 720-724 (1995).
130. Omura, S., Tanaka, Y., Kanaya, I., Shinose, M. and Takahashi, Y.: Phthoxazolin, a cellulose biosynthesis inhibitor, produced by a strain of *Streptomyces* sp., J. Antibiot. (Tokyo), 43, 1034 – 1036 (1990).
131. Gräfe, U., Kluge, H., and Thiericke, R.: Biogenetic study on oxazolomycin, a metabolite of *Streptomyces albus* (strain JA 3453), Leibigs Ann. Chem., 429 – 432 (1992).
132. Zhao, C., Coughlin, J. M., Ju, J., Zhu, D., Wend-Pienkowski, E., Zhou, W., Wang, Z., Shen, B., and Deng, Z. : Oxazolomycin biosynthesis in *Streptomyces albus* JA 3453 featuring an “acyltransferase-less” type I polyketide synthase that incorporates two distinct extender units, J. Biol. Chem., 285, 20097 – 20108 (2010).
133. Hashimoto, K., Nihira, T., Sakuda, S., and Yamada, Y.: IM-2, a butyrolactone autoregulator, induces production of several nucleoside antibiotics in *Streptomyces* sp. FRI-5, J. Ferment. Bioeng., 73, 449 -455 (1992).

134. Partida-Martinez, L. and Hertweck, C.: A gene cluster encoding rhizoxin biosynthesis in "*Burkholderia rhizoxinia*", the bacterial endosymbiont of the fungus *Rhizopus microsporus*, ChemBioChem, 8, 41-45 (2007).
135. Zhou, Y., Murphy, A. C., Samborskyy, M., Prediger, P., Dias, L. C., and Leadlay, P. F.: Iterative mechanism of macrodiolide formation in the anticancer compound conglobatin, Chem. Biol., 22, 745-754 (2015).
136. Perlova, O., Gerth, K., Kaiser, O., Hans, A., and Müller, R.: Identification and analysis of chivosazol biosynthetic gene cluster from myxobacterial model strain *Sorangium cellulosum* Soce56, J. Biotechnol., 121, 174-191 (2006).
137. Pistorius, D. and Müller, R.: Discovery of the rhizopodin biosynthetic gene cluster in *Stigmatella aurantiaca* Sg a15 by genome mining, ChemBioChem, 13, 416-426 (2012).
138. Bockamp, E., Maringer. M. Spangenberg,C, Fees, S.,Fraser,S., Eshkind, L., Oesch,F., and Zabel, B.: Of mice and models: improved animal models for biomedical research. Physiol. Genomics, 11,115–132 (2002).
139. van Duyne, G. D.,:Cre-recombinase, Microbiol.Spectrum, MDNA3-0014 (2014).
140. Pulsawat, N., Kitani, S., Fukushima, E., and Nihira, T.: Hierarchical control of virginiamycin production in *Streptomyces virginiae* by three pathway-specific regulators: VmsS, VmsT and VmsR, Microbiology, 155, 1250-1259 (2009).
141. Ikeda, H., Kotaki, H., and Omura, S.: Genetic studies of avermectin biosynthesis in *Streptomyces avermitilis*, J. Bacteriol., 169, 5612-5621 (1987).
142. Komatsu, M, Tsuda, M., Omura, S., Oikawa, H., and Ikeda, H.: Identification and functional analysis of genes controlling biosynthesis of 2-methylisoborneol, Proc. Nat., Acad. Sci. USA, 105, 7422-7427, 2008.
143. Musiol, E.M., Greule, A., Härtner, T, Kulik, A., Wohlleben, W., and Weber, T.: The AT2 domain of KirCI loads malonyl extender units to the ACPs of the kirromycin PKS, ChemBioChem, 14, 1343-1352 (2013).
144. Yadav, G., Gokhale, R. S., and Mohanty, D.: Computational approach for prediction of domain organization and substrate specificity of modular polyketide synthases, J. Mol. Biol., 328, 335-363 (2003).
145. He, M., Varoglu, M., and Sherman, D. H.: Structural modeling and site-directed mutagenesis of the actinorhodin β-ketoacyl-acyl carrier protein synthase, J.

Bacteriol., 182, 2619-2123 (2000).

146. Lai, J. R., Koglin, A., and Walsh, C. T.: Carrier protein structure and recognition in polyketide and nonribosomal peptide, Biochemistry, 45, 14869-14879 (2006).

147. Reid, R., Piagentini, M., Rodriguez, E., Ashley, G., Visvanathan, N., Carney, J., Santi, D. V., Hutchinson, C. R., and McDaniel, R.: A model of structure and catalysis for ketoreductase domains in modular polyketide synthases, Biochemistry, 42, 72-79 (2003).

148. Matilla, M.A., Stöckmann, H., Leeper, F. J., and Salmond, G. P. C.: Bacterial biosynthetic gene cluster encoding the anti-cancer haterumalide class of molecules: Biogenesis of the broad spectrum antifungal and anti-oomycete compound, oocydin A, J. Biol. Chem., 287, 39125-39138 (2012).

149. Wu, J., Zalesky, T. J., Valenzano, C., Koshla, C., and Cane, D. E.: Polyketide double bond biosynthesis. Mechanistic analysis of the dehydratase-containing module 2 of the picromycin /methymycin polyketide synthase, J. Am. Chem. Soc., 127, 17393-17404 (2005).

150. Schoenafinger, G., Schracke, N., Linne, U., and Marahiel, M. A.: Formylation domain: an essential modifying enzyme for the nonribosomal biosynthesis of linear gramicidin, J. Am. Chem. Soc., 128, 7406-7407 (2006).

151. Bork, P. and Koonin, E. V.: A P-loop like motif in a widespread ATP pyrophosphatase domain: Implications for the evolution of the sequence motifs and enzyme activity. Protein. 20, 347-355 (1994).

152. Soehano, I., Yang, L., Ding, F., Sun, H., Low, Z. J., Liu, X., and Liang, Z. X.: Insight into the programmed ketoreductions of partially reducing polyketide synthase: stereo-and substrate-specificity of the ketoreductase domain, Chem. Sci., 00, 1-7 (2012).

153. Caffrey, P.: Conserved amino acid residues correlating with ketoreductase stereo specificity in modular polyketide synthases, ChemBioChem, 4, 649-662 (2003).

154. Keatinge-Clay, A. T.: A tylosin ketoreductase reveals how chirality is determined in polyketides, Chem. Biol., 14, 898-908 (2007).

155. Wagner, D. T., Zeng, J., Bailey, C. B., Gay, D. C., Yuan, F., Manion, H. R., and Keatinge-Clay, A. T.: Structural and functional trends in dehydrating bimodules from trans-acyltransferase polyketide synthases, Structure, 25, 1045-1045 (2017).

156. Piel, J: A polyketide synthase-peptide synthetase gene cluster from uncultured bacterial symbiont of Paederus beetles, Proc. Natl. Acad. Sci. USA, 99, 14002-14007 (2002).

List of Publications

1. Suroto, D. A., Kitani, S., Miyamoto, K. T., Sakihama, Y., Arai, M., Ikeda, H., and Nihira, T.: Activation of cryptic phthoxazolin A production in *Streptomyces avermitilis* by the disruption of autoregulator-receptor homologue AvaR3, J. Biosc. Bioeng., 124(6):611-617(2017). https://doi.org/10.1016/j.jbiosc.2017.06.014.

2. Suroto, D. A., Kitani, S., Ikeda, H., and Nihira, T.: Characterization of the biosynthetic gene cluster for cryptic phthoxazolin A in *Streptomyces avermitilis*. PLoS One, 13(1): e0190973 (2018). http://doi: 10.1371/journal.pone.0190973

Acknowledgements

Firstly I would like to express my gratitude to my supervisor, Professor Takuya Nihira, for his support, guidance and advice during my study. I also extend my gratitude to Associate Prof. Shigeru Kitani for all the discussions, truthful advice, support, and encouragements, to Assistant Prof. Hiroshi Kinoshita for his helpful advice and support.

I would like to thank my co-supervisor, Prof. Eiichiro Fukusaki and Prof. Hajime Watanabe for their valuable suggestion and comments to improve this thesis. I sincerely thank all professor in Department of Biotechnology for their support and assistance which made this achievement possible. I would like to extend my thanks to Prof. Kazuhito Fujiyama for his support and assistance in the final step of my study.

I am especially grateful to Prof. Haruo Ikeda from Kitasato Institute for his valuable advice and experimental supports. Associate Prof. Yasuko Sakihama from Faculty of Agriculture, Hokkaido University for undertaking anti-*Aphanomyces* bioassay and Associate Prof. Masayoshi Arai from Graduate School of Pharmaceutical Sciences, Osaka University for the assistance on the anti-mycobacterial bioassay and MS analysis.

I am thankful for Ministry of Education, Cultures, Sports, Science, and Technology (MEXT) for financial support during my five years stay in Japan.

I would like to thank all members in the Nihira Laboratory for providing an incredible working atmosphere during my stay. Thanks for being great and friendly lab buddies.

Lastly, I wish to thank my family, especially my husband, my son Ivan, and my daughter Nadia for their love, patience and extraordinary support, throughout my PhD studies. To my mother and father for constant reminders and sincere prayers. It would be impossible for me to finish this project without their support. For this, I am indebted.

Appendix 1.[1] H-NMR Spectrum of Phthoxazolin A in Methanol-d4 (600 Mhz)

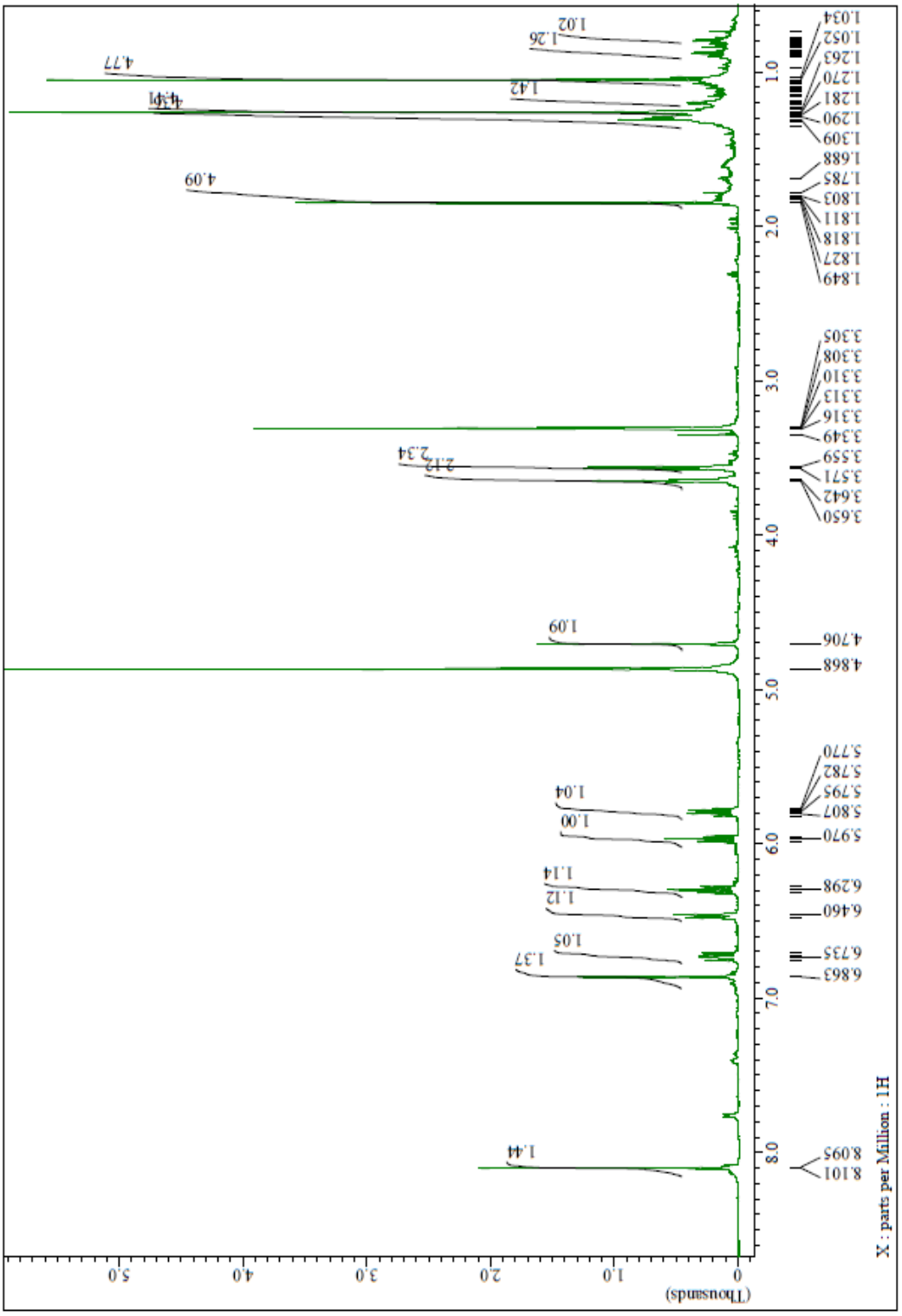

Appendix 2. ^{1}H- NMR Spectrum of Phthoxazolin A in Chloroform $CDCl_3$ (600 Mhz)

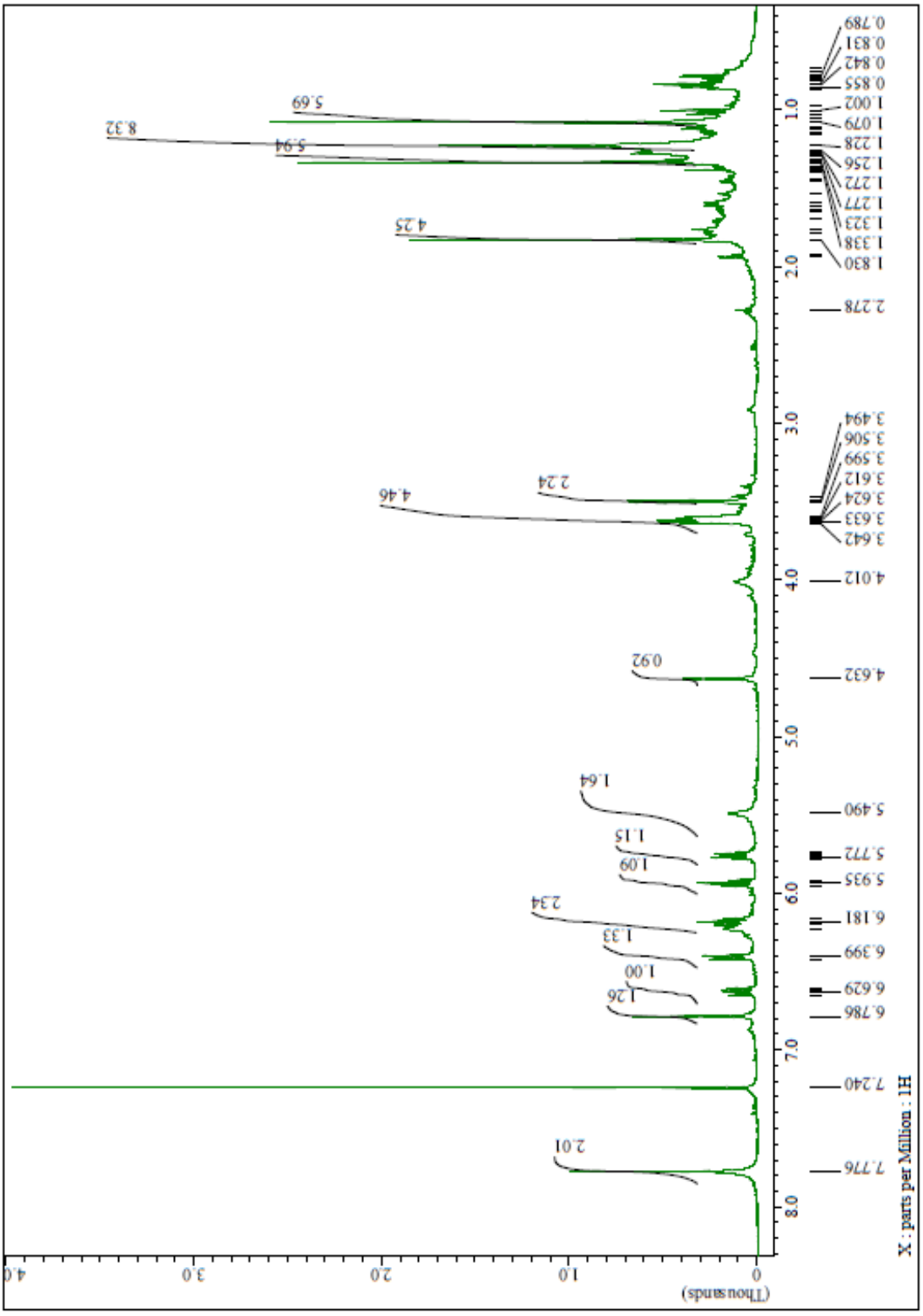

Appendix 3. ^{13}C-NMR Spectrum of Phthoxazolin A in Methanol-d4 (600 MHz)

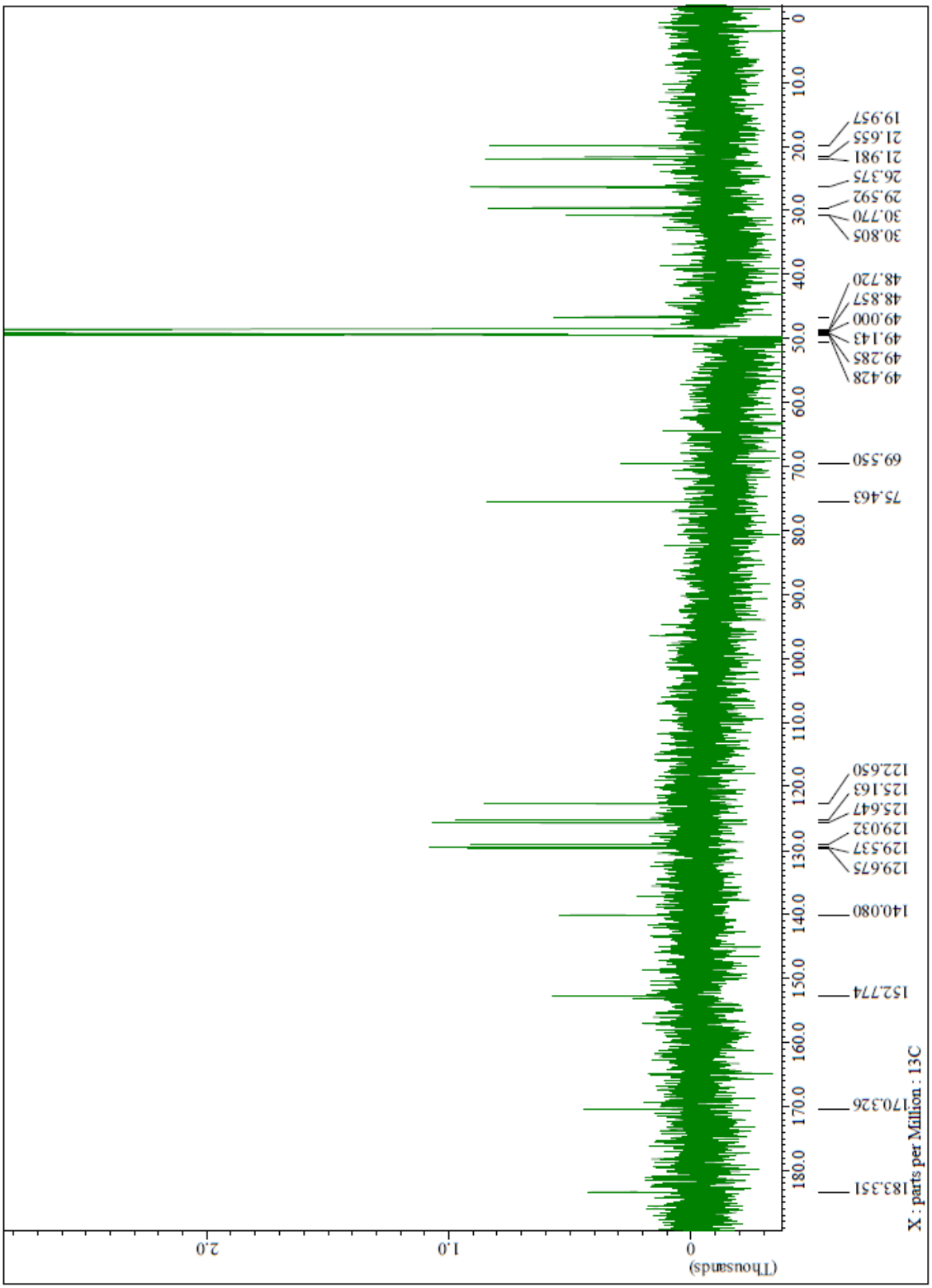

Appendix 4. IR Spectrum of Phthoxazolin A

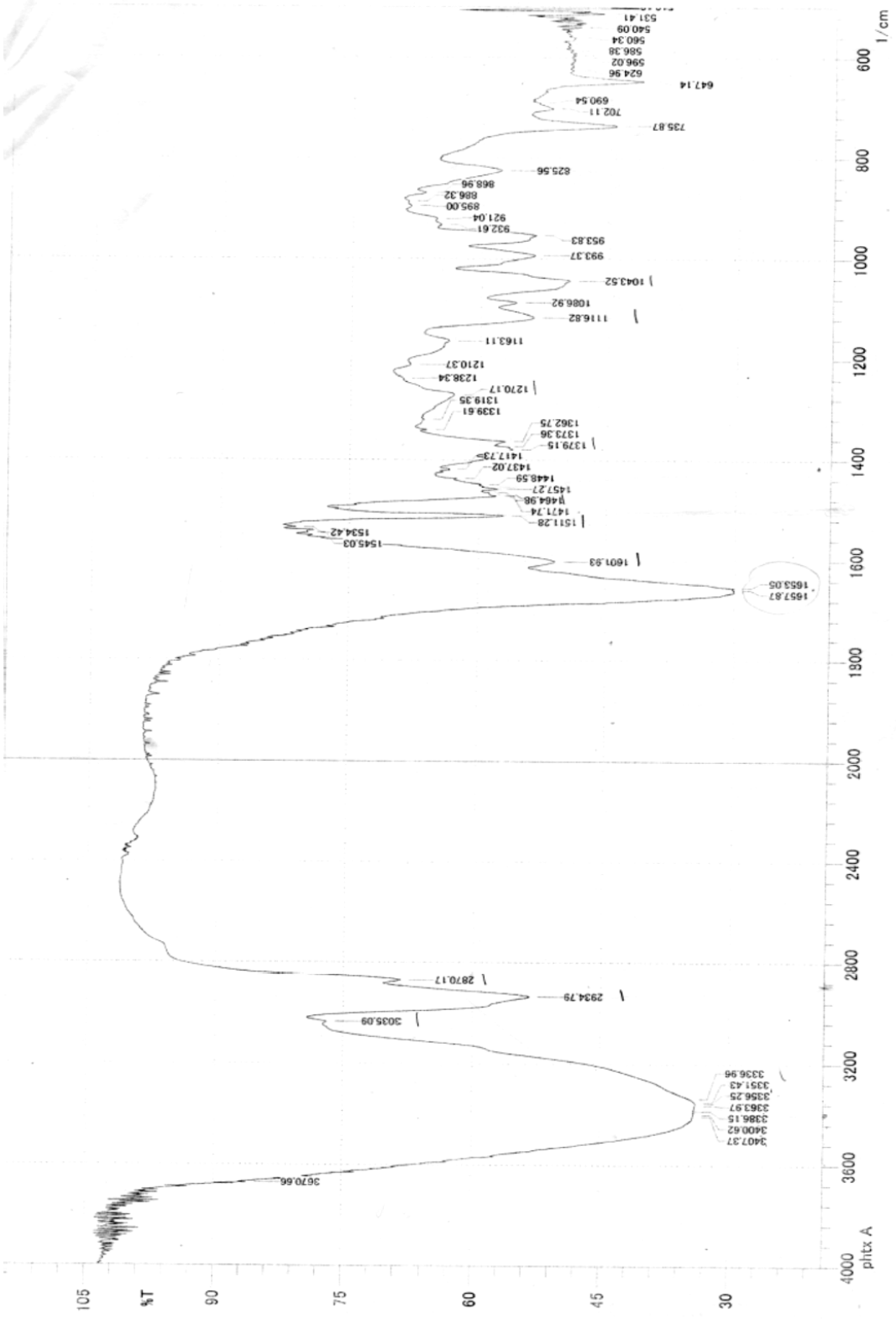

Appendix 5. Plasmids for vectors constructions

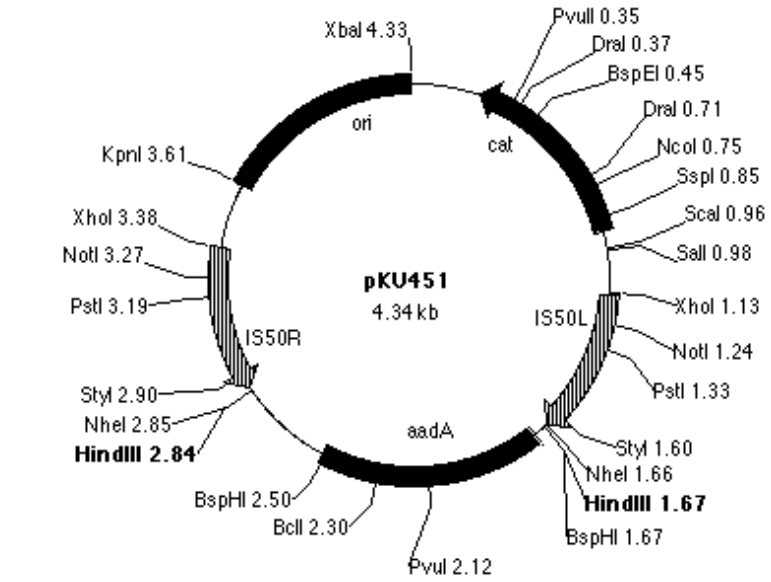

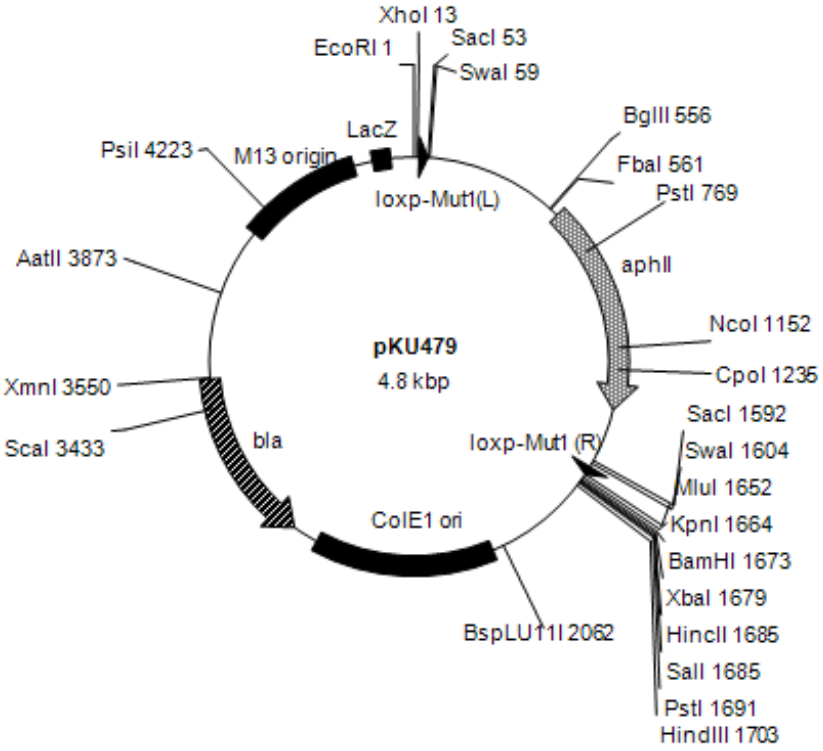

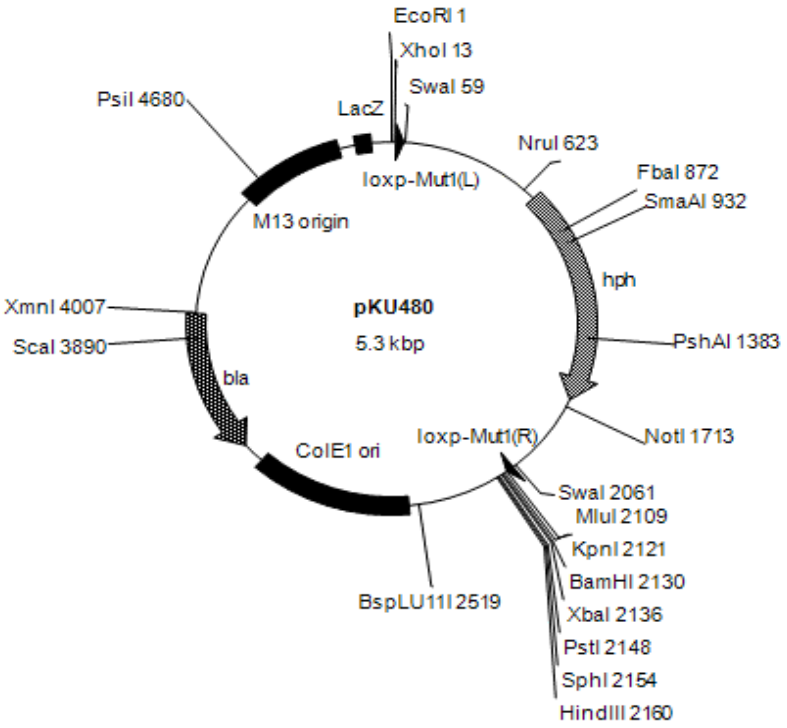
EcoRI 1
XhoI 13
SwaI 59
PsiI 4680
LacZ
NruI 623
FbaI 872
SmaAI 932
loxp-Mut1(L)
M13 origin
hph
pKU480
5.3 kbp
XmnI 4007
ScaI 3890
PshAI 1383
bla
NotI 1713
loxp-Mut1(R)
ColE1 ori
SwaI 2061
MluI 2109
KpnI 2121
BamHI 2130
XbaI 2136
PstI 2148
SphI 2154
HindIII 2160
BspLU11I 2519

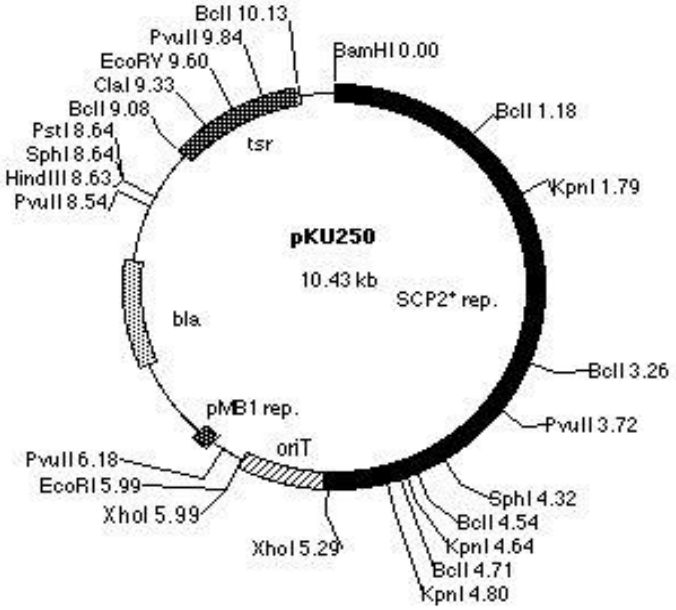
BclI 10.13
PvuII 9.84
BamHI 0.00
EcoRV 9.60
ClaI 9.33
BclI 1.18
BclI 9.08
PstI 8.64
tsr
KpnI 1.79
SphI 8.64
HindIII 8.63
PvuII 8.54
pKU250
10.43 kb
SCP2* rep.
bla
BclI 3.26
pMB1 rep.
PvuII 3.72
oriT
PvuII 6.18
SphI 4.32
EcoRI 5.99
BclI 4.54
XhoI 5.99
KpnI 4.64
XhoI 5.29
BclI 4.71
KpnI 4.80

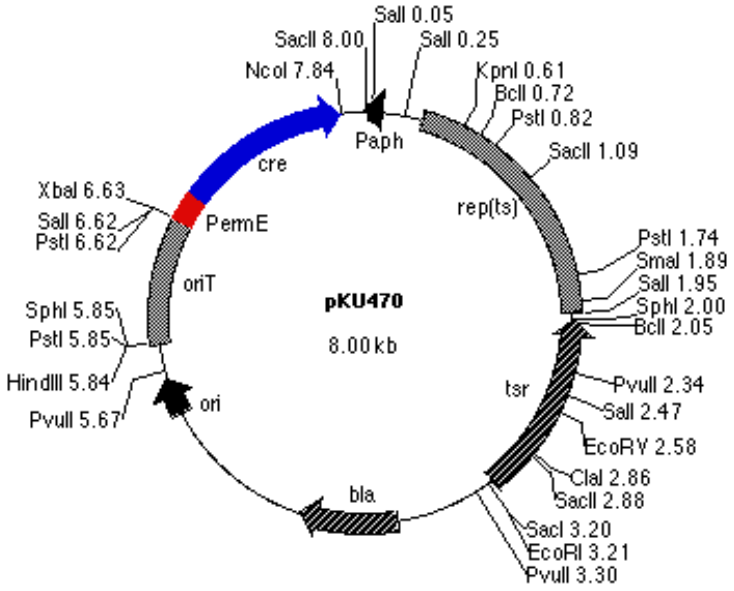
SalI 0.05
SacII 8.00
SalI 0.25
NcoI 7.84
KpnI 0.61
BclI 0.72
PstI 0.82
Paph
SacII 1.09
cre
XbaI 6.63
rep(ts)
SalI 6.62
PermE
PstI 6.62
PstI 1.74
SmaI 1.89
oriT
pKU470
SalI 1.95
SphI 5.85
SphI 2.00
PstI 5.85
8.00 kb
BclI 2.05
HindIII 5.84
tsr
PvuII 2.34
ori
SalI 2.47
PvuII 5.67
EcoRV 2.58
ClaI 2.86
bla
SacII 2.88
SacI 3.20
EcoRI 3.21
PvuII 3.30

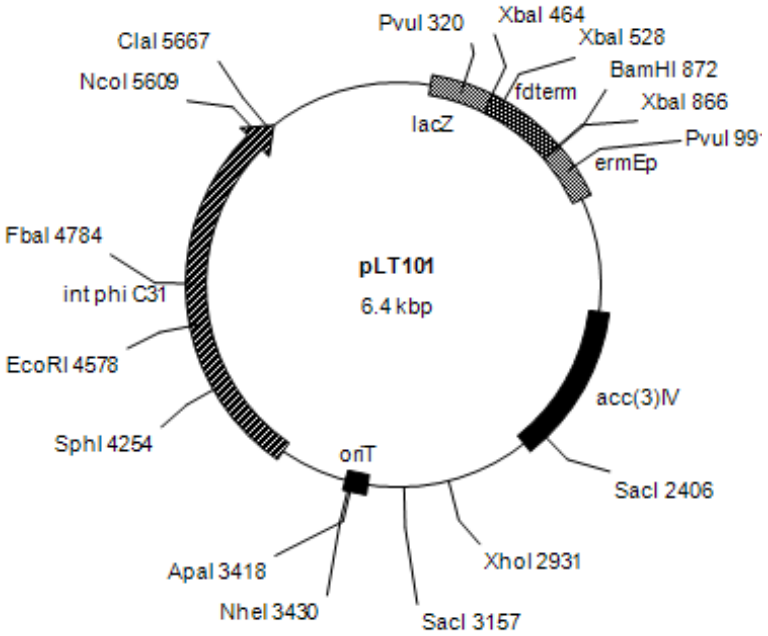
PvuI 320
XbaI 464
ClaI 5667
XbaI 528
NcoI 5609
BamHI 872
fdterm
XbaI 866
lacZ
PvuI 99
ermEp
FbaI 4784
pLT101
int phi C31
6.4 kbp
EcoRI 4578
acc(3)IV
SphI 4254
oriT
SacI 2406
XhoI 2931
ApaI 3418
NheI 3430
SacI 3157

Appendix 6. The discreet AT domains and their accession numbers subjected for phylogenetic analysi**s**

Protein	**NCBI Accession number**	**Gene cluster**	**Source organisms**
BaeC	CAG23950	Bacillaene	*Bacillus amyloliquefaciens* FZB4
BaeD	CAG23951	Bacillaene	*Bacillus amyloliquefaciens* FZB4
BaeE	CAG23952	Bacillaene	*Bacillus amyloliquefaciens* FZB4
BatH	ADD82949	Batumin	*Pseudomonas fluorescens* BCCM_ID9359
BatJ	ADD82951	Batumin	*Pseudomonas fluorescens* BCCM_ID9359
BryP	ABK51299	Bryostatins	*Candidatus endobugula sertula*
DifA	CAG23974	Difficidins	*Bacillus amyloliquefaciens* FZB42
DzD	AAY32968	Disorazols	*Sorangium cellulosum* So ce12
ElsA	WP_012792904	Elansolids	*Chitinophaga pinensis* DSM 2588
ElsB	WP_012792903	Elansolids	*Chitinophaga pinensis* DSM 2588
KirC1	CAN89639	Kirromycin	*Streptomyces collinus* Tü 365
LnmG	AAN85520	Leinamycin	*Streptomyces atroolivaceus*
LkcD	BAC76473	Lankacidins	S*treptomyces rochei*
MmpC	AAM12912	Mupirocin	*Pseudomonas. fluorescens* NCIMB 10586;
OzmM	ABS90474	Oxazolomycin	*Streptomyces albus* JA3453
OzmM	ADI12766	Oxazolomycin	*Streptomyces bingchenggensis* BCW-1
PedC	AAS47559	Pederin	*Pseudomonas* symbiont of *Paederus fuscipes*
PedD	AAS47563	Pederin	*Pseudomonas* symbiont of *Paederus fuscipes*
PsyH	ADA82589	Psymberin	symbiont of sponge *Psammocinia* aff. *bulbosa*
RhiG	CAL69887	Rhizoxins	*Burkholderia rhizoxina*
SorO	ADN68489	Sorangicins	*Sorangium cellulosum* So ce12
VirI	BAF50719	Virginiamycin	*Streptomyces virginiae*
FabD*	CAA77658	Fatty acid synthase	*Escherichia coli*
SAV5788*	BAC73500	Fatty acid synthase	*Streptomyces avermitilis*-MA460

*Out group